NUMERICAL EXPLORATION OF RESIDUAL STRESS MECHANISMS IN ROCK

by

Maxzender Trzop

Submitted in partial fulfilment of the requirements
for the degree of Master of Applied Science

at

Dalhousie University
Halifax, Nova Scotia
July 2024

Dalhousie University is located in Mi'kma'ki, the
ancestral and unceded territory of the Mi'kmaq.
We are all Treaty people.

TABLE OF CONTENTS

LIST OF TABLES

LIST OF FIGURES

ABSTRACT

Residual stresses are known to exist within the microstructure of crystalline materials as a result of material formation processes and exists in a state of equilibrium with their own internal forces. Research has proven their existence, and engineering applications have been derived for glass and metal to achieve desirable material properties. In the field of rock mechanics and rock engineering, the existence of residual stress has been acknowledged, but beyond that, little research has been performed to investigate their behaviour and implications and they are often omitted from design considerations due to their state of equilibrium. Using numerical modelling techniques such as grain-based modelling, insights on the effects of residual stress in rock can be explored. Grain-based models were created in 2D with *RS2*, and in 3D with *3DEC*, to explore potential implications for residual stress in the field of rock mechanics and rock engineering. Methods to implement residual stress in numerical models were developed and used to explore the effects of residual stress on modelling outcomes. In *RS2*, three main implications were investigated. The first examines a relationship between residual stress and crack closure strains in compression tests. The second investigates the influence of residual stresses on the formation and propagation of damage (microcracks) within rock specimens. The final simulation relates to the stresses and displacements associated with a mobilized residual stress field due to the addition of a circular excavation in a rock block. In *3DEC*, the formation of damage due to unloading a specimen containing residual stresses was examined. Compression tests were performed on the unloaded specimens to investigate for crack closure strains as a result of the damaged formed through residual stress redistribution during unloading. The investigations undertaken in this study suggest that residual stresses have a real and non-negligible influence on rock behaviour and their omission may not be a valid approach when performing design in rock that contains these stresses.

LIST OF ABBREVIATIONS AND SYMBOLS USED

2D	Two-dimensional
3D	Three-dimensional
AE	Acoustic Emission
BEM	Boundary Element Method
DGR	Deep Geologic Repository
DIC	Digital Image Correlation
EDZ	Excavation Disturbed Zone
EDZ_{CI}	Construction Induced Excavation Damage Zone
EDZ_{SI}	Stress-Induced Excavation Damage Zone
FDM	Finite Difference Method
FEM	Finite Element Method
HDZ	Highly Damaged Zone
HF	Hydrofluoric Acid
LdB	Lac du Bonnet Granite
NaCl	Sodium Chloride
MgO	Magnesium Oxide
REV	Representative Elemental Volume
SEM	Scanning Electron Microscope
UCS	Uniaxial Compressive Strength
URL	Underground Research Laboratory
XRD	X-Ray Diffraction
E	Young's modulus
$E_{impurity}$	Young's modulus for an impurity embedded in a matrix
E_{matrix}	Young's modulus for a matrix containing an impurity
K_n	Joint normal stiffness
K_s	Joint shear stiffness
$\mu\epsilon$	Microstrain
ν	Poisson's ratio
ϕ	Friction angle
ρ	Material density
σ_1	Major principal stress
σ_3	Minor principal stress
σ_x	Stress in the x-direction
σ_y	Stress in the y-direction
σ_z	Stress in the z-direction

ACKNOWLEDGEMENTS

I would like to thank my supervisor, Dr Andrew Corkum for his support and guidance throughout my thesis. Thank you for providing me this opportunity and allowing me to work under your supervision; and thank you for all the knowledge you have provided to me. I would not have been able to complete this without your help.

I would also like to thank my committee members, Dr Navid Bahrani and Dr Craig Lake, and my colleagues, Gomez and Ryan, for their input and feedback on my research.

Finally, I would like to thank my friends and family for supporting me throughout this journey.

CHAPTER 1 - INTRODUCTION

1.1 Background for Thesis Research

Residual stresses are a self-equilibrated stress field that exists within the microstructure of crystalline materials such as metal, glass, and rock. These stresses are sometimes referred to as microstresses due to their nature of existing within the microstructure of materials and therefore interacting on the micro (grain-to-grain) scale. Friedman (1972) discusses residual stresses as a system of "locked-in" and "locking" strains. As residual stress forms as a result of a locked-in residual strain, in this thesis, the terms residual stress and residual strain are used interchangeably due to their relationship, and, unless specifically referring to one component, the term "residual stress" is preferred to reference this phenomenon. If a material is subjected to applied stress and, as a result, residual stress forms, the complete dissipation of the strain associated with the applied stress does not occur and a portion remains locked in the microstructure. The non-dissipated strains would be representative of the locked-in strains, and the forces restricting the complete dissipation of the induced strain would be referred to as the locking strains. As these stresses are self-equilibrating, the locked-in and locking strains should result in a net zero force acting on the material. If the residual stress state becomes disturbed or disrupted, then the net force acting on the material is no longer zero, and the residual stress will mobilize and dissipate until a new net zero stress state is achieved. This can occur through the complete dissipation of residual stress, or if partial dissipation occurs, the residual stresses would reach a new state of equilibrium and thus continue to exist within the microstructure with lower overall magnitudes. Friedman (1972) presents residual stress magnitudes measured in various studies and rock types with magnitudes of up to 27 MPa in tension and 22 MPa in compression, and Chapter 2.4 presents the results of additional residual stress measurements.

As residual stresses are self-equilibrated stresses, they are often omitted from rock mechanics and rock engineering consideration and typically, only in situ, and excavation-induced stresses are considered. Residual stresses, if mobilized, can have a significant influence on structures and excluding them from analysis can likely lead to design issues. An example of the consequences of omitting residual stresses from consideration is presented by Nau (2015) and is illustrated in Figure 1-1. In their research, they presented the case of the split I-beam. The I-beam was created by casting, and as a result, residual stresses formed within the beam. Once the beam was fully hardened, it was cut on the ends to the desired shape and length. As a result of cutting the beam, the residual stress state was disturbed, and the I-beam fully split through the web destroying the entire beam. This illustrates the importance of considering residual stress as a mechanism that exists within the structure of a material, as neglecting to consider residual stress resulted in significant damage to the material.

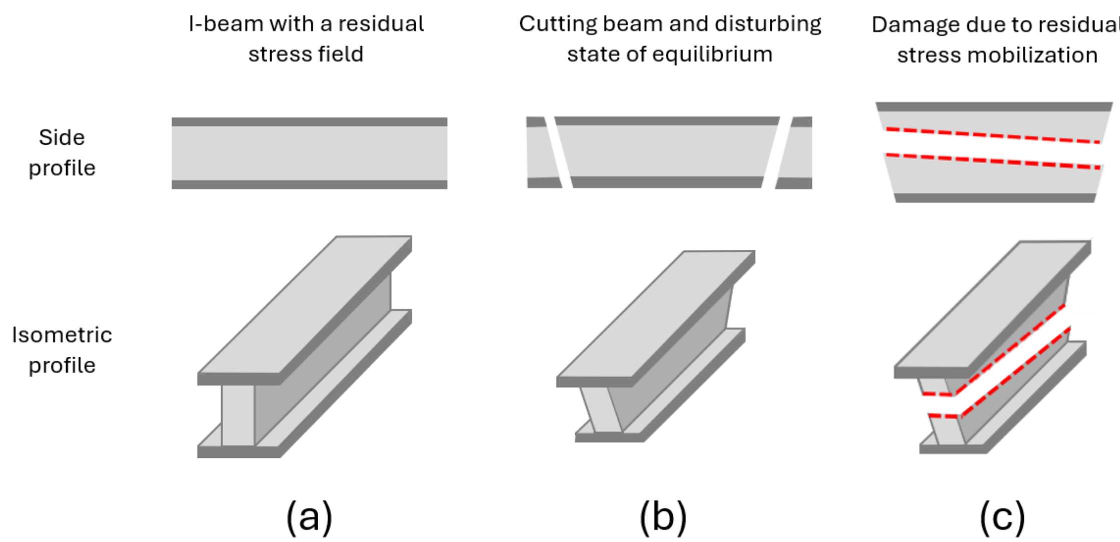

Figure 1-1 Representation of damage formation in an I-beam from residual stress redistributions as a result of cutting the beam (after Nau 2015). a) I-beam created by casting the metal resulting in the formation of a residual stress field. b) Cutting the beam to size and shape thus disturbing residual stress equilibrium resulting in residual stress redistributions. c) Damage in the form of complete web splitting due to the residual stress redistributions overcoming the material strength

Similar to the case of the split I-beam, in the field of rock mechanics and rock engineering, omitting residual stresses from design considerations and field measurements may lead to design flaws or measurement errors. As shown in Figure 1-1, disturbing a residual stress field results in the mobilization of residual stress that can overcome the local strength of a material.

This process can also occur in rock, and if the magnitude of the redistribution overcomes the material strength, grain fracturing or microcracking along grain boundaries may occur. If microcracks are present prior to the redistribution of residual stress, then crack propagation can occur as well. When performing in situ stress measurements the rock is typically overcored, and as a result, disturbs the state of equilibrium and mobilizes residual stresses. As residual stresses are not considered in the field of rock engineering, the mobilization of residual stress likely leads to a source of error for in situ stress measurement. On a larger scale, residual stress redistributions around underground or surficial excavations can lead to unaccounted-for stresses and strains to be mobilized which may have effects on tunnel convergence or wall displacement, and more importantly, on support structures.

With an increase in demand for mineral resource deposits, the economic near-surface deposits are largely being mined resulting in a greater need for underground mining operations to meet societal demands (Ghorbani et al. 2023). With increasing depth, an increase in in situ stress magnitude is also observed. With larger stress concentrations surrounding excavations, a detailed understanding of the complete in situ stress state will allow engineers to better develop mine plans and excavation designs. Residual stress is a component of the complete in situ stress state, and therefore an understanding of the local residual stresses will allow engineers to develop a better description of the stress fields influencing their designs. Similar to underground mining, a Deep Geologic Repository (DGR) also requires a detailed understanding of the stress state as illustrated by Corkum et al. (2018) who underwent a detailed investigation of the in situ stress magnitudes surrounding the access shaft for Ontario Power Generation's DGR for low and intermediate-level storage of nuclear waste. A detailed understanding of the stress state is an important consideration for the design of DGRs. Minimizing the damage surrounding DGRs becomes an area of concern as with increased levels of damage, there exists increased potential for the transportation of radioactive waters through the damaged zones and into the surrounding rockmass. Siren et al. (2015) described the levels of damage that can surround an excavation and are summarized in Figure 1-2. Residual stresses are a contributing factor to the stress magnitudes surrounding the excavations and therefore can contribute to the level of damage around tunnels. Specifically within the HDZ, EDZ_{CI}, and EDZ_{SI} regions illustrated in

Figure 1-2, residual stresses can influence the depth and degree of damage in each layer. Therefore, developing an understanding of the local residual stresses is likely an important consideration to quantify the damage for DGRs and reduce the likelihood of transportation of radioactive wastewater.

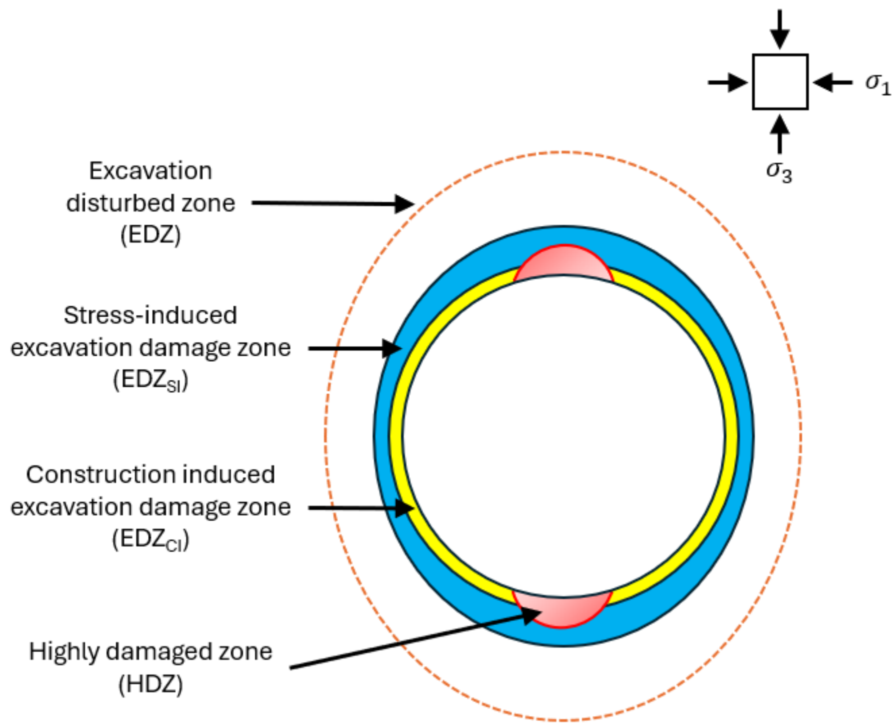

Figure 1-2 Representation of the damaged zones surrounding a tunnel (After Siren et al. 2015). In the excavation disturbed zone, stresses are altered due to the presence of the tunnel but the material remains undamaged. Stress-induced excavation damage is the zone where mining-induced stresses result in damage. Construction induced damage arises from blasting, TBM, or other excavation methods. The highly damaged zone occurs at the location of maximum induced stresses surrounding the tunnel

Residual stresses have been a long-studied phenomenon with investigations in glass taking place as early as 1660 (Brodsley et al. 1986). This phenomenon began with glass items called Prince Rupert's drops, and the concepts were later adapted in 1870 for use in automobile windscreens (Brodsley et al. 1986). In the 1940s, the understanding of residual stress in metallurgy increased, and these stresses were implemented through the peening process to strengthen materials (Maleki et al. 2021). Engineers in both the glass and metallurgy fields developed an understanding of the processes at hand for residual stress formation and understood the detrimental and beneficial effects of their presence. Engineers in these fields adapted the positive characteristics to intentionally create these stresses within their designed materials resulting in desirable material properties. Residual stress concepts derived from research in glass and metal structures were adapted in the field of rock mechanics and rock engineering in the mid-1960s (Voight 1966; Friedman 1967). Research on residual stress in rock continued to be published until the mid to late 1990s, were after such time, few studies were presented relating to residual stress. In rock, the effects of residual stresses are largely deemed negligible and have been omitted from the majority of studies on rock behaviour.

1.2 Thesis Goals

The goal of this thesis is to include residual stresses in numerical simulations related to rock mechanics and rock engineering to evaluate their influence on modelling outcomes and determine if omitting these stresses from consideration is a valid approach. Through a review of available literature, and with the use of numerical modelling tools, implications for residual stresses in rock are explored using 2D continuum and 3D discontinuum software. In the 2D simulations, implications for these stresses are explored. Some of these implications are best described using a discontinuum framework, and therefore, some findings from the 2D simulations are reassessed using 3D discontinuum software to validate their findings. By creating numerical models that contain residual stresses and exploring their results, the effects of residual stress are presented to provide examples of their influence on rock behaviour. Residual stresses appear to have broad implications in the field of rock mechanics and rock engineering. With continued research, understanding, and discussion of these stresses, the number of potential implications increases and can be used as a mechanism to describe observations that cannot currently be modelled or predicted with the tools available to engineers.

1.3 Thesis Structure

This thesis is paper-based and therefore there may be some overlap between the material presented within the introduction, literature review, and conclusion chapters with the chapters containing the submitted papers (Chapters 3 and 4). The layout of the chapters contained in this thesis is as follows. Chapter 2 contains the literature review section. In this section, residual stress measurement methods, residual stresses in non-rock materials, and residual stresses in rock are discussed. An overview of the modelling methodologies and inputs used in this thesis is also presented. Chapter 3 contains a journal paper submission to the Journal of Engineering Geology and the Environment. In this chapter, background is provided on the topic (some material in this section overlaps with Chapter 2) and residual stresses are investigated with 2D continuum micromechanical models created in *RS2*. Implications for residual stress such as the opening of microcracks visualized through crack closure strains, crack formation and propagation due to residual stress redistributions, the influence of residual stress on a propagating crack, and the effects of residual stresses surrounding excavations are discussed. Chapter 4 contains a conference paper submission for the American Rock Mechanics Association (ARMA) Golden 2024 conference. In this chapter, background is provided on the topic (some material in this section overlaps with Chapter 2), and 3D discontinuum micromechanical models are created using *3DEC*. Implications for residual stress such as crack formation, and the opening of microcracks visualized by crack closure strains in compression tests are explored. In Chapter 5, the thesis will be concluded. A brief discussion section will be presented followed by the main findings from the research along with recommendations for future research to continue developing the understanding of residual stress in rock mechanics and rock engineering.

CHAPTER 2 - LITERATURE REVIEW

Studies on residual stress began in glass and then progressed to the field of metallurgy, followed by rock mechanics and rock engineering. Many methods have been developed in the various fields to quantify these stresses using different techniques, some of which are described here. The initial discovery of residual stress in glass is presented along with some of its applications and its development into the field of metallurgy. Residual stresses are discussed in depth in the field of rock mechanics and rock engineering illustrating their measured magnitudes using various techniques, as well as observations and models for residual stress in rock.

2.1 RESIDUAL STRESS MEASUREMENT TECHNIQUES

To measure residual stresses in crystalline materials such as metal, glass, or rock, two main categories of strain measurement techniques are commonly used. These techniques are classified in either the non-destructive methods or destructive methods categories. As the name implies, non-destructive methods measure strains within specimens without the need for damage such as drilling to initiate strain mobilization. These methods can be advantageous as they measure internal strains locked in a sample which can then later be used for property testing or other investigations. However, techniques in this category are often more difficult to use and require a detailed understanding of the method to employ them. On the other hand, destructive methods use drilling, cutting, grinding, or other forms of physically altering a specimen to disrupt the state of equilibrium within a microstructure to initiate strain mobilization. These methods are simpler and easier to use, but after measurement, the specimen can no longer be used for any property measurements or other laboratory investigations. The following section briefly describes some common techniques used in both the non-destructive and destructive method categories to measure residual stresses contained within the microstructure of crystalline materials.

2.1.1 Non-Destructive Methods

A common approach in non-destructive measurement methods is to use diffraction techniques. X-ray diffraction (XRD) is a method that relies on X-ray beams and their interaction with the crystal lattice structure of a material and is based on the fundamentals of Bragg's law (Fitzpatrick et al., 2005). Crystalline materials consist of many grains, and within each grain, the atomic structure consists of an array of atoms that create sheet-like structures, that when layered together, create the crystal structure. These atomic sheet structures form parallel to each other, and the distance that separates the layers of atoms is known as the *d-spacing*. *D-spacings* are known to change when it is exposed to an elastic load as the crystal structure compresses or separates due to either applied compressive or tensile loading. To measure a strain within a material using this method, an X-ray beam is shot into the sample, which through its interactions with the crystal structure, results in diffraction patterns. These diffraction patterns are then scanned, and diffraction peaks are located and related to the current *d-spacing* of the material. Changes in the *d-spacing* are reflected in the scanned diffraction measurements which allows for changes in *d-spacings* to be measured. Therefore, this method can be used to evaluate strain progression in loading or unloading scenarios by monitoring changes in *d-spacing* with the progressive changes in load. It can also be used to measure the current state and compare it to a known unloaded state to determine strain. A crystal known to have no load acting internally or externally can be scanned with this method to determine the unloaded value for *d-spacing*. The measured *d-spacing* can then be used with the unloaded value to correlate the associated strain magnitude within the crystal structure.

Neutron diffraction, a similar method to XRD, relies on elastic distortions of the crystal structure to result in *d-spacings* that are different from their unloaded state (Rossini et al., 2011). This method measures the diffraction of a neutron beam as opposed to an X-ray beam through the crystal structure to produce a measured value of *d-spacing*. The main difference between the neutron diffraction method and the XRD method is the depth within a specimen at which strains can be measured. The neutron diffraction method allows for a penetration depth (sampling depth) of up to a few centimetres, which compared to XRD methods that can only measure strains near the surface of the material, is significantly larger. Due to the increase in depth, strain fields can be more accurately mapped with this method as strains below the surface can also be recorded. The downside to employing this method is the associated costs as the equipment is more expensive than the equipment required for XRD measurements.

Synchrotron diffraction is another diffraction technique that exists as a method to measure strains. This method is also similar to XRD in its measurement technique but uses X-rays that are more intense than those of standard XRD measurements. This method allows for higher resolution and improved sensitivity of diffraction peaks compared to XRD methods (Sharma & Hesterberg, 2020). With a better understanding of the diffraction peaks, measurements of strain become more accurate which allows for a better understanding of the strain state within the material. Due to the increased intensity (higher X-ray energy), this method also allows for a deeper penetrating depth compared to standard XRD methods (Withers & Webster, 2008). Measurement times are also quicker with this method compared to the others, but due to the higher energy X-rays that are used, the depth of strain measurements and their associated directions have greater restrictions compared to that of the neutron diffraction method.

The ultrasonic method, also called the refracted longitudinal wave method, can be used to measure stress states and is based on the use of acoustic elasticity theory. This method is based on a relationship between the elastic wave propagation velocity and the magnitude of stress which affects the wave velocity (Rossini, 2011). The ultrasonic method is a type of stress measurement that has many different forms including direct measurement, phase comparison, echo amplitude, ultrasonic goniometer, spectral, and tomography methods (Guo et al., 2019). Stress states can be mapped within the specimen being measured by adjusting the wave frequency to reach different depths. In general, the accuracy of this method is around ± 30 MPa, and after calibration, the accuracy can be improved to about ± 10 MPa. Measurements with this method are more common in fields of metallurgy where residual stresses are expected to have larger magnitudes, and it is unlikely that this method could be used in rock engineering unless the accuracy of the method is greatly improved.

The Raman spectroscopy method was designed to study molecular structures and is based on the Raman effect and the scattering of light (Guo et al., 2019). As mentioned previously, when a crystal structure is exposed to stress it results in a shortening or extension of the molecular structure depending on the direction of stress (compressive or tensile). The light is scattered by the molecular structure, and changes in the observed frequency or wavenumber of the light are recorded. When using this method, due to stress, changes in the frequency can be seen on the Raman spectrum, called Raman shift, and can be converted to stress by using a mathematical formula. This method has been successfully used by Harker et al. (1970) to illustrate its effectiveness in measuring stress by applying uniaxial stress in a quartz crystal and determining the stress state through the use of this method. The accuracy of measurements with this method can be highly dependent on external factors such as focusing depth, laser thermal effects and room temperature, and this method is more commonly used for residual stress measurements in metals.

The non-destructive methods discussed above are only some of the more prominent methods used for residual stress measurements in crystalline materials. While most of these methods were developed for analyzing residual stresses in metals, some have been adapted to measure residual stresses in rocks. The most common methods of residual stress measurement in rock are through the use of diffraction measurement techniques. Some of the uses for these methods are discussed later in Chapter 2.4.1. While other methods such as the ultrasonic and Raman spectroscopy methods have not been used in rocks quite yet, the continued progression of their accuracy and measurement methods may allow for future use of these methods.

2.1.2 Destructive Methods

When using destructive methods, the sample must be permanently altered by cutting, drilling, grinding, or other similar processes which result in deformations that can be measured. Sectioning is a destructive method used to measure residual stresses. This method was developed to measure the internal stresses contained within metals (Tebedge et al. 1973) and consists of cutting up a specimen into longitudinal strips. Due to the residual stress field present within the sample prior to sectioning, once the specimen has been cut, it is expected to have changes in length that can be measured and converted to stress using elastic theory. This method is commonly used with strain gauges that are attached to the specimen which then has parts of the material cut out, creating "sections" (Schajer 2010). These measured strains are then converted into stresses which illustrate the magnitudes required to cause the measured change in dimension due to the presence of an internal stress field (residual stresses). Progressive cutting of the specimen creates a large amount of data that can then be used to recreate the original residual stress field that existed prior to cutting.

The slitting method is another form of destructive residual stress measurement and is similar to the sectioning method. In the sectioning method, the material was fully cut into sections, but in the slitting method, the cut is only partially through the material leaving it somewhat intact. This method can also be referred to as the saw-cut method, or the slotting method, as it essentially creates a slot in the material due to a saw-cut, disturbing the residual stress' state of equilibrium and resulting in a change in shape due to the partial dissipation of residual stresses (Schajer 2010). The cutting of the material takes place over multiple passes of the saw, and with each pass of the saw, residual stresses are released resulting in deformations. This method is typically used with strain gauges to measure the deformations after cutting has been performed to correlate a value of residual stress to the associated displacements. This method has been used in multiple materials (metal, glass, crystals, and plastics) and shapes (blocks, beams, plates, rods, and tubes) to measure residual stresses, illustrating its versatility (Lee and Hill 2007).

The layer removal method is another method that is similar to the sectioning method. In this method, thin layers are removed from a specimen through machining or other methods which results in a bending action on the remaining layers of the specimen (Eijpe and Powell 1997). The deformations or curvature of the specimen after a layer is removed is then investigated and related to a force and moment which could cause such a deformation. The combinations of both of these acting forces are then assessed for their relationship to stress which allows for residual stress measurements to be deduced. This method is more commonly employed in metals which allows for the use of electro-chemical polishing (Ekmekci et al. 2004) which is a method to remove thin layers from the sample without inducing any stresses, as might be done with a grinder or machining. Nonetheless, this method could still be adapted to other materials as long as a method to remove thin layers (such as grinding) has a control on parameters that could induce stress such as temperature or applied force from the grinding wheel.

The contour method is a residual stress measurement technique that is similar to the sectioning method, but this method allows for a 2D residual stress field to be determined normal to the cut surface (Hosseinzadeh et al. 2014). In this method, a specimen is cut into two halves, and as a result of the residual stress field constrained within the microstructure, the cut surface deforms. Deformations can occur due to tensile residual stresses which cause the material to bow inward from its initial surface, or due to compressive residual stresses which cause the material to bow outward. After the sample has deformed, the surface is then scanned creating a contour profile of the deformations on the cut surface. The stresses that result in such deformations are then back-calculated to produce the original residual stress field on that plane prior to cutting. This method can be repeated on the sample to release further residual stress and provide contour maps of deformations for other planes within the material to determine the state of residual stress in more than just a single 2D plane.

The hole drilling method is the most versatile residual stress measurement technique as it requires only drilling a hole within a material and measuring the deformations around that hole (Schajer 2010). This method is typically used with strain gauges that surround the cutting location, and after the hole has been drilled, the strain gauges record the deformations that occur. These deformations are then converted to stress and a residual stress magnitude can be determined. Aside from using strain gauges, there are also optical methods that can be used to measure the deformations surrounding the drill hole (Nelson 2010). Brittle coatings, such as a brittle lacquer, can be applied to the surface of a specimen prior to drilling, and as a result of the residual stress redistributions caused by drilling, the coating cracks and illustrates areas of movement which can then be used for stress interpretation. Photoelastic coatings can be applied to the surface, and using a reflection polariscope, redistributions of residual stress can be seen as a pattern of isochromatic fringes that can be used to interpret residual stress. Digital Image Correlation (DIC) requires a speckled pattern to be applied to the surface of a material prior to drilling, during/after drilling the specimen is recorded with a camera to track movements of the speckle pattern that can be inferred by software to determine a 2D stress state normal to the surface that produced the deformations. Other optical methods than the ones listed here that can be used to infer residual stresses are discussed in Nelson (2010).

Some of the existing destructive methods used for residual stress measurement have been summarized above, but other methods exist, and new methods are frequently developed. Destructive methods are easier to employ for residual stress measurement when compared to non-destructive methods. Although not all of these methods have been used in rock, they may have applications in the future if the processes can be adapted to suit the requirements for rock measurement. The most common method used for residual stress measurement in rock is the hole drilling method, and some examples are provided later in Chapters 2.4.2 and 2.4.3.

2.2 Residual Stress in Non-Rock Materials

One of the earliest observations of residual stresses was through glass objects called Prince Rupert's drops. In the mid-1600s, Prince Rupert sent five glass items as a gift to King Charles II, two of which contained liquor, and the other three were solid glass. The King became interested in their odd mechanical properties and gave them to the Royal Society for investigation, who would later term these glass items Prince Rupert’s drops (Aben et al. 2016). Prince Rupert’s drops are teardrop-shaped glass items known to contain residual stresses that can significantly alter their mechanical properties. These drops are created when molten glass is dripped into cold water (Brodsley et al. 1986). Due to the large thermal gradient that is produced by this method, the cooling of the glass takes place at different rates throughout the material. The glass that contacts the water hardens first and creates a sort-of “shell” that contains the remaining molten glass in its interior. As the molten glass within the shell starts to cool, it contracts and hardens. The contraction of the molten glass results in the generation of tensile stress as it pulls on the already-hardened shell, and as the shell is being pulled inwards, compressive stress is generated within it. After the glass is fully cooled, the Prince Rupert’s drop reaches a state of equilibrium in which the tensile stresses in the core generated by contraction during cooling, balance the compressive stresses in the shell generated from being pulled inward.

Prince Rupert’s drops are known to have altered mechanical properties as a result of the residual stresses that are generated during their creation. The larger section of these drops, referred to as the head, can withstand fairly large forces. The head of these drops can be hit with a hammer and survive the impact without damage and can also be placed within a loading frame and loaded up to 15 kN before breaking (Aben et al. 2016). The reason these drops can withstand such forces is due to the compressive residual stresses that exist within the outer region of the glass. These compressive stresses resist the formation of tensile microcracks that form on the surface during loading, essentially increasing the compressive strength of the material. However, as residual stresses are a self-equilibrating stress field with equal and opposite compressive and tensile magnitudes, the large magnitude of compressive stress required to increase the strength is accompanied by a large tensile magnitude that can result in further damage if it is exposed. At the tail section of Prince Rupert’s drops, the glass is quite thin. As less material is present within this section, less compressive stresses are generated in the outer layers which creates a section that can be broken quite easily. When the drops are broken, the damage typically initiates from the tail section and propagates towards the head of the drop. Due to tensile stresses contained within the core, the glass becomes very brittle when these stresses are exposed, resulting in the rapid disintegration of the glass into small powder-like fragments as it dissipates the large tensile stresses within it.

As research developed further into Prince Rupert's drops, an understanding of the mechanisms that result in residual stress formation, and the implications of their presence, allowed engineers in the field of glass to utilize these stresses to their advantage. Thermal tempering is a process used in glass to strengthen the material by inducing residual stresses within it (Aronen and Karvinen 2018). This tempering process is similar to the formation of Prince Rupert's drops in that a large thermal gradient is used to induce the residual stress field. Sheets of glass are heated to temperatures over $600°C$ and then are rapidly cooled, typically with cold air, to produce the thermal gradient that is required to generate residual stress. Another method of inducing residual stress into glass materials is with chemical methods. With this method, the glass is submerged in a molten alkali salt (Gy 2008). While the glass is submerged, an exchange between ions in the glass, and the molten salt occurs. As a result of this process, residual stresses are formed due to the ions in the glass being exchanged for larger ions from the salt which induces a compressive stress into the surface of the glass that is balanced by a tensile stress below the surface. The advantage of tempering with chemical methods over thermal methods is that larger compressive stresses are induced, which effectively creates glass with a higher strength compared to thermally tempered glass. Tempered glass is used for its high strength compared to annealed glass, and its safety as when it breaks, it fragments into small pieces preventing large shards that could puncture or injure people. It has a range of uses such as for windows in vehicles due to its strength and safety (Brodsley et al. 1986), and even for screen protectors for cell phones or tablets due to its increased compressive strength (Terakado et al. 2020).

Engineers in the field of metallurgy also use residual stresses to their advantage. The shot peening process was developed to introduce compressive residual stresses on the surface of metals to reduce wear and improve the material's strength (Montross et al. 2002). Shot peening relies on shock waves to induce strain into the surface of the material that can be used to create residual stresses. Using lasers, upon contact with the surface of the material, a plasma is created, and a shock wave is induced. As a result, compressive stress is generated in the direction of the shock wave through the plasma and into the solid metal below. The generated compressive stress results in plastic deformations up to a certain depth in the material, and once the surface plasma hardens, the residual stresses are stored within the material. With this method, residual stresses are used to increase the strength and ductility of a material, but residual stresses can also be detrimental to a material if unaccounted for. Throughout the machining process of metals, residual stresses can be generated unintentionally which can impact material properties such as fatigue strength, creep, and crack resistance (Jacobus et al. 2000). An understanding of the formation mechanisms of residual stress can help reduce the magnitudes produced during machining to ensure the component has the desired strength and is not impacted by residual stress. In these fields, an in-depth understanding of residual stress allowed engineers to improve material strength, and also understand the detrimental effects of their presence if unaccounted for.

2.3 RESIDUAL STRESS FORMATION IN ROCK

Residual stress can form for many different reasons in different rock types. A few of the possible origins of residual stresses in igneous, metamorphic, and sedimentary rock types are discussed here. In igneous rock types, the rock forms as a magma deep below the surface of the earth and then over geologic time the material is uplifted to the surface or near-surface depths. Varnes (1969) created a model to simulate the formation of residual stresses in igneous rock types. Their model consisted of numerous units that simulated the grains of rock which exerted a repulsive force when in contact with one another and could also be restrained from separating by attaching them with various types of restraints. They created an array of these units and proceeded to apply external load to the boundaries of the system. Under load, they applied elastic restraints on the units and then removed the external load. As a result of attaching the units with elastic restraints, the model did not completely relax and instead, illustrated a residual stress field as the units themselves were under compression and trying to separate, but they were restrained by the elastic bands under a tensile force resisting the relaxation. This process effectively simulated residual stresses that could arise as a result of a rock crystallizing under in situ stresses that cannot fully relax when removed from in situ due to the crystallization of the grains and the "welding" of the grain interfaces under such loads.

Another possible origin of residual stress in igneous rock types originates from the anisotropic heating/cooling of grains within the rockmass due to variations in mineralogy at the grain scale. Russell and Hoskins (1972) discuss the effects of varying coefficients of thermal expansion due to a heterogeneous rockmass on the formation of residual stress. Due to non-uniform thermal expansion, strains are induced within the grains and some grains expand/contract more than others which further induces strains into neighbouring grains that are expanding/contracting at a different rate. After cooling, strain remains in the system due to the varied local magnitudes (tensile and compressive) produced from heating which results in a residual stress field. Savage (1978) created a basic model to simulate the relationship between different thermal coefficients and residual stress formation. In their model, they simulated a granite with a quartz sphere embedded in a feldspar matrix. The model then had a temperature of $300°C$ set as the initial temperature, and the model was allowed to cool. As a result of cooling, the quartz contracted creating a tensile residual stress within it, and due to the magnitude of stress exceeding the local strength, microcracking was noticed to occur within the quartz grain. Other researchers (Holzhausen and Johnson 1979; Tan and Kang 1980) have also explored the effects of thermal heating/cooling on the formation of residual stress in igneous rock bodies.

In metamorphic rock, plastic deformations and recrystallization processes are likely sources of residual stress formation. Processes such as folding or tectonic collisions can produce plastic deformations (Molli and Heilbronner 1999) that will free grain boundaries and create damage within the rock structure. Due to the plastic deformations, grain boundaries will be broken thus leaving frictional interfaces. If sliding of grain boundaries has occurred, due to the neighbouring grains having their movement restricted or due to complex interlocking, interfaces will then have a frictional resistance to back-sliding that prevents the complete relaxation of built-up stress. This results in the formation of residual stress surrounding the interfaces as there is a sliding force acting on them and their relaxation is resisted by the interlocking of neighbouring grains. Molli and Heilbronner (1999) discuss the effects of recrystallization in Carrara marble and illustrate that plastic deformations can be recrystallized. Recrystallization is another method in which residual stress can be locked in rock as the plastic strains have been hardened within the material to prevent their relaxation as opposed to relying on interlocking forces to restrict their relaxation. The formation of residual stresses due to recrystallization under in situ stresses is also similar to the formation of residual stress due to crystallization. During recrystallization, deformations due to in situ stresses can also be recrystallized and can be combined with plastic deformations from folding or other processes to create residual stress fields.

In sedimentary rocks, the interlocking forces that occur in metamorphic rocks can also occur here. Due to the structure of sedimentary rocks, interlocking can occur as a result of frictional grain-to-grain interfaces. As the material is compacted, sliding along grain boundaries occurs, and when unloaded, back-sliding is prevented due to the frictional forces acting on them. Another method for residual stress to form in sedimentary rocks is via the cementation process. This process is similar to crystallization/recrystallization processes, but differs as a cement binder is added to the granular structure of the rock to cement the deformations and prevent their relaxation. Gallagher (1971) performed an experiment in which they loaded 68 discs in an array where all were contacting one another and then cemented the discs under load. They then completely removed the load and investigated the stresses in the system with fringe patterns. They noted that stress remained locked in the grains of the material and that stress had also developed within the cement. The addition of the cement prevented the complete relaxation of the discs as the cement had gained stress after unloading, illustrating that the cementation process restricts the relaxation of the grains and thus can lead to the formation of residual stresses.

The grains within a rock are typically composed of crystalline materials (i.e., quartz, feldspar etc.). Within the crystal structure of the grains lies the atomic structure where internal deformations and creep mechanisms can occur. Passchier and Trouw (2005) discuss the microstructures of rock and detail some of the internal mechanisms that can occur within it.

Crystal structures are typically composed of sheet-like layers of atoms that become bonded together in their normal directions. Within the atomic structure, lattice-preferred orientations exist where the sheet-like structures are bonded together in a state that requires the least amount of energy to be stable (Mainprice and Nicolas 1989). When a rock, and therefore the crystal structures within it, are under load, the atomic structure undergoes deformations. A process called crystal plastic flow can occur in these situations where the crystal undergoes permanent deformation. This process is a result of the atomic bonds between the sheet-like structures breaking and rebonding throughout the deformation. After a period of deformation, the crystal structure can reach a new lattice-preferred orientation where the relaxation of the deformation is resisted by the strong atomic bond associated with the new atomic configuration. This process results in a permanent deformation within the crystal structure that can then lead to the formation of residual stresses.

2.4 Residual Stress Measurement in Rock

In the field of rock mechanics and rock engineering, residual stress measurements have been performed in both the laboratory and in situ. Both non-destructive and destructive methods have been used to estimate the magnitudes of residual stress fields that can be found in rocks. The use of diffraction methods (non-destructive) and coring methods (destructive) in the laboratory, as well as the use of coring methods in situ, have previously been used by researchers. The results of their residual stress measurements taken in various geologic materials and settings are discussed here. By using various residual stress measurement methods, it becomes clear that these stresses are not an artifact of a specific measurement technique, but rather that they are real stresses that exist within the microstructures of rock.

2.4.1 Laboratory Measurement with Non-Destructive Methods

The first investigation of residual stress in rock with non-destructive methods was conducted by Friedman (1967). In their work, they tested five different cemented sandstone specimens, two calcite cemented, and three silica cemented, for the presence of residual stress. XRD was used to measure residual strains that were released from the five specimens. To release residual stress, they freed the boundary constraints on individual grains by using hydrofluoric acid (HF) to dissolve the cement. The state of strain was measured with XRD prior to removing the cement as a baseline measurement. HF was then placed one drop at a time, measuring the strain state in between each drop until no further change in strain was measured. The number of drops required to completely free the grains from the cement varied from 4 to 25 drops. Both tensile and compressive magnitudes of strain were released with magnitudes of up to 170 microstrains ($\mu\epsilon$) measured in contraction illustrating a release of tensile residual stress, and up to 240 ($\mu\epsilon$) in extension illustrating a release of compressive residual stress.

Residual stresses contained within a quartz vein were measured by Sekine and Hayashi (2009) with XRD methods. In their work, they collected a schist block from the Kanto Mountain outcrop that had a quartz vein within it. The vein was approximately 5 mm thick and was exposed on all sides of the block. They prepared samples from the block and measured residual stresses contained within them using XRD methods. In their measurements, they reported compressive residual stresses with magnitudes of 5 to 30 MPa and tensile residual stresses with magnitudes of 4 to 12 MPa. When measuring residual stresses within the vein, they noted that measurements parallel to the vein often had higher magnitudes of compressive residual stresses compared to measurements taken perpendicular to the vein where these measurements had lower compressive stresses and, in some cases, low magnitudes of tensile stress. The parallel direction was found to be the principal residual stress direction throughout the vein which agreed with the reported magnitudes in parallel and perpendicular directions. The influence of thermal expansion on residual stress formation was investigated for the vein in their rock and concluded that to produce residual stress with the reported magnitudes, the vein must have formed under in situ stresses in the range of 550 to 660 MPa.

Residual stresses have been measured using synchrotron X-ray microdiffraction in a coarse-grained metamorphic marble by Chen et al. (2011a). The samples they recovered were moderately deformed during metamorphism and contained fairly large grains with lamellar twinning (a microtectonic deformation process) after recrystallization. Thin sections were prepared from the recovered material to analyze the magnitudes of residual stresses contained within the microstructure. They reported residual strains with magnitudes of several hundred to over a thousand $\mu\epsilon$. These strains, converted to stress, are in the magnitude of 60 to 120 MPa. Due to the deformation and recrystallization that occurred during metamorphism, the large magnitudes of strains reported were likely recrystallized during this process and trapped within the microstructure. The authors concluded using their observations of the residual stresses that the twinning process resulting in residual stress formation must have occurred under in situ stresses of 100 to 200 MPa.

A quartz sample was retrieved from a meteorite impact in South Africa and was tested for residual stress using synchrotron X-ray diffraction by Chen et al. (2011b). From their recovered material they cut thin sections, and then using a grinder, thinned them even further for residual stress measurement. Several grains within the thin section were measured to determine residual stress magnitudes. They recorded a total of 1600 diffraction measurements throughout multiple thin sections. Due to the meteorite impact, the shock waves that occurred induced large strains into the rock that were later recrystallized after the impact zone had cooled. Residual strains on the order of several thousand $\mu\epsilon$ were reported, and after conversion, the reported stresses were in the range of 40 to 140 MPa.

To try and quantify the mechanisms that occur during earthquakes, Chen et al. (2015) retrieved cores from depth in active fault zones to study the fault gauge material. Residual stresses were measured using X-ray Laue microdiffraction from quartz samples retrieved from the San Andreas fault at a depth of 2.7 km. Thin sections were taken from the recovered material and four scans were performed. They noted that the measured residual strains were fairly heterogeneous, illustrating that residual stresses were inconsistent throughout and had areas with high and low magnitudes. They noted both compressional and extensional deformations illustrating a release of both tensile and compressive stresses respectively. They noted that in the direction normal to the thin section, little to no residual strains were noted as most were released during the creation of the thin sections. They reported common residual strains of about 1000 $\mu\epsilon$ which converted to approximately 130 MPa, and in some cases, residual stresses of over 300 MPa were reported.

Boudinage structures occur in rock during deformation which results in a series of long block-like structures that form next to one another in a sheet-like orientation and can be deformed by in situ stresses. Specimens with quartz veins infilled in the openings between these structures are recovered and investigated for residual stresses with XRD methods by Chen et al. (2016). A total of five scans were performed in two separate quartz veins (one 8 mm thick and the other 1 mm thick) that were parallel in situ and were turned into thin sections for measurement. Scans were taken from the scale of a single grain up to a scan that included about 50 grains. Strains on the order of a thousand $\mu\epsilon$ were reported and it was noted that strains perpendicular to the vein wall consisted of shortening strains (release of compression) while strains parallel to the vein were mostly extensional (release of tension). These strains were then converted to stresses and had peak magnitudes of up to 250 MPa.

Samples of Carrara marble were investigated for the presence of residual stress using neutron diffraction methods by Voigtlander et al. (2020). Prior to investigating residual stresses, some samples were subjected to a creep test under both dry and saturated conditions by axially loading a notched sample and inducing bending stresses. The samples were subject to creep loading only, and loading was stopped before the samples broke to have intact samples for residual stress measurements. The presence of some newly formed microcracks along grain boundaries due to creep loading was noted. One sample was not exposed to creep loading to determine the residual strain state prior to the creep test. A core was taken from the untested sample and the measured residual strains were mainly contractional with magnitudes ranging from 435 to 890 $\mu\epsilon$. cores were also taken for measurement in the notched sample subjected to creep loading. In the cores, near the location of the notch in the initial sample, measured strains were extensional intergranular strains with magnitudes on the order of thousands of $\mu\epsilon$ and as the distance from the notch location increased, the strains returned to the contractional state illustrated in the untested sample. Their creep loading experiment illustrated the effects of creep loading on potential residual stress formation.

Seven samples of quartzite recovered from the central Alps were used with synchrotron Laue microdiffraction by Wenk et al. (2020) to measure the state of residual stress contained within the microstructure. The recovered samples were initially sandstone samples that were deformed and metamorphosed into the material they recovered for testing. From the recovered material, thin sections were cut for investigation. In the thin sections, they noted that most grains within the quartzite were flattened with some undulations due to plastic deformations that occurred prior to recrystallization. The magnitudes of residual strains within the measured samples were noted to be highly variable in magnitude and direction. They reported residual strains of 1000 to 2000 $\mu\epsilon$ which they related to residual stress magnitudes of 300 MPa in both tension and compression.

Wang et al. (2023) measured residual stresses in a siliceous slate-containing quartz vein that was obtained from Mongolia by using XRD methods. The veins within the rock were approximately parallel to the bedding planes and were 1 to 4 mm in width, as well as a few veins that were perpendicular to the bedding and were 1 to 3 mm in width. The veins contained both uniform small grains (30 to 40 $\mu\epsilon$), and non-uniform large grains (70 to 400 $\mu\epsilon$). They noted that the measured residual stresses were all compressive with magnitudes of 10 to 30 MPa. Residual stresses parallel to the bedding were significantly higher than those measured perpendicular to the bedding. Their work illustrated that a potential relationship between residual stress magnitudes and the orientation of vein formation may exist.

2.4.2 Laboratory Measurement with Destructive Methods

Residual stresses were measured in 11 rock samples (nine from underground and two from near surface) using coring methods by Gentry (1972). Cores were retrieved from their respective environments and then cut to size for testing. Upon retrieving the specimens, they were sprayed with a clear lacquer to reduce the effects of humidity and abrasion during transport. The cut ends of the core specimens were then cleaned, and a strain gauge was attached and covered with epoxy for protection. A metal washer was then placed over the strain gauge to create a pilot hole to keep the core barrel centred during overcoring. The strain gauge was then overcored to a depth of 7.62 cm. Strain readings were recorded after overcoring until the readings stabilized and no further strain was indicated, which in some cases took up to ten weeks. The magnitudes of residual strains reported after overcoring were up to 190 $\mu\epsilon$ in extension, and 125 $\mu\epsilon$ in contraction.

Russell and Hoskins (1972) recovered a core of Redfield granite from South Dakota for laboratory testing of residual stress with coring methods. The recovered core (4.13 cm diameter by 15.24 cm tall) was equipped with 11 strain gauges on the top of the sample with three located in the centre, three located in a ring pattern halfway from the centre to the edge, and five located near the edge (three of which were located together). The specimen was cored through from the back side with an 8.26 cm bit, essentially “overcoring” the six inner strain gauges and “undercoring” the outer five strain gauges located on the top of the specimen. The same core was then overcored twice from the top side, first with a 4.13 cm bit overcoring the inner six strain gauges and undercoring the outer five strain gauges. The second cut was with a 1.11 cm bit over coring the inner three gauges and undercoring the middle three gauges. All strain readings were recorded until no further changes in strain were noticed, and magnitudes of up to 80 $\mu\epsilon$ were reported

A nearly cubic block of granite (approximately 22 cm per side) was cut out of a larger rock block recovered from Barre Vermont that originated from a depth of 67 m for residual stress investigations by Nichols (1975). Their experiments on the rock block consisted of three phases. The first of which investigates changes in strain measured on the surface of the block as a result of concentric overcoring with strain gauges. Phase two used dyes on the surfaces that had been drilled to examine any microcracking that may have formed from strain release/redistributions. The third phase consisted of a petrofabric analysis. The block was equipped with a total of 34 strain gauges with 13 located on the top surface running vertically and horizontally through the center of the block. Another 13 gauges were placed on the bottom side following the same orientation as the top, and eight gauges were placed on the right side in a circular shape with a single gauge at the centre. A chip of the rock block was taken from the center of the block's top surface for XRD analysis prior to the coring programme which determined that magnitudes of 130 and 250 $\mu\epsilon$ existed in the rock prior to coring. The drilling program consisted of first coring the top of the block with a 5.1 cm core barrel centred on the surface of the block to just under halfway through and allowing strain redistributions to be measured for a total of three days after coring. Once strain readings stabilized, the top surface was concentrically drilled with a 10.1 cm core barrel and strains were measured for another three days, and then the top of the sample was cored for a final time with a 15.0 cm core barrel. This process in its entirety was repeated on the bottom surface of the block, and then again on the right side of the block but with only the 10.1 cm cut. From their cuts, strains of 75 to 275 $\mu\epsilon$ in both contraction (release of tension) and extension (release of compression) were measured. Their strain measurements illustrated similar magnitudes in the surrounding area measured from XRD measurements prior to coring. Their phase two analysis indicated that little to no microcracks were noticed as a result of the coring programme, except for near the freshly cut surfaces which had an area of 1 mm thick around the cuts that could be identified as an area where microcracks formed.

To determine if residual stresses can be completely dissipated due to time dependency, Bock (1979) measured residual stresses in a basaltic column. The column had been separated from the rock mass by naturally formed tensile joints that suggested the unit had been separated from the adjacent units for long periods of time, if not since its formation. Therefore, any residual stresses measured would be deemed trapped-in, and the relationship between time dependency and residual stress release could be investigated. The basaltic column had been recovered from a near-surface outcrop not covered by any thick sediment deposits from Australia, and was classified as a simple gneiss rock unit. The specimen was a nearly perfect pentagon in shape and was 38 cm tall by 18 cm in diameter. To measure residual stress release, a rosette containing three strain gauges centred around a pilot hole for undercoring was adapted from metallurgy measurements and used here. A total of 24 measurements were taken (22 on the top surface, and two along its axis). The drilling depth continued until strain readings became unaffected by drilling, after which, the strains were recorded for an additional 24 hours. Residual stress magnitudes of 15.2 MPa in compression and 12.6 MPa in tension were reported as the maximum magnitudes released from drilling.

Residual stress measurements in large single crystals using overcoring have been performed by White (1984). A quartz and orthoclase crystal (each a block with side lengths of about 0.3 m) were retrieved from the Tin Mountain mine in South Dakota. A plagioclase feldspar crystal was also obtained for testing, but it was received from the South Dakota School of Mines and therefore its origin was unknown. For all three crystal specimens, smooth surfaces were cut and cleaned for the installation of strain gauges. The strain gauges were then concentrically overcored with decreasing core barrel sizes of 5.0 cm, 3.6 cm, and 2.5 cm. The overcoring process was repeated twice on the quartz and orthoclase crystals, and three times on the feldspar crystal. Residual strains of up to 381 $\mu\epsilon$ were reported in the crystals from their investigation.

2.4.3 In Situ Measurement with Destructive Methods

In situ measurements of residual strain have been performed by Engelder et al. (1977) in three separate outcrops of Barre granite, a rock shown by Nichols (1975) to contain residual stress in a laboratory setting, that were all within 150 m of the lip for their respective quarries, and some outcrops of the surrounding metasediments in Barre Vermont. Residual strain measurements were performed using the concentric overcoring method. A strain rosette containing three strain gauges was attached to the surface of the rock and overcored with a 15.2 cm diameter core barrel to remove in situ stresses, and then the rosette was overcored again with a 7.6 cm diameter core barrel to measure residual strains. To compensate for the thermal effects on the strain results, a rosette was placed near the overcored locations and was not overcored. This provided a baseline strain that was then subtracted from the measured strains to compensate for thermal drift during the measurement period which took place over several days after overcoring. The largest measured strains were about 25% of the initial overcored value and were reported to occur in one measurement location, and the lowest measured strains were 25 $\mu\epsilon$ and reported to occur in a separate measurement location. In the surrounding metasediment outcrops, measurements of up to 1350 $\mu\epsilon$ were reported, and in one of their measurements, the residual strain measurement exceeded that of the initial overcore which removed the in situ stresses. This study illustrated that residual stress magnitudes can vary by location likely due to the volume of rock required to maintain the state of equilibrium.

A companion paper to Engelder et al. (1977) was published by Engelder and Sbar (1977). In this paper, five outcrops of Potsdam sandstones from New York were tested for residual strains measured in situ. The same methodology was used for concentric overcoring with a 15.2 cm core barrel to remove in situ stresses followed by a 7.6 cm core barrel to release residual strains. For all five outcrop measurements, three strain rosettes, containing three strain gauges each, were attached to the surfaces of the rock at spacings of 1 to 2 m. They monitored the strain gauges prior to overcoring to provide a baseline for thermal drift to increase the measurement accuracy and monitored the strains after overcoring for a few days. After overcoring, residual strains with a magnitude of more than 100 $\mu\epsilon$ were reported in one case, but it was noted that strains near the experimental error ($10\mu\epsilon$) were reported in other cases. Again, their work illustrated the regional variation in residual stress magnitudes that can occur due to the volume of rock required for the equilibrium of different residual stress fields.

Measurements of in situ residual stress at the Underground Research Laboratory (URL) located in Manitoba, Canada have been performed by Lang et al. (1986) and Read (1990). At the 240 m level near the location of the shaft, Lang et al. (1986) used concentric overcoring to measure residual stress. A stress cell was secured in a borehole and was overcored with a 200 mm diameter core barrel to remove in situ stresses. A 150 mm diameter cut followed by a 96 mm diameter cut was performed to release residual stress. Three separate holes were used for residual stress measurement, and within each hole, three stress cells (ranging from 2 to 5 m from the excavation wall) were placed to confirm the results obtained in each hole. From all measurements, residual stresses of about 1 MPa were reported. To confirm the magnitude of residual stress on the 240 m level, Read (1990) re-measured the residual stress magnitudes. Measurements were taken in two orthogonal boreholes and overcores with diameters of 600 mm, 300 mm, 200 mm, 150 mm, and 96 mm were performed. Their work confirmed the previous residual stress measurement with a magnitude of about 1 MPa present on the 240 m level of the URL.

2.5 Residual Stress Observations and Implications in Rock

Residual stresses have been proposed by Durrance (1969) as a mechanism for the weathering of rock. They mention that when a sample is released from in situ stresses, some residual stresses will be released instantaneously, while the rest will dissipate over long periods of time, and what doesn't dissipate will remain locked in the structure of the rock while it remains an intact material (i.e., not disaggregated). With the formation of rock joints, a release of residual stress will occur, but as the rock joints do not disturb the entire rock mass, some residual stress remains within. After this material has been uplifted to the surface or near the surface, there exist mechanical, chemical, and organic factors that can further release residual stresses that are not present at the depths where the residual stress fields originate. They propose that when these weathering processes occur, the residual stress fields are further disturbed, which can then lead to further destruction of the material after the release of residual stress.

A series of creep tests were performed by Price (1969) where a siltstone specimen was subjected to various loads and the deformations were monitored over time. The test loaded the specimen to a certain stress and maintained that stress for 40 to 50 days. After the allotted time, the specimen was then unloaded, concluding the loading cycle. The magnitude of induced stress between each test iteration was increased, starting at 36 MPa in the first cycle and ending at 80 MPa in the ninth. In the first five cycles, a typical reaction to the creep loading occurred. When the Specimen was subjected to the sixth cycle at a stress of 64 MPa, the specimen underwent elastic shortening due to the load, but the material suddenly started to expand without any change in the testing conditions. The seventh and eighth creep cycles then again illustrated the expected time-strain relationship illustrating that the observed phenomenon in cycle six did not affect the structural integrity of the material. Under the ninth and final cycle, halfway through the loading period, the material started to suddenly expand under a load of 80 MPa. The unexpected expansion when shortening was expected to occur in cycles six and nine was attributed to the release of residual stress. The magnitude of residual stress required to cause the anomalous measurements was stated to be about 60 to 70 MPa.

A study to examine the influence of residual strains on the orientations of tensile and shear failures was undertaken by Friedman and Logan (1970). Rock samples of Tennessee sandstone, Uinta Mountain quartzite, and Tensleep sandstone were used for their investigation. Residual strains were measured for each rock type using XRD methods, and strains were reported with magnitudes of up to 90 $\mu\epsilon$ in Tennessee sandstone, 250 $\mu\epsilon$ in Uinta Mountain quartz, and 200 $\mu\epsilon$ in Tensleep sandstone. Brazilian and point load tests were performed on Tennessee sandstone and Uinta Mountain quartz, and triaxial compression tests were performed on all three materials. To study the influence of residual strains on failure orientations, the magnitudes of residual strain were superimposed with the magnitudes of induced stress, and along with some known Mohr-Coulomb criteria and the maximum tensile stress, predictions of failure orientations were made. They noted that the tensile strengths of the materials determined by Brazilian testing had lower strengths at orientations matching the greatest tensile residual strain or with the least compressive residual strain. In their point load testing, they predicted the failure orientation that would occur by superimposing the residual strains and applied stresses, and the orientations aligned with the maximum net tensile stress. In their triaxial tests, they predicted the strike of the failure plane by superimposing the residual strains with the applied stress state and determined that it would occur at the net intermediate stress. With a knowledge of the entire stress state within the material, they concluded that residual strains were an influencing factor in the failure orientations, and this knowledge allowed them to successfully predict them.

Some implications of residual stress for rock-engineered structures such as mines, tunnels, or slopes are discussed by Varnes and Lee (1972). If new free surfaces are created in a rock mass, then the state of equilibrium is disturbed and can result in immediate or time-dependent residual stress mobilization. They state that if this occurs, then near excavated surfaces residual stresses will re-distribute faster than at a location deeper into the excavation face suggesting that they may have a size dependency. Concerning rock supports, they state that when residual stresses are mobilized, they can then do work on support structures and tunnel liners and can then influence their effectiveness. It is also stated that for in situ stress measurement, if the volume used for stress measurement is greater than the volume required for residual stress equilibrium, then the effects of residual stress would be none; but, if the measurement volume is less than the equilibrium volume, then residual stresses will influence the results. This relationship between stress measurement and equilibrium volume is also discussed by Tullis (1977).

In situ stress measurements in a Tully limestone located in New York were performed by Engelder and Geiser (1984) and anomalous readings were reported. The Tully limestone measured in this study interrupts thicker layers of clastic rocks and has a thickness of 1 to 7 m throughout. They performed in situ stress measurements on the surface near a creek bed, and a 25 m vertical cliff face existed 50 m away from the measurement location. A set of joints exists at their site with 5 m spacing, and five measurements were made within a single block isolated by joints to ensure the measurements were within the same rock unit. Overcoring of four door stopper strain measurement devices and one USBM device in 1 m deep holes was performed. Differential stresses up to 14 MPa were reported and given that the measurements were located on the surface, near a cliff face, and in a jointed rock mass, the readings were deemed too high for in situ stresses alone. The effects of moisture on the readings were dismissed due to overcoring below the water table and with drilling water temperatures near the groundwater temperature. Then they investigated the rock fabric as a reason for the anomalous strain readings but deemed that they were also an unlikely cause. It was then suggested that the anomalous readings were a measurement of released residual stress. The possibility for residual stress formation at that location with the reported magnitudes was investigated, and it was concluded that residual stresses could form within the given conditions and produce the stress magnitude measured in situ.

A sandstone core was retrieved from a depth of 5300 m and was used for residual stress investigations by Zang and Berckhemer (1989). The 66 mm diameter core was equipped with three strain gauges located radially in the center of the core, and three strain gauges located circumferentially along the outer boundary. A secondary overcore (overcoring the retrieved core) was then performed with a 30 mm diameter core barrel to mobilize residual strains. The strains illustrated an anisotropic contraction of the core where at an orientation of 45° the core contracted with a magnitude of about 50 $\mu\epsilon$, and at an orientation of 135° the core contracted with a magnitude of about 20 $\mu\epsilon$. P-wave velocities were measured on the large core prior to secondary overcoring, and on the small core after overcoring. These measurements confirmed the contraction of the core as the measured velocities decreased after overcoring as the contraction of the material would effectively increase its density and slow p-wave velocities. From the inner core, thin sections were cut for analysis and testing. A microscopic inspection was performed on one of the sections which determined the average strike of microcracks within the sample to be at 135°. When looking at the residual stress redistributions, larger contractions occurred at 45°, and therefore the larger magnitude can be attributed to the closing of open microcracks, as this orientation aligns with the normal to the microcracks. Other thin sections were used for point load testing and Brazilian testing. In the point load tests, consistent failure orientations occurred at 135° which was associated with the orientation of least compressive residual stress redistributions. Brazilian tests were performed with the load acting against both 45° and 135° orientations. When loaded against 45°, the tensile strength was about 12 MPa, and when loaded against 135°, the tensile strength was about 8 MPa. The 4 MPa increase in tensile strength can be attributed to the larger magnitude of compressive residual stresses acting in that orientation. This work illustrates some effects of residual stresses on measured properties of rock specimens in the lab.

A similar study to Zang and Berckhemer (1989) was performed by Zang et al. (1996) to continue investigating the effects of residual stress redistributions on rock specimens in the lab. Cores with 60 mm diameter were recovered from depths of 935 to 3747 m, and secondary overcoring was used to mobilize residual strains with a 30 mm core barrel. Six strain gauges were used on the top surface of the core with three located radially in the centre, and three located along the same radial directions but towards the halfway point from the core's centre and core's edge. Strains were reported in both extension and contraction with magnitudes of up to 220 $\mu\epsilon$. Crack orientation and p-wave velocity measurements were performed on the inner cores after secondary overcoring. Half of the results illustrated principal strain redistributions perpendicular to the average microcrack strike, while the other half illustrated principal strain redistributions parallel to the average crack strike. P-wave velocities were always well aligned with the average strike of the microcracks. This study further investigated the relationship between residual strain redistributions and the orientation of microcracks. While not all results agreed with the previous study in that residual stress redistributions are affected by microcrack orientations, it does provide further data on a relationship between residual stress redistributions and the opening/closing of microcracks.

In examining the Opalinus clay formation as a suitable material for the storage of nuclear waste materials, Corkum (2020) proposed residual stress as a mechanism for unexpected behaviour that occurred during excavation. Two mine-by experiments were conducted in the Opalinus clay formation with extensive instrumentation. Piezometers were monitoring pore pressure ahead of the excavation, and once it neared the sensors, a rapid drop in pore pressure was observed. The piezometers were located outside of the EDZ and therefore effects of plastic yielding were unlikely to be a mechanism responsible for the pore pressure drop. The author then proposed that residual stresses may be influencing the formation and/or aperture of microcracks near the piezometers which can result in a decrease in pore pressure due to the availability to transport the surrounding water. This concept was then applied in a simplified numerical simulation to compare to the physical results. When incorporating a release of residual stress due to excavating in their model, they had success in reproducing the rapid pore pressure drop that other simulations that do not consider residual stress have a difficult time reproducing.

2.6 Numerical Simulation of Residual Stress

The purpose of this section is to present existing residual stress simulations and the modelling methods that will be used for the simulation of residual stress in this thesis. Limited research using numerical models to study residual stress in rock have been discovered, but the available research is presented. In this thesis, 2D continuum, and 3D discontinuum micromechanical models are created using Voronoi structures to investigate residual stresses in rock mechanics. As such, background information is presented to discuss the use of continuum and discontinuum modelling methods, as well as some existing uses of Voronoi structures, and micromechanical models in the field of rock mechanics. The models presented in this thesis are based on a study of Garibaldi grey granite, which is presented here, and quantifies many aspects of the rock structure that are required to create a micromechanical model.

2.6.1 Existing Residual Stress Simulations

Residual stress formation in rock salts is a phenomenon examined from core samples, and numerical simulations by Aptukov and Volegov (2020). Cores of salt rock were taken from an underground drift used as a roadway at 350 m depth for study. Unloading the core (removal from in situ) resulted in the formation of damage which the author noted could be related to the residual stresses contained within it, and in some cases, core discing occurred during core preparation. Numerical simulations were used to investigate residual stress as a mechanism for damage. Rock salt cores were modelled using 2D simulations with three loading stages to produce residual stress. The modelled specimen had dimensions of about 40 mm in diameter by 80 mm tall, with an average grain diameter of 3 mm. In the first model stage, the simulated core was loaded in one of two directions simulating the loading in the roof and sidewalls of the roadway. The second stage involved simulating a time-dependent change in stress that occurs due to the addition of a roadway over a set time period (1 to 30 years), simulating the effects of creep within the rock structure. In the third stage, the loads were removed to simulate the removal of the core from in situ. It was noted that samples taken after 1 year at a depth of 1 to 3 m into the excavation had no initial damage, and residual stresses of up to 1.3 MPa were reported. After a simulation of 10 years, cores taken from the same depth were reported to have residual stresses of up to 2.3 MPa, with little damage reported. After a simulation of 30 years, samples from the same depth exhibited residual stresses up to 4.9 MPa and high levels of damage were reported. Compression tests were modelled on samples recovered after a simulation of 1, 10, and 30 years. It was noted that with an increase in modelled time, a strength decrease was observed, illustrating the varying levels of damage within the cores due to residual stress formation.

Rock salt specimens were collected from a 500 to 800 m depth in Pakistan to investigate their fatigue life (number of cyclic loads before failure) under triaxial cyclic loading by Fan et al. (2020). They noted that the fatigue life over numerous loading cycles was reduced with increasing magnitudes of the applied load. It was then hypothesized that residual stresses were formed within the specimen during cyclic loading which affected the internal stress field and thus influenced the results. To explore the possibility of residual stress formation during cyclic loading of rock salt, numerical investigations were used. They performed a Scanning Electron Microscope (SEM) investigation for their cores and determined that Magnesium Oxide (MgO) was a common impurity embedded within Sodium Chloride (NaCl). The MgO was reported to be much harder than the NaCl, therefore, variations in material stiffness were present. The NaCl matrix was assigned an elasto-plastic behaviour while the MgO impurity was assigned a purely elastic behaviour. The model was then loaded by applying force on the upper boundary, while the sides remained free, and the bottom was restrained in the direction of loading. As a result, plastic deformations occurred in the NaCl material surrounding the impurity, and after removal of the load, stresses up to 3 MPa remained in the plastic zones of the NaCl, while in the elastic NaCl and MgO impurity, the stresses completely dissipated. They concluded that the effect of time on the cyclic loading of rock salt cores can influence the results of their tests due to the progressive formation of residual stresses altering the internal stresses and displacements throughout testing. Other materials were simulated for both the host and impurity to further investigate the formation of residual stress, and it was noted that with larger variations in stiffness ($E_{matrix} - E_{impurity}$), larger magnitudes of residual stresses were formed.

2.6.2 Continuum, Discontinuum, and Micromechanical Simulations for New Residual Stress Research

The use of continuum and discontinuum numerical models for tunnel engineering is described by Barla and Barla (2000) and is discussed to provide a background for the use of each numerical model for rock simulation. In continuum methods, the rock mass is assigned an equivalent continuum which simplifies the rock mass into a single material that constitutes the larger rock domain. The equivalent continuum is then assigned properties that are measured from intact specimens in the lab which are scaled to the rock mass through the use of constitutive models. The domain is then assigned a constitutive relationship (elastic, elasto-plastic, strain-softening, strain-hardening, elastic-brittle, etc.) which governs the post-peak strength of the material. In continuum models, the boundary element (BEM) and domain element (FEM/FDM) methods are the two methods that can be used for simulation. Using BEM, the domain is simulated as a discretized excavation boundary contained within an infinite continuum. Results are obtained on the excavation boundary and within a specified domain of the infinite continuum. Using FEM/FDM, the actual geometry of the problem is simulated within a specified domain containing all pertinent structures, and then the entire domain is discretized to obtain results throughout.

In the discontinuum method, the rock mass is simulated as an assemblage of discrete blocks separated by interfaces within a specified domain. Joints, faults, or other geologic discontinuities are typically modelled as the interfaces between the discrete blocks, and both blocks and joints are assigned properties and constitutive models. When using this method, blocks are allowed to completely detach or separate from their neighbouring blocks, and the model continues to calculate the displacements of the separated blocks. After block separation, the model recognizes any new contacts that form (surface to surface, surface to edge, edge to edge) and continues to apply the desired strength in those regions. The discontinuum method differs from the continuum method in that complete detachment of blocks can take place, whereas, in a continuum method, no material separation can occur due to the assumption of an equivalent continuum even if joint elements are used. The appropriate selection of a continuum or discontinuum model to accurately interpret results for a given scenario depends upon the conditions that occur in situ. Using a continuum method to simulate a blocky ground with equivalent properties is not as accurate as the explicit simulation of the blocky ground that can be reproduced using discontinuum methods, but the continuum simulation can achieve results much quicker than the discontinuum simulation.

Brittle failure has been simulated using Voronoi tessellations in both continuum and discontinuum models, as well as with the particle flow code (*PFC*) by Potyondy and Cundall (2004). Damjanac (2008) uses a Voronoi structure in *UDEC* (a 2D discontinuum code provided by *Itasca*) to investigate the stability and damage surrounding a cavern under various loading conditions that could occur over 100,000 years as the cavern is to be used as a DGR for the storage of hazardous materials. Two cavern sizes are to be used for the storage of low, and intermediate-level waste materials, and the larger of the two is used for simulation. An array of caverns will be developed in situ, but numerically, only a single cavern is simulated due to the symmetry of the proposed design. Through the use of correct boundary conditions, the results will be equally as accurate as simulating all caverns but will take less time to compute the results. The model is loaded with in situ stresses of 18.3 MPa vertically, and 36.7 MPa horizontally. A Voronoi structure was simulated in the rock formation surrounding the cavern to simulate failure depths around the cavern. Although blocks in discontinuum models typically represent discontinuities, the Voronoi blocks used here are not representative of discontinuities within the rock mass but are instead used to provide regions where the rock can fail thus allowing for the modelling of progressive damage. The Voronoi properties (strength and stiffness for both block and interface) were calibrated for the rock by simulating UCS, direct tension, and triaxial tests. By implementing a Voronoi structure, the simulations were able to model progressive damage in the cavern walls illustrating the degree of damage that could be expected over the 100,000-year loading period.

As discussed previously, in continuum models, rock is simplified to an equivalent continuum. Using Voronoi structures in continuum models allows for the rock to be represented as either a series of variations in materials and geometry, or like in Damjanac (2008), it can be used to simulate brittle failure. Using Voronoi structures in continuum models allows for further analysis of rock strength than if the material is represented by a single equivalent continuum. Li and Bahrani (2021) used a Voronoi structure in a Wombeyan marble to simulate the fracturing of the material under axial compression. In their work, only one material was used for the grains (represented by Voronoi blocks), but due to the heterogeneous nature of the grain shapes, tensile stresses were generated which resulted in accurate representations of failure in unconfined, and confined compression tests. Sanipour et al. (2022) also utilized Voronoi structures in a continuum model to simulate brittle failure, but their work simulated the failure around the URL mine-by tunnel. The Voronoi structure in this research was not representative of grains but rather provided the model with areas that could yield, which illustrates damage more accurately than that of a typical continuum model. When implementing the Voronoi structure, they were able to reproduce damage around the tunnel, illustrated by the yielding of Voronoi blocks and block interfaces, and produced similar results to the actual damage profile measured at the URL. It should be noted that although the Voronoi structure allows for the modelling of brittle failure, it is still a continuum method, and therefore the blocks created by the structure can not physically separate. The separation that should occur is interpreted by the software which outputs displacements for the blocks as if they have or could separate. This acts as a source of error in Continuum Voronoi models, but under low levels of displacement/strain, the results can be similar to discontinuum simulations.

A hydro-mechanically coupled micromechanical model has been used by Farahmand and Diederichs (2020) to simulate the EDZ around circular tunnels. A Voronoi structure was simulated in *RS2* to create a specimen satisfying the conditions for a UCS test, and a Brazilian tensile test for Lac du Bonnet (LdB) granite. The simulated Voronoi structures were then exported from *RS2* and imported into *UDEC* for model calibration. A cohesive crack model was implemented, and the Voronoi structure was allowed to fail along the block (grain) contacts only, i.e., no grain failure occurred. The following calibration process was then applied to their simulations: First, the elastic and strength properties for the grains and contacts were calibrated to reproduce observed macro properties for UCS and Brazilian tests. Secondly, the initial and residual apertures of the interfaces were calibrated to reproduce the permeability of the material under various levels of deformation and damage. Finally, the contact apertures were refined so that their model produced similar poroelastic properties to their laboratory measurements. Their calibrated model was then used to simulate the EDZ surrounding the URL tunnel by inputting the calibrated micromechanical model as the material surrounding the tunnel. Using a micromechanical model to simulate damage, their model was able to illustrate the failure depth, the shape of damage surrounding the tunnel, and stress-induced pore pressure changes at the URL.

The model geometry and mineralogy used in this thesis are based on the Garibaldi grey granite reported by Griffiths et al. (2017), and the compression tests performed in their study were used for model calibration and as a means to investigate the effects of residual stress on samples with various levels of damage. In their work, they describe the mineralogy of Garibaldi grey granite as 45% quartz grains, 45% feldspar grains, and 10% mica grains. The geometry of the grains was described to be fairly homogenous in size with about 20 grains in the width of the sample (1 mm average grain diameter, 20 mm sample diameter). In their investigation on the influence of thermally induced damage on rock strength, they prepared 11 specimens in total: one un-treated, and 10 exposed to temperatures varying from 100 to $900°C$. Crack density measurements were then taken on these specimens to quantify the damage, and using a micromechanical model, they attempted to predict the rock strength based on the levels of damage. UCS tests were performed on the specimens after crack density measurement to create a data set that could be compared to their model predictions. In samples with damage originating from temperatures of $550°C$ or less, there was a fairly good agreement between their predicted and measured UCS, but in specimens damaged with higher temperatures, there was little to no correlation between the measured and predicted UCS. It was noticed that with increasing levels of thermal damage, increased magnitudes of crack closure strain were reported as well as an overall decrease in rock strength. This phenomenon was also observed in metamorphic rocks (Rong et al. 2018; Peng et al. 2019) and in sedimentary rocks (Li et al. 2021). An investigation into the effects of residual stress on specimens with various levels of damage is undertaken later in this thesis to determine if the release of residual stress can be associated with the evolution of crack closure strains with increasing damage.

CHAPTER 3 - RESIDUAL STRESS IN ROCK: INSIGHTS FROM CONTINUUM-BASED MICROMECHANICAL NUMERICAL MODELLING

A version of a journal paper submitted to the Bulletin of Engineering Geology on April 16th.
Status: Under review

3.1 Introduction

Residual stress is a phenomenon where a microstress field exists within the material's crystalline structure in a state of internal equilibrium independent from external boundary conditions (e.g., in situ stress field). Residual stresses are commonly observed in metallurgy and glass engineering fields and have also been observed to exist in rock as a result of complex geological processes. Although their presence in rock has been observed, they have been largely disregarded and considered to have negligible practical implications.

In the 1660s, a phenomenon was discovered in man-made glass specimens that were cooled rapidly in water where an increase in strength was observed, but also an increase in the brittleness of the glass upon failure. Further investigation into this phenomenon led to an understanding of the concept of residual stress, or stresses that remain locked into a sample, and through continued investigation, in the 1870s an application for residual stress was adapted in sheeted glass which would later be used for windscreens in vehicles around the 1930s (Brodsley et al. 1986). Researchers began understanding and adapting the concepts laid out in previous work, and in the 1940s a similar adaptation was provided for residual stress in the field of metallurgy, through the peening process (Maleki et al. 2021). Reaching the 1960s, research into the now well-documented residual stress phenomena began in the field of rock engineering (Voight 1966; Friedman 1967). Research progressed on this topic for nearly 40 years until the late 1990s to early 2000s, at which point, researchers noted the difficulty associated with achieving an in-depth understanding of residual stresses with the tools available to them at the time, and only limited studies were presented thereafter. However, studies on the topic continued largely in the fields of metallurgy and glass.

Figure 3-1 illustrates an approximate timeline for studies quantifying and investigating residual stresses in the fields of glass, metallurgy, and rock engineering.

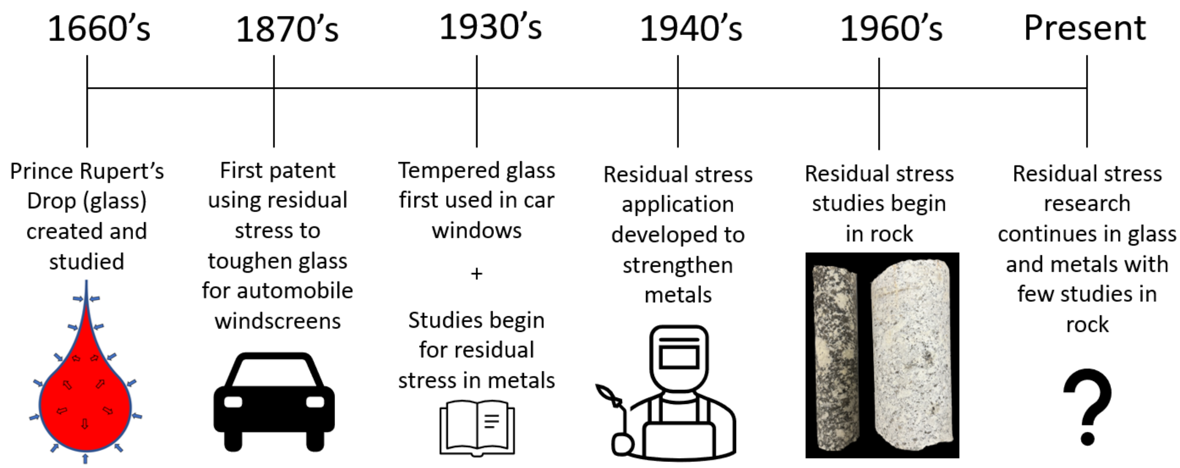

Figure 3-1 Residual stress research timeline for glass, metallurgy, and rock engineering fields

Due to the limited active research on the topic in rock engineering, a literature review is presented in this paper to formulate a comprehensive background on a topic seldom discussed in the field that presents previous research leading to the application of such stresses in other fields, as well as the major research that has been performed in the rock engineering field. Early studies quantifying residual stresses in glass and metals were investigated, and the applications for these stresses are discussed. In the field of rock engineering, these stresses are discussed more broadly to provide background information and an understanding of the concepts that are applied in the micromechanical investigation section of this paper. A few formation mechanisms for these stresses in rock are presented, and the existence of such stresses is discussed at various scales. The studies presented investigate the existence of residual stresses in singular grains constrained in the microstructure, up to the in situ scale containing a complex grain structure.

To explore residual stresses in rock, 2D continuum-based micromechanical numerical models were created using RS2 to investigate scenarios potentially related to residual stress. The first of which is the crack opening/closure effect in compression tests. For crack closure to exist, there must exist a prior state of open microcracks within the microstructure. Residual stresses are investigated as a potential mechanism responsible for opening microcracks in rock specimens by undergoing compression testing and examining the associated crack closure in their stress-strain curves. Residual stresses may also possess the potential to induce existing cracks to propagate, or for new cracks to form as a result of the redistribution of residual stresses present within a sample. To further explore a connection between residual stress and crack propagation, the influence of a residual stress field on the propagation of a slot cut under a direct tensile load is also investigated. A final simulation is undertaken related to the displacements produced by residual stresses surrounding a small-scale circular excavation in a rock block and the impacts these stresses may have on the anticipated results for designs that do not consider such stresses. These models were used to investigate potential implications for residual stresses in the field of rock mechanics. The focus of this investigation was not to perfectly recreate the complex and varied residual stress formation processes, but to provide insight into mechanisms that these stresses may be responsible for producing. Residual stresses were implemented using a simplified method that manipulates the Young's moduli of mineral grains to entrap strains and produce a residual stress field with magnitudes similar to those reported in the literature. As the discussion continues on the results of residual stress modelling, and the understanding of the concepts presented in the literature progresses, the topic becomes more complex with potential relationships to an increasing number of scenarios that currently cannot be accurately modelled with the methods and tools available to engineers and researchers.

3.2 Observations of Residual Stress

In the field of rock mechanics, limited publications have been found regarding residual stress, especially in the past 20 - 30 years. As such, a comprehensive background was provided on the concepts of residual stress, and the research performed in the field of rock mechanics. Residual stresses, also referred to as residual strains, exist within the microstructures of crystalline materials and are present when no external load exists. These stresses exist as a result of the partial dissipation of strains induced during previous loads associated with various geological processes. The entire magnitude of an induced strain is not recovered after external loads are removed, and a portion remains stored within the microstructure. Friedman (1972) states that residual stress fields are a product of "locked-in" and "locking" strains, where locked-in strains represent non-recovered strains from prior loading, and locking strains are those that prevent the complete recovery of the initial strain. As residual stresses are produced by the trapped residual strains trying to dissipate and relax, these terms are used interchangeably throughout this paper. In the following sections, a review of the literature on residual stress applications in glass and metal, as well as some formation mechanisms and quantifications of residual stress in rock are presented.

3.2.1 Materials Engineering Applications of Residual Stress

One of the earliest known residual stress observations is the Prince Rupert's drop (Brodsley et al. 1986). In the 1660s, glass baubles with intriguing properties were gifted to the King and would become an area of investigation for the Royal Society who would later term them Prince Rupert's drops. These drops are created when molten glass is dripped into cold water producing a large thermal gradient. As a result, these glass drops cool rapidly, hardening from the outside in. During cooling, the hardened outer layer acts as a shell, containing molten glass at the core. As the molten glass cools, it contracts, pulling inward on the already hardened outer shell inducing compressive stresses in it, and as cooling continues, the magnitude of compressive stress increases. Once the glass completely cools, a state of equilibrium is reached, and compressive stresses in the outer shell are balanced by tensile stresses at the core producing a residual stress field (Brodsley et al. 1986). Due to the large magnitudes of compression in the grains of the outer shell, the formation of tensile microcracks is resisted effectively increasing the strength. When Prince Rupert's drops break, the large magnitude of tensile stresses at the core are displayed as they rapidly disintegrate into small powder-like pieces. This process occurs due to disturbing the residual stress' state of equilibrium. The material attempts to re-equilibrate, and an internal redistribution of stress occurs which then overcomes the strength of the material and results in further damage, or complete sample failure (violent fragmentation).

A continuation of studies on Prince Rupert's drops led to an understanding of the residual stress formation processes that occurred. These processes were later adapted to large-scale glass projects and in the 1930s, the tempering process, first envisioned by principals exhibited in Prince Rupert's drops, was employed for use in windscreens (Brodsley et al. 1986). Tempered glass is used in many different areas for its increase in strength and its small fragment size during fracturing. The typical tempering process uses thermal methods, heating glass sheets to high temperatures and rapidly cooling them with cold air, a similar process to Prince Rupert's drops. An alternative method of chemical tempering can be used, where under this method a higher overall strength is obtained due to an increase in the magnitudes of residual stress (Gy 2008). The understanding of residual stresses derived from Prince Rupert's drop studies allowed material engineers to innovate new processes to intentionally use these stresses to strengthen glass products to achieve a functional advantage.

The concept of residual stress was also adapted for studies in the field of metallurgy. Throughout the manufacturing of metals, many processes such as exposure to large thermal gradients or strains induced by machining or metalworking occur that can result in the formation of residual stress. Like engineers using residual stress in glass to strengthen materials, engineers in the field of metallurgy have taken a similar approach to understanding these stresses and manipulating them to their advantage for applications such as aerospace engineering or power generation (Ulutan and Ozel 2011). Engineers in the metallurgy field have been able to derive processes for inducing residual stresses after the material has been produced. This process is the peening process. Peening can be performed by hammer methods, as well as shot or laser methods. The hammer peening process is applied during the welding of joints. While the material is molten, it is hit with a ball peen hammer until the weld has cooled which induces a compressive residual stress within the weld. To apply this process more broadly (i.e., to not only weld joints) the laser peening process was developed. This process uses the impacts of high-power density laser pulses to induce large compressive shockwaves that are capable of inducing local plastic deformations (Montross et al. 2002). This process results in compressive residual stresses forming on the surface that transition to tensile stresses towards the core of the material, like that of Prince Rupert's drops. The presence of compressive residual stresses on the surface of the metal aids in resisting the formation of tensile microcracks effectively increases the material's strength.

3.2.2 Geologic and Microtectonic Origins of Residual Stress

Residual stress forms when strains have been stored within a microstructure reflecting a history of induced stresses, whether induced physically (in situ loads, earthquakes, etc.), chemically (interaction of solutions within the microstructure) or by thermal methods. Throughout the long-term geologic history of rock, various events or processes may occur that induce a portion of residual stress. Researchers have described some of the mechanisms for the formation of residual stresses in rock as a result of geologic events (Russell and Hopkins 1972; Savage 1978; Holzhausen and Johnson 1979; Passchier and Trouw 2005). This section will provide details on some of the proposed mechanisms outlined in the literature that can lead to the development of residual stress in rock.

The cooling, or crystallization of magma under in situ stresses can lead to residual stress formation after rock crystallization occurs. An example of a similar process that can lead to the formation of residual stresses was illustrated in a laboratory setting by Friedman (1967). As part of their work, they examined if residual stresses could form and be measured as a result of cementing quartz grains under an applied load as a physical analogy to rock formation processes. The grains were randomly arranged in a cylindrical container and mixed with a binding agent. The samples were then placed in a loading frame under various magnitudes of axial stress, and the binding agent was allowed to cure. After curing, the samples were removed and the magnitudes of residual stresses within the grains were measured. Their results illustrated residual stresses, both compressive and tensile, were induced in the sample which allowed the residual stress field to equilibrate under the applied load. While the work of Friedman (1967) showed residual stress formations under artificial laboratory conditions, the concepts from their work can be adapted to a geologic setting to provide context for residual stress formations in igneous rocks. As these rock masses form when magma cools deep below the surface, the crystallization process occurs under large magnitudes of in situ stress. As the magma is deposited, it deforms, reacting to the in-situ stresses, and crystallizes in this state. This allows for a portion of the strain induced through the in situ stresses to be entrapped within the fully crystallized rock structure.

Interlocking occurs in metamorphic rock through plastic deformations that arise during metamorphism. Due to the complex geometrical configuration of the microstructure, the relaxation of local and neighbouring deformations is resisted leading to the formation of local residual stresses. When the interlocking of grain interfaces occurs in a system with crystallized, recrystallized, or cemented grains, these interlocking forces can contribute to the formation of residual stresses. Throughout metamorphism, reorganization of the microstructure occurs through various processes. In samples of Carrara marble, elevated stresses and temperatures were shown to lead to the re-organization of the microstructure (Molli and Helibronner 1999). After deformation ceases, recrystallization occurs within the microstructure, and metamorphic strains may be present in the newly crystallized structure. Metamorphism induces large strains through deformations and thermal gradients that can be entrapped during recrystallization leading to residual stress formations. Voigtlander et al. (2020) measured residual stresses in unrelated samples of Carrara marble using grain-based measurement techniques. Their results indicated that residual stresses were present, providing confidence that metamorphism and the processes it accompanies can induce residual stress. In sedimentary rocks, residual stresses can form as a result of cementation as illustrated by Friedman (1967), and discussed previously, due to similar interlocking processes. In situ, stresses force the microstructure to compact which leads to frictional resistances on the grain interfaces, and as in metamorphic rock, if interlocking occurs in conjunction with cementation, these processes can contribute to the formation of residual stresses.

In crystalline materials such as rock, a system of grains exists within their microstructures. Each grain is comprised of layers of crystal structures, and when overlain, creates the commonly seen grain structure. Within the crystal structure lies the atomic structure where internal deformation and creep mechanisms may occur leading to the formation of residual stress. Within the microstructure, there exists a lattice-preferred orientation, where the deformed crystal structure of a specific mineral grain will have a frequently occurring crystal lattice orientation. Lattice-preferred orientations typically accompany a structure that requires the least amount of energy to form (Mainprice and Nicolas 1989). When loaded, crystal structures deform elastically unless defects such as dislocation or gliding of atoms within the crystal structures occur. For residual stresses to be created, a permanent crystal deformation is required; otherwise, the deformation is purely elastic. For permanent deformation, a change in the relative position of the atoms comprising the crystal structure must occur. Under load, shear stresses in the atomic structure are induced. These shear stresses displace the atoms in the layers of the crystal structure. The atoms within each layer are bonded, but due to the shear stresses, the bonds between the layers break and re-bond which allows the crystal structure to creep (Passchier and Trouw 2005). This process is sometimes referred to as *crystal plastic flow*. Figure 3-2 illustrates the process of permanent internal deformations that can occur within a crystal structure.

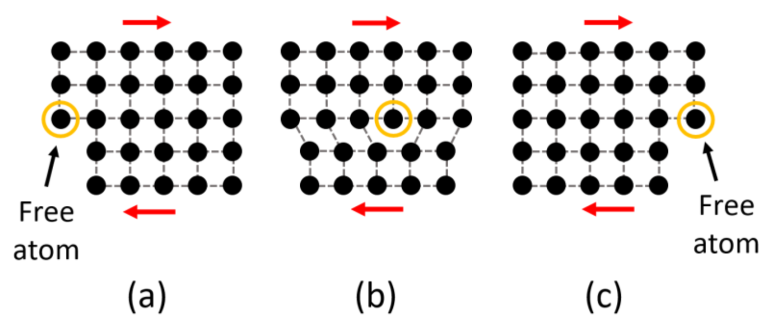

Figure 3-2 Crystal plastic deformations resulting in permanent strain. a) Undeformed crystal structure in its lattice-preferred orientation with a free atom. b) Deformed crystal structure undergoing displacement with a translation of the free atom. c) Deformed crystal structure in its lattice-preferred orientation with a displaced free atom. Modified after Passchier and Trouw (2005)

In Figure 3-2a, the crystal structure is undeformed and in its lattice-preferred orientation. Due to the applied shear stresses, Figure 3-2b illustrates the bond breakage and re-bonding of the atomic structure throughout the creep process. Finally, the crystal structure reaches its lattice-preferred orientation in a deformed state in Figure 3-2c. Once the crystal structure re-achieves the lattice-preferred orientation after deformation, the relaxation of such deformations is resisted due to the strong atomic bonds associated with the lattice-preferred orientation. These permanent strains due to crystal plastic deformations can then lead to the formation of a residual stress field as the atomic structure resists the relaxation of strains. The formation of residual stress through crystal plastic deformation can occur in each grain within the rock mass that is exposed to the required conditions. Overlaying the effects of grain-to-grain interactions and other residual stress mechanisms described earlier with the residual stresses from crystal plastic deformations, a complex and highly variable residual stress field can be produced within a rock mass.

3.2.3 Residual Stress Studies in Rock Engineering

Research on residual stresses in rock engineering began around the mid-1960s (Voight 1966; Friedman 1967). At this time, residual stresses were well documented in metals, and researchers were adapting residual stress concepts from literature in the metallurgy field (Russell and Hopkins 1972). Rock engineers, now aware of residual stresses, began investigating the potential for these stress formations in rock through experimentation and observations. The following section outlines some of the research on residual stresses in rock.

If residual stresses exist within rocks, then strains would need to be measured in samples that are free from external boundary loads. To determine if residual strains exist within the microstructures of rocks, X-ray Diffraction (XRD) techniques have been used. The XRD process, based on the fundamentals of Bragg's Law, measures internal strains constrained within a crystal structure. The crystal structure illustrated in Figure 3-2 can be used to explain how XRD is used for physical strain measurements. Horizontally, the atoms are bonded in a sheet-like structure. Vertically, the atoms within the sheet structures are bonded perpendicularly to the adjacent layers of atoms. The spacing between the vertical layers of atoms is known as the *d-spacing*; and as a result of induced stresses, the associated strains are reflected in the d-spacing. When exposing a crystal structure to an X-ray beam, the crystal structure diffracts the beam, and through scanning of the diffracted beams, a diffraction pattern is observed and interpreted for the measurement of d-spacings. These measurements can then be compared to known d-spacings for load-free conditions, and the current state of strain can be determined (Fitzpatrick et al. 2005).

As described in Chapter 3.2.2, the cementing of grains under in situ stresses can lead to residual stress. The cementing process constricts the grains and prevents their relaxation, and thus if the cement is broken, residual stresses (if present) should mobilize and result in measurable strains. Friedman (1967) investigated residual stresses contained within the grains of cemented sandstones using XRD techniques. The author's work consisted of breaking the cemented bonds by dripping hydrofluoric acid (HF) and monitoring changes in the d-spacing of a single grain using XRD techniques. A total of five cemented sandstone samples (three silica cemented, and two calcite cemented) from two separate locations were tested. The total number of drops of HF required to relax the grains varied by sample from a minimum of four drops, to a maximum of 25 drops. All five XRD measurements confirmed the presence of residual stresses within the grains of sandstone samples. Four samples measured extensional strains with magnitudes from 150 to 240 microstrains ($\mu\epsilon$), and one sample measured a contractive strain with a magnitude of 170 $\mu\epsilon$. This work presented some of the earliest observations of residual stress in rock and confirmed that residual stresses were present, at least within the grains, with non-negligible magnitudes. Other authors have also investigated the presence of residual stresses using diffraction methods. Measurements on samples from in situ, faults, and meteorite impacts have been performed with significant magnitudes reported in their studies as well (Wenk et al. 2020; Chen et al. 2015; Chen et al. 2011).

Through the use of diffraction techniques, researchers confirmed that residual stresses were constrained within the grains of rock specimens. As these stresses are self-equilibrating and exist under no applied load, the question arises as to whether these stresses can result in measurable strains due to coring methods, or if they can only be mobilized by completely removing the boundary constraints on any individual grain. Nichols (1975) explored the existence of residual stresses in a block of Barre granite by measuring the redistributions of residual strains using strain gauges as a result of concentric overcoring, i.e., overcoring the same position with an increasing core barrel diameter. The results of their study are discussed to build on the work of Friedman (1967) illustrating the effects residual stresses may impose on a larger scale specimen with numerous grains, as opposed to the stresses constrained within a single grain.

A nearly cubic block of granite was prepared from a larger master block excavated from the 67 m level at the Wetmore and Morris quarry to test for the presence of residual stress with no applied external boundary conditions. The work of Nichols (1975) followed three testing phases. In the first phase, residual stress redistributions due to concentric drill core cuts were examined. The second phase consists of a surface fabric investigation where the presence of newly formed microcracks was investigated with the aid of surface dyes. Finally, the third phase consisted of measuring residual stresses in a chip from the block using XRD methods. In their Phase 1 investigation, a total of three surfaces were cored. The top and bottom surfaces of the sample were equipped with 13 strain gauges oriented in a cross shape, and the right side of the sample was equipped with eight strain gauges in a circular pattern with a gauge in the middle. Concentric overcoring commenced on the top surface with a 5.1 cm diameter cut to a depth of just under half of the block's depth. Strain readings were taken continuously for three days, and after the stabilization of strain readings, a second 10.1 cm diameter cut was concentrically placed over the first. After another three days, the block was overcored for the final time with a 15 cm diameter bit. This process in its entirety was repeated on the bottom surface. On the right side only the 10.1 cm cut was drilled. With the addition of each cut, redistributions of residual strains were measured with magnitudes being the highest located near the freshly cut surfaces and decreased as the distance from the cut surface increased. This phenomenon was seen with each progressive cut, indicating the largest redistribution of residual stresses was located around the newly created free surface. The measured release of residual strains was within the magnitudes of 75 to 275 $\mu\epsilon$ in both compression and tension representing significant magnitudes of strain to be released from a block isolated from externally applied loads. The dyes applied to the surface in Phase 2 indicated that little to no microcracks were produced on the surface. Minor microcracking was reported near the freshly cut surfaces which may be a result of residual stress redistributions, sample disturbance from during drilling, or a combination of the two. The XRD measurements taken in Phase 3 confirmed the existence of residual strains with magnitudes of up to 250 $\mu\epsilon$. In their work, Nichols (1975) illustrated the existence of residual stresses constrained within a laboratory scale sample through redistributions that occurred as a result of drill cuts releasing local residual stresses.

Other coring methods to relieve residual stresses, such as spot undercoring, have been used to examine the potential for measured strains in a rock block specimen. Bock (1979) proposes that most, if not all residual stress measurements come from specimens that are retrieved from in situ stresses. A research question was then proposed as to whether or not residual stresses could be measured in specimens that had been separated from the rock mass over geologic time, or if residual stresses are time-dependent and dissipate over long periods. To examine the time-dependency of residual stresses, spot undercoring was used in a specimen taken from a basaltic column rock mass which had been separated from surrounding units by tensile joints and was proposed to be separated over long periods of time, if not since its formation. The undercoring method was chosen to examine the residual stress state, as it was the least disruptive method and measurements could be taken throughout drilling. The author used a special rosette, adapted from undercoring measurements in metallurgy, equipped with three strain gauges centred around a pilot hole for drilling. A total of 24 core cuts were made in the sample, and redistributions of strains were measured for 24 hours following all cuts. Drilling released residual stresses from within the sample with magnitudes varying from 12.6 MPa in tension to 15.2 MPa in compression. The author concluded that residual stresses were present in samples that had been separated from a host rock for geologic time, with significant magnitudes of released residual stresses. In both undercoring and overcoring scenarios, the existence of residual stress at the specimen scale has been proven to exist with non-negligible magnitudes.

Residual stresses are present when removed from in situ, and therefore it can be assumed that these stresses are also present in situ. Investigating in situ residual stresses determines if they exist in a specimen from micro (microstructure) to macro (geologic) scales with non-negligible magnitudes. Measuring residual stress in situ follows a similar process to concentric overcoring. A strain gauge rosette must first be secured in a borehole and then initially overcored with a larger bit to remove in situ stresses. After the complete relaxation of the rock surrounding the strain gauge, a secondary overcore, smaller than the first, is made to relieve residual strains. Engelder et al. (1977) used this process in their investigation of a Barre granite rock mass, the rock studied by Nichols (1975) and known to contain residual stress at the specimen scale, and in some surrounding metasediments by first overcoring with a 15.2 cm diameter bit to relax in situ stresses, and then a 7.6 cm diameter overcore to measure residual strains. A total of three separate locations were chosen to perform in situ measurements in Barre granites, and all strain measurements were performed within 150 m of the nearest lip on the surface of the quarries. In their measurements, the author illustrated that residual strains could be measured in situ with significant magnitudes of up to 1350 $\mu\epsilon$ measured in metasediments, and up to 25% of the initial overcore in Barre granite. It was noted that residual strain measurements were not consistent with location. Some measurements were recorded having as little residual strains of 25 $\mu\epsilon$ suggesting the local residual stress scales that satisfy the equilibrium conditions can vary significantly upon the location of the measurement. Engelder and Sbar (1977) in a similar study examined residual stresses in situ in sandstone outcrops. In this study, the same concentric overcoring process was used. Residual strain measurements were lower in the sandstone outcrops than those of the previous study, but nonetheless, the presence of residual stresses in situ was illustrated.

Another in situ residual stress measurement program was performed at the well-documented Underground Research Laboratory (URL) in Manitoba Canada (Lang et al. 1986; Read 1990). Using the same overcoring methods to measure in situ residual stresses, Lang et al. (1986) and Read (1990) quantify the magnitudes of residual stresses at the 240 m level. Lang et al. (1986) used triple overcoring with an initial overcore diameter of 200 mm to remove the in situ stresses, followed by 150 mm and 96 mm concentric cores to quantify the magnitudes of residual stress. Two separately oriented boreholes were used, and each borehole was equipped with three strain cells. The residual strains at the measured location had a low magnitude of about 1 MPa. The study of Read (1990) acted as a sort of check for the residual strains measured just a few years earlier. Overcoring was performed with core diameters ranging from 600 mm to 96 mm with a minimum of two secondary overcores being performed in all measurements. The second study confirmed that the magnitudes of residual stress at the measured locations were indeed low with magnitudes of about 1 MPa. The presence of residual stresses in situ is the main finding regardless of the magnitude, as Engelder et al. (1977) showed residual stresses have spatial variability with local highs and lows due to the volume of rock that results in the local equilibrium of residual stress.

Residual strains have been proven to exist at different scales within rock specimens. Literature quantifying relationships between the residual stress field contained within the microstructure of a rock, and the macro properties that can be measured under laboratory, or in situ conditions are reviewed. The work of Zang and Berckhemer (1989) quantified residual stress magnitudes from sandstone samples using secondary coring methods and related them to macro properties measured in the laboratory. Calcite cemented sandstone samples were initially cored and retrieved from 5300 m depth for testing. The core was equipped with a total of six strain gauges, three on the top center of the sample and three on the exterior. Secondary overcoring, or overcoring the core retrieved from depth, was performed with a 30 mm core bit on the 66 mm diameter initial core. The results from their strain measurements indicated that the interior core had contracted anisotropically, with the maximum contraction at an orientation of 45° and the least contraction at 135°. P-wave velocity measurements were performed on the sample before and after secondary overcoring. The measurements confirmed the strain gauge's results in that the inner core had contracted. The p-wave velocity measurements indicated a slowing of the waves after secondary overcoring which likely occurred due to the contraction of grains in the microstructure. Through microscopic inspection, the author was able to identify the average strike of microcracks which were preferentially aligned with a 135° orientation. The closing of microcracks as a result of residual stress redistributions is a likely cause for the increase in contraction at the 45° orientation as this orientation is normal to the microcracks average strike. After inspection, thin sections from the inner core were cut for fracture testing to determine if a preferred failure orientation was observable. Performing Brazilian tests on discs oriented at 45°, and 135° illustrated that when loading against the least compressive residual stress redistribution (135°) a tensile strength of nearly 8 MPa was measured compared to the tensile strength of nearly 12 MPa measured at the 45° orientation. In point load tests, loads were applied to the center of the disc allowing them to fail in their weakest orientation. Similarly, the failure orientation was consistently aligned with the least compressive residual stress redistribution (135°). Zang et al. (1996) continued the work laid out by repeating a similar process on multiple samples. Their work produced similar results in p-wave velocity and crack analysis, but fracture tests were not performed. In both of these works, residual stresses, or more specifically, the redistribution of residual stresses, could be seen to influence the measured macro properties that are used by engineers for their design.

Corkum (2020) analyzed claystone as a potential host formation for the storage of nuclear waste. In the analysis, an unexpected rapid decrease in pore pressures occurred as a result of the excavation nearing the pore pressure sensors. It is mentioned that a dilatational behaviour may result in the occurrence of a rapid pore pressure drop, but as the location of the sensors was outside the excavation disturbed zone, this process alone was unlikely to explain the observations. As excavation-induced damage was not occurring in the areas of the sensors, an alternative mechanism was proposed in that residual stresses may be influencing the observations. The author proposed the redistribution of residual stresses as a result of excavating could overcome the tensile strength of the clay stone, resulting in the formation, and opening/dilation of local microcracks. The newly formed dilational microcracks provides a mechanism for the observed rapid pore pressure drop in areas where it was unexpected.

The largest contribution that research has illustrated for residual stress is that these stresses do exist within rock. Numerous rock types have been used in residual stress investigations, and the studies have proven their existence in all. This illustrates that these stresses are not a result of a single rock formation method, but rather they can be created through various geologic processes that result in the formation of different rock types. In studies that quantify residual stress, various measurement methods and techniques have been used. This provides confidence that these stresses are not an artifact of a single measurement technique, but rather that they can be measured with comparable magnitudes using different methods. The reported magnitudes of residual stresses and strains are non-negligible, and have been illustrated to have spatial variability within rock. Through the analysis of existing literature, the effects of residual stress fields have been shown to have clear implications in the macro-effects of rock, and rock-like materials.

3.3 Micromechanical Modelling Investigation of Residual Stress in Rock

Current practice in rock mechanics and rock engineering does not consider residual stresses in rock behaviour, but their existence and mobilization may impact the mechanical and hydromechanical behaviour of rocks. For such reasons, the purpose of this study was to include residual stresses in different modelling scenarios to illustrate potential effects of residual stresses on modelling outcomes. Through the use of 2D continuum-based micromechanical numerical models, implications for residual stresses in rock were explored. A hypothetical residual stress field was implemented with magnitudes similar to those of literature observations using a simplified method. Accurately recreating all mechanisms for residual stress formation is not possible with the current understanding and numerical implementation of residual stress. The following section presents the justification of the selected modelling method and the processes used for model formulation, as well as presents results for numerical investigations containing residual stresses. RS2 models were used to investigate modelling scenarios related to crack closure in compression tests, microcrack formation and propagation due to the redistribution of residual stresses, the influence of a residual stress field on the propagation of a slot cut under a direct tensile force, and the displacements associated with a residual stress field surrounding a small-scale excavation in a rock block. The results were then analyzed and compared to model scenarios without residual stress to determine if there were any differences in modelled results. If differences were observed, residual stresses would be the cause for discrepancies suggesting that such stresses are not negligible in rock behaviour. It is important to note that the modelling studies presented within this section were not intended to recreate literature findings, but to use residual stress as a potential mechanism to describe common observations.

3.3.1 Modelling Methodology

3.3.1.1 Overview of Modelling Approach

Micromechanical models are used when the scale of an object can be enhanced to visualize the micro-components that constitute the macro-structure. These models are used to investigate the behaviour of the micro-components and their effects on the macro-behaviour of a material. Micromechanical models have been used in the field of rock mechanics by numerous authors (Potyondy and Cundall 2004; Damjanac 2008; Farahmand and Diederichs 2021; Sanipour et al. 2022). Farahmand and Diederichs (2021) investigated the behaviour of a hydro-mechanically coupled rock specimen under various loading conditions. In their work, grain-based models were used to simulate laboratory tests for their model calibration, and large-scale excavation-induced brittle damage. Their work illustrated that the interaction of the micro-scale behaviours produced the emergent observed macro-scale behaviours. Therefore, the use of a micromechanical model to represent the grain structure of rock specimens to investigate the interaction of micro-scale stresses (a residual stress field) is justified.

As the micromechanical models will be created using a continuum-based approach, the models are limited in the physical separation of materials. Within this study, the separation of materials was likely to occur as the models represented a granular structure and thus the associated grain boundaries had potential for relative movement. While this was a potential source of error within the models, the displacements and thus the strains of the separating grains were expected to be relatively low. In addition, while this study was mainly concerned with the presence of residual stress and its impacts on the outcomes of modelling, subtle variations in the magnitude of displacements and strains were negligible on the outcomes. The use of continuum-based models to simulate grain-based structures has been performed by Li and Bahrani (2021) to simulate the brittle failure of rock. While in this study brittle failure was not generally an area of concern, the model formulation and methodology were similar to their work in the application of a continuum-based Voronoi model to simulate discontinuous processes. Although a discontinuum model is more likely an accurate representation of the physical processes illustrated by modelling, advances in continuum modelling methods have allowed for the use of such models to produce comparable results to discontinuum methods under small strains. Therefore, for this study, the use of a continuum-based model was valid due to the small strains, but the associated error with employing this method should not be entirely disregarded.

The model geometry and properties used within this study were based on the work of Griffiths et al. (2017) as they had quantified many aspects of a rock required to reproduce a realistic sample for numerical use. Their work provided detailed microstructure measurements such as grain size and mineralogy for samples of Garibaldi grey granite from British Columbia, Canada. In their work, samples were exposed to various levels of thermal damage ranging from room temperature (no damage) to 900°C, which resulted in the formation of microcracks. After thermal treatment, multiple measurements were taken to quantify the level of damage, such as crack density and UCS test measurements. Due to the detailed measurements and description of the microstructure, the formulated model geometry and mineralogy were based on the rock type presented in their work, and their UCS testing was used as a source for model calibration.

3.3.1.2 Model Setup

Models were created using Rocscience's 2D continuum software, RS2. Within RS2, joint elements can be used to represent structural discontinuities in a rock mass (Rocscience, 2023). If the representative elemental volume (REV) is enlarged to the grain scale, then it is reasonable to assume that joint elements can be used to describe the grain boundaries in a Voronoi structure, as at that scale, grain boundaries are representative of structural discontinuities. Using the Voronoi feature, grain-based models were created to represent the microstructure of rock. Figure 3-3 illustrates the typical Voronoi model used in the analysis of residual stress implications.

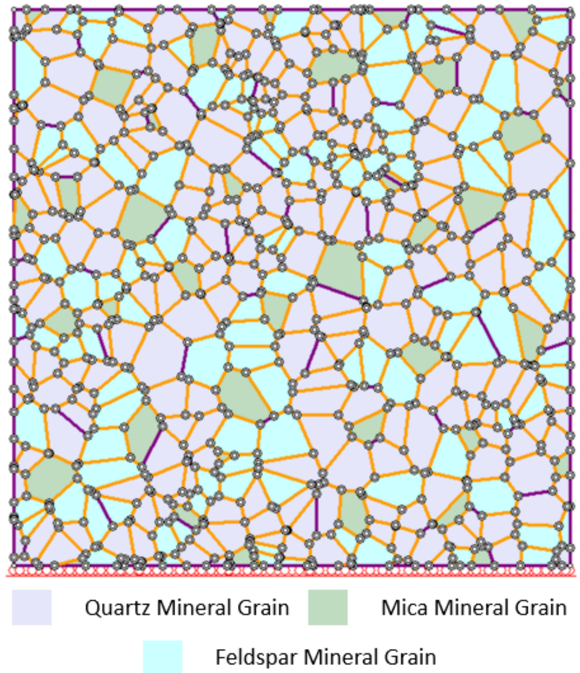

Figure 3-3 Micromechanical model of rock represented by a Voronoi geometry created in RS2 for the investigation of residual stress under various modelling scenarios

The micromechanical model illustrated in Figure 3-3 consists of a system of joint boundaries that divides a total of three mineral types. The model's external boundary is 1 m square and is scaled to be representative of a granular structure. The size of the irregularly shaped grain elements were scaled to those of Griffiths et al. (2017) ensuring the number of grains reported across the width of the sample in their work was similar to the model input, effectively creating a scaled model geometry representative of their 20 mm diameter specimen with appropriately sized grains. The mineralogy of Garibaldi grey granite was described by Griffiths et al. (2017) as 45% quartz, 45% feldspar, and 10% biotite mica grains. Each grain within the model was randomly assigned one of three materials by manual selection to blocks produced by the Voronoi structure, and measurements were taken to determine the distribution of minerals. Adjustments were then made until the modelled mineralogy was representative of Garibaldi grey granite. It is important to note that the model geometry used here is a zero porosity system and is a reasonable representation of low porosity granites, and any porosity within the model is a result of grain boundary separation. Within RS2's software, when using joint systems, the end condition of joints must be specified as "open" or "closed".

When setting the condition to open, the joint is represented by two nodes on each end which allows the joint tip to open and close relative to the position of the opposing node. As grains of rock can displace relative to each other, the open condition was set as it was the best description for the actual physical processes that occur and are illustrated by the circles at the end of each joint element seen in Figure 3-3.

Within the models, two types of joint elements were used. The joints were either assigned as grain boundaries (illustrated as orange lines) or crack elements which are the residual strength properties of the intact grain boundaries (illustrated as purple lines). A total of three model geometries were created based on the work of Griffiths et al. (2017) for future residual stress analysis under various levels of sample damage. The first and simplest model geometry contained three materials for grains and only grain boundaries (i.e., the crack density was zero). The second model geometry was based on their undamaged sample and was termed the “low crack density” geometry. This model contained three materials for grains and contained both cracks and grain boundaries for joint elements. Crack elements were arbitrarily distributed throughout the model by manually selecting and assigning cracks to joint elements without following any pattern to ensure their selection was as random as possible. Through the use of digital image processing using Mathematica software (Wolfram 2023), the crack density of the modelled geometry was measured and compared to the author's measurements using the following equation provided by Griffiths et al. (2017): $\gamma = N_A c^2$; where γ is the 2D crack density, N_A is the number of cracks per unit area, and c is the average crack half-length. Adjustments were then made to the modelled crack density until a reasonable depiction of the crack density was achieved. It is important to note that the crack density measurement methods employed depend on the number of cracks as well as their lengths, and as such, crack densities can vary largely. In samples with a low number of long striking cracks, the crack density reported may be larger than a sample with numerous small striking cracks. The third and final model geometry termed the “high crack density” geometry, was based on the measured crack densities from damaged samples in the range of 600 - 900°C. This model geometry contained three material types for grains, and both cracks and grain boundaries for joint elements following the same crack density measurement process as used in the low crack model geometry to correct to the author's measurements.

For all modelling scenarios, the geometry was meshed with uniform six-noded triangular elements resulting in a total of approximately 12,000 elements. The model was then calibrated. This process was performed on the stiffness of the grain and joint elements, and on the strength of joint elements to produce similar peak strength and bulk stiffness to that of Griffiths et al. (2017). Within the model, the grain elements were set to behave elastically, and the joint elements were set to allow for a plastic-brittle behaviour following a Mohr-Coulomb criterion. The initial elastic mineral properties were based on typical properties obtained from Mavko et al. (2020). To reduce parameters for calibration, some assumptions were used for grain interface properties. The first assumption was that the post-peak cohesion and tension had zero strength. The second assumption was a joint normal-to-shear stiffness ratio of 2 existed within the rock. The final assumption was that the crack elements were purely in a post-peak state. Therefore, their stiffness was lower than those of grain boundaries, as crack elements will have similar stiffnesses to naturally formed rock joints. The bulk material stiffness was the first calibration target. An iterative process was undergone increasing the joint element stiffnesses until the model became numerically unstable, i.e., a sporadic stress-strain response and premature yielding of all joint elements, and then increasing the grain stiffness until the model numerically restabilized. This process was performed until a target modulus of elasticity of approximately 70 GPa was measured from the simulated stress-strain curve. After the calibration of stiffness parameters, the model's peak strength was calibrated. Starting from the initial parameters, the properties were slightly increased until a peak strength of approximately 280 MPa was reached. This process was repeated with the intact cohesion, tension, and friction angle as the main calibration targets. The calibration of strength properties was prioritized in the pre-peak phase, and proper calibration of the post-peak parameters was not performed as the majority of the parameters were governed by the assumptions mentioned above. Tables 3-1, 3-2, and 3-3 below show the initial, and calibrated properties for elastic grains, plastic grain boundaries, and plastic crack elements, respectively.

Table 3-1 Initial and calibrated elastic grain properties

Property	Value suggested by Mavko (2020)	Calibrated value
Quartz: ν	0.07	0.07
Quartz: E (GPa)	96	340
Feldspar: ν	0.35	0.35
Feldspar: E (GPa)	69	250
Biotite: ν	0.21	0.21
Biotite: E (GPa)	85	300

Table 3-2 Initial and calibrated plastic grain boundary properties

Property	Initial value	Calibrated value
Tensile strength (MPa)	10	28
Residual tensile strength (MPa)	0	0
Peak cohesion (MPa)	50	110
Residual cohesion (MPa)	0	0
Peak ϕ (°)	35	55
Residual ϕ (°)	35	55
K_n (MPa/m)	100,000	1,800,000
K_s (MPa/m)	50,000	900,000

Table 3-3 Initial and calibrated crack element properties

Property	Initial value	Calibrated value
Residual tensile strength (MPa)	0	0
Residual cohesion (MPa)	0	0

Residual ϕ (°)	35	55
K_n (MPa/m)	100,000	180,000
K_s (MPa/m)	50,000	90,000

3.3.1.3 Residual Stress Initialization Methods

Residual stresses represent long-term geological processes that can be difficult to accurately depict within numerical models. Such processes could involve the solidification of magma, the recrystallization of strains accumulated throughout its loading history, or other geologic processes. As the objective of this study was to investigate the effects of residual stress in rock mechanics models, the goal was to create a reasonable representation of a hypothetical residual stress field. For this reason, two simplified methods for creating self-equilibrating residual stress fields with magnitudes similar to those reported in the literature were investigated.

The first method was based on the storage of plastic strains in grain boundaries as a result of in situ stresses and crack sliding. This method is a simplified representation of the formation of in situ microcracks, simulated through the staging of grain boundary properties. The storage of residual stresses within the interfaces occurs as a result of crack sliding and their residual strength (friction only), as well as interlocking forces due to the distribution of grains to prevent the complete relaxation of the crack interface, thus locking-in residual stress. The presence of residual stress using this method was investigated using the low crack density geometry described earlier. The model was set up using four stages to create the residual stress field. In the first stage of the model, the geometry was created, and the model properties were applied with staged crack element properties. The properties were stages so that during the first two stages, the crack elements would have intact grain boundary properties (illustrating a crack free material), and then at the third stage, the properties would change to crack element properties (zero cohesion and tension) representing the formation of in situ microcracks. The second model stage applied a bi-directional isotropic stress of 50 MPa through stress boundaries along both the sides and top boundaries, and a roller boundary was placed on the bottom. In the third stage, the transition from grain boundary properties to crack element properties was applied to the crack elements while the in situ stress remained acting along the external boundaries. In the fourth and final stage, the in situ stress was removed creating free boundary conditions on both the sides and top boundaries, and the model was investigated for the presence of residual stresses. Figure 3-4 illustrates the resulting residual stress field with maximum stress magnitudes varying from nearly 30 MPa in tension to upwards of 70 MPa in compression with stress concentrations surrounding the crack elements. This residual stress method was altered to induce higher average magnitudes. To increase the magnitudes, higher in situ stresses were applied to induce larger plastic strains on the joint interfaces that could be stored. Due to the increased stress magnitude, model instability occurred and therefore, the second method for creating residual stresses was adopted.

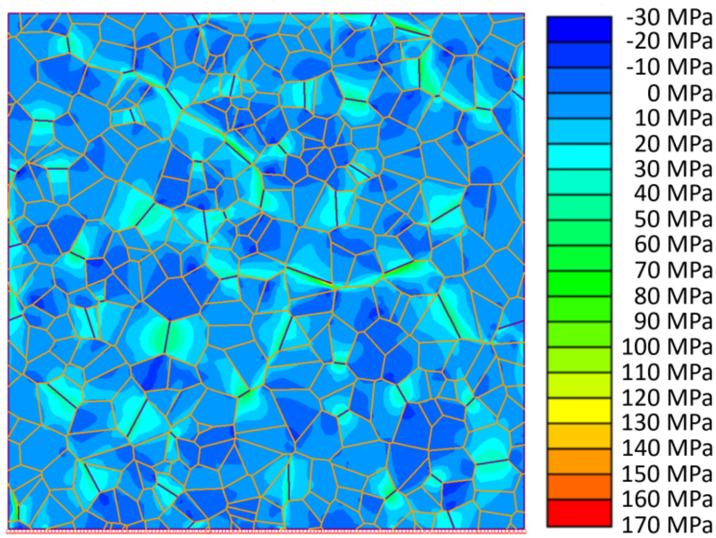

Figure 3-4 Plot of residual stress field (contours of σ_1 are shown) from the storage of plastic strain in joint elements due to in situ stresses and residual interface strength

The second method, consisting of Young's modulus manipulation, was based on the storage of elastic strains within the grain's model zones. While employing this approach, the residual stress formation method is similar to the solidification of magma under in situ stresses, but may also be representative of recrystallization or cementation processes under in situ stresses. As magma is a viscous fluid, its resistance to stresses must be lower in this state than if it were hardened. Therefore, staging the elastic modulus can be applied to simulate the hardening process. As igneous rock is stiffer than magma, strains can be trapped within the microstructure due to the limited rebound that occurs after cooling with the increase in stiffness. Figure 3-5 illustrates how strain from the initial load could be trapped within the microstructure and only partial dissipation of the initial strain occurs resulting in a residual stress field.

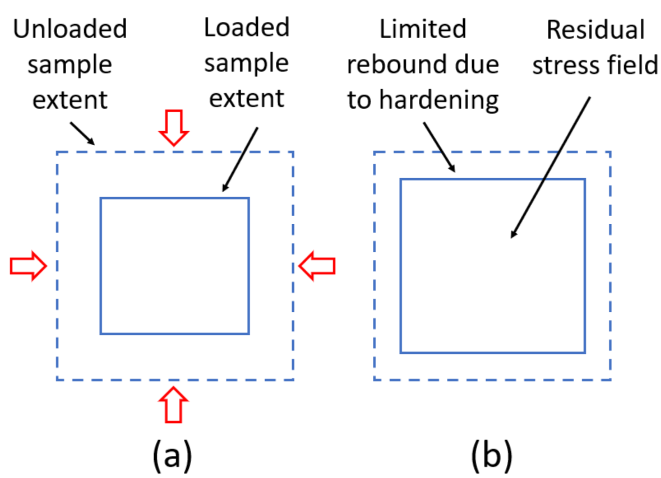

Figure 3-5 Depiction of the Young's modulus manipulation process used for the creation of residual stresses. a) Deformed sample under in situ stresses with a lowered Young's modulus to represent a magmatic state. b) Partial relaxation of the initial deformation due to an increase in Young's modulus entrapping strain in the microstructure illustrating the solidification process

Using the low crack density geometry and taking advantage of the staging feature, the presence of residual stress using the Young's modulus manipulation method was investigated. Residual stresses were induced in the model by staging the elastic moduli for each grain material simulating the hardening process for each mineral. The manipulation of the elastic modulus was performed through the staging of the modulus. The materials representing mineral grains were staged so that in the initial stages, the elastic moduli were 35% of their fully hardened value, and at a later stage, the value would change to the typical hardened value. For each mineral, the reduced and full Young's moduli illustrate the "soft" and "stiff" states respectively throughout the cooling process. This method also uses a similar process to the first method in that the crack elements were staged to have intact grain boundary properties during the initial loading, and at a prescribed stage, the transition in grain boundary to crack element properties was undergone. The model was set up over five stages, and in the first stage the geometry was created, and the material properties were applied. In the second stage, an in situ stress was applied to the left, right, and top boundary using displacement boundaries of 2.5 mm with a roller restraint boundary on the bottom. In stage three, the in situ stresses remain acting on the boundaries, and the transition from the mineral grains soft, to stiff state was applied. In the fourth stage, the displacement boundaries were removed from the sample and a residual stress field was produced within an intact sample. In the fifth and final stage, the crack element properties were transitioned from intact to crack properties and thus a micromechanical model containing residual stresses and a pre-described level of cracks now existed. Figure 3-6 illustrates the residual stress field produced from this method with magnitudes that are more distributed throughout the model with no zones of stress concentrations compared to the results of Figure 3-4.

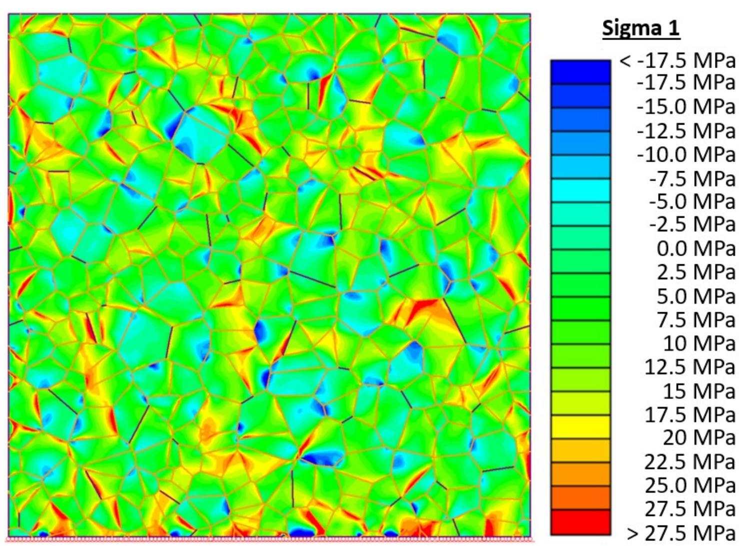

Figure 3-6 Plot of residual stress field (contours of σ_1 are shown) from the storage of elastic strains in grains as a result of hardening under in situ stress

Repeating this method with increased and decreased magnitudes of displacement boundaries allowed for various magnitudes of residual stress fields to be created. As this method was the most versatile, it was adapted and used for future modelling with residual stress. All modelling scenarios presented in the following sections will implement the described geometries, and residual stress with the Young's modulus manipulation method. Detailed descriptions of the methods used for each specific modelling scenario will be presented at the start of each of their respective sections.

3.3.2 Residual Stress as a Mechanism for Microcrack Opening

Research has shown residual stresses (a distributed microstress field) can have observable macro effects on rock specimens (Zang and Berckhemer 1989; Zang et al. 1996). Griffiths et al. (2017) in their work with thermal damage indicated that with increasing levels of damage, or an increased presence of microcracks, increased magnitudes of crack closure strains were observed. While this study was not concerned with residual stress, their results could be interpreted with an understanding of it. The question arises as to how increased levels of crack closure strains with increasing damage could be measured when there are no applied stresses to maintain an open state of microcracks. An investigation into residual stress as a potential mechanism for open microcracks was undertaken in this section by applying compression tests to samples with varied levels of pre-existing damage and residual stress magnitudes.

Low crack density and high crack density model geometries were used to investigate the effects of residual stresses with equal magnitudes on samples with varied levels of pre-existing damage. These models were built upon the existing residual stress formation model by adding a compression test staged to take place over 22 additional loading stages. The compression test was performed by using a displacement boundary along the top of the sample, a roller boundary on the bottom of the sample, and staging the magnitudes after the formation of residual stresses was complete. In the early stages of loading, the load step was small to capture crack closure strains accurately. The model samples were loaded to their peak stress and finished loading in the early post-peak stages. To create stress-strain curves from the modelled results, a query of 200 points was taken along the top of the sample to achieve an average stress throughout loading. This stress value was calculated for every stage and correlated to strain, which was determined as the magnitude of applied displacement at the top boundary for each respective loading stage. Figure 3-7 illustrates the stress-strain curves produced from compression testing for both low and high crack-density samples, and the modelled results were plotted with those of Griffiths et al. (2017) to determine if including residual stresses could produce similar shaped stress-strain curves to those of other compression tests with known crack closure strains and various levels of pre-existing damage.

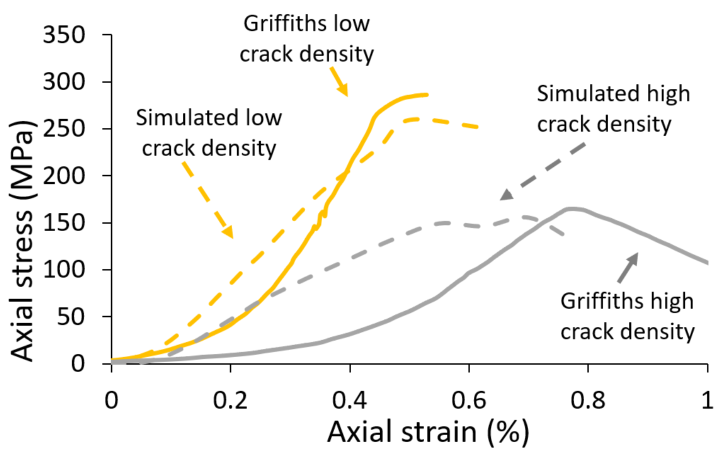

Figure 3-7 Effects of varied levels of existing damage with residual stress on the shape of the stress-strain curve from compression testing

The magnitude of residual stress within the sample was varied to examine the impacts on the stress-strain curves produced in the same manner as previously described. A baseline model was created following the processes laid out for the previous compression tests with residual stress, but no manipulation of Young's modulus occurred. As a result, a sample containing no residual stress was produced, while still undergoing the same loading and unloading processes in each stage. To compare the effects of residual stresses being present, three average residual stress magnitudes were produced. Low, intermediate, and high magnitude residual stress fields were created with average magnitudes of 4.5, 8, and 8.8 MPa, respectively. It should be noted that the magnitudes of residual stress could not be increased past the current maximum level with the current model configuration. Further increasing the residual stress magnitudes resulted in model instabilities that would occur during compression testing, and therefore no further increase in the magnitude of residual stresses was attempted. Figure 3-8 illustrates the results from modelling compression tests on samples with low crack density and varied levels of residual stress magnitudes.

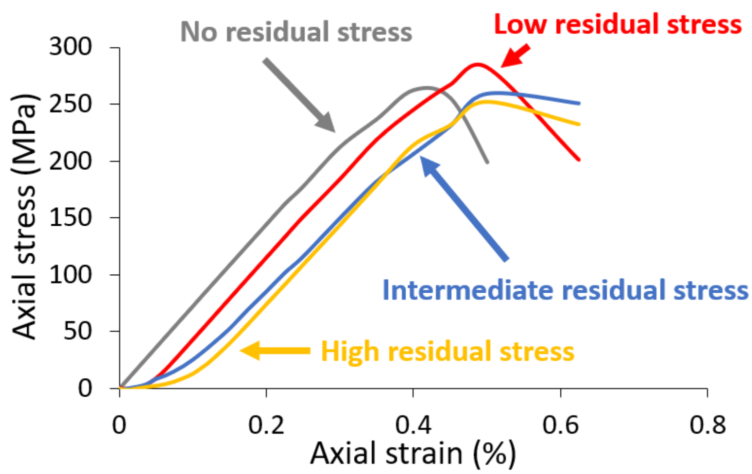

Figure 3-8 Effects of varied levels of residual stress magnitudes on the shape of the stress-strain curve from compression testing

The presented modelling results indicate that with increasing magnitudes of residual stress, the magnitude of crack closure strain increases. To further examine the effects of residual stress on crack closure strains, a distribution of the normal displacements for all joint elements was created. By selecting all grain boundary and crack element interfaces and exporting their data at respective stages, histograms of relative joint displacement in micrometres (μm) were created. Within RS2, separating or opening joint elements have negative displacements, while closing joints have positive displacements. Figure 3-9 illustrates three separate histograms for different loading stages throughout compression testing. In Figure 3-9b the state of stress prior to loading is shown, and it can be seen that about 45% of interfaces were in a tensile state of strain which tended to open the grain boundaries and crack elements. In Figure 3-9c it can be seen that this number drops to about

20% of interfaces in a state of tensile strain due to the applied external boundary load. In Figure 3-9d the percentage of interfaces in a tensile strain state started to increase due to crack initiation processes that were starting to occur.

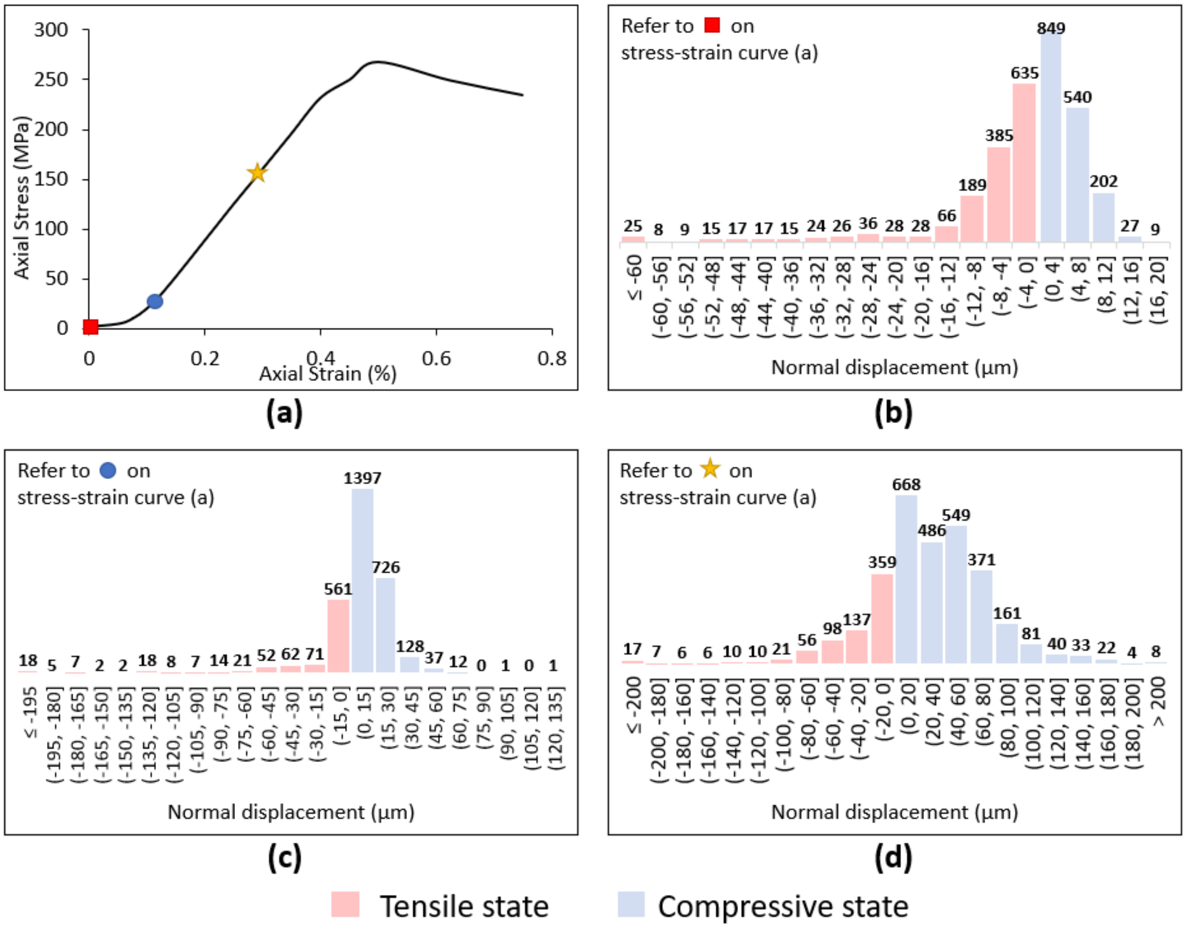

Figure 3-9 Normal displacement histograms in micrometres for the 3150 total grain boundary and crack element interfaces during compression testing with a 6 MPa average residual stress field. a) Stress-strain plot. b) Interface normal displacement prior to loading. c) Interface normal displacement at crack closure stress. d) Interface normal displacement near crack initiation stress

3.3.3 Crack Formation and Propagation Due to Residual Stresses

The redistribution of residual stresses has been shown to contribute to a sample's macro strength (Zang and Berckhemer 1989; Zang et al. 1996). As sample damage is known to decrease the strength of a specimen, this section aims to investigate the likelihood of sample damage as a result of residual stress redistributions occurring during the removal of in situ stresses. The potential for microcrack formation in undamaged samples and microcrack propagation in low crack-density samples were investigated. Crack densities were measured to quantify the level of damage after the sample had been relieved of some residual stress to compare the damage associated with each model. Modelling scenarios were created with various levels of interface tensile strengths and average residual stress magnitudes. The modelling procedure for all models within this section follows that of the residual stress implementation method. As the only concern was the redistribution of residual stress due to removing in situ stresses, no additional staging was required, and therefore resulted in free boundary conditions and residual stress within the model. Interface strengths were varied by model to examine the potential impacts that residual stress redistributions may have on local weak zones within the rock structure. Figure 3-10, and Figure 3-11 illustrate the modelling results on the effects of residual stress redistributions for the formation and propagation of microcracks respectively (illustrated as red line segments in the figures) in samples with the anticipated and lowered interface tensile strengths.

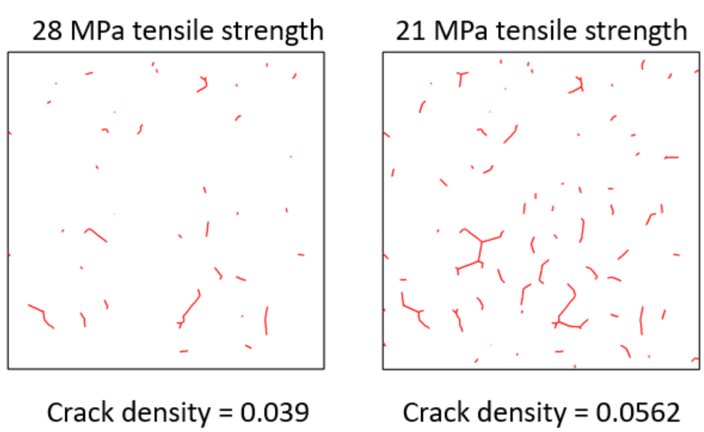

Figure 3-10 Formation of new microcracks due to the redistribution of residual stress caused by in situ stress unloading with varied interface tensile strengths

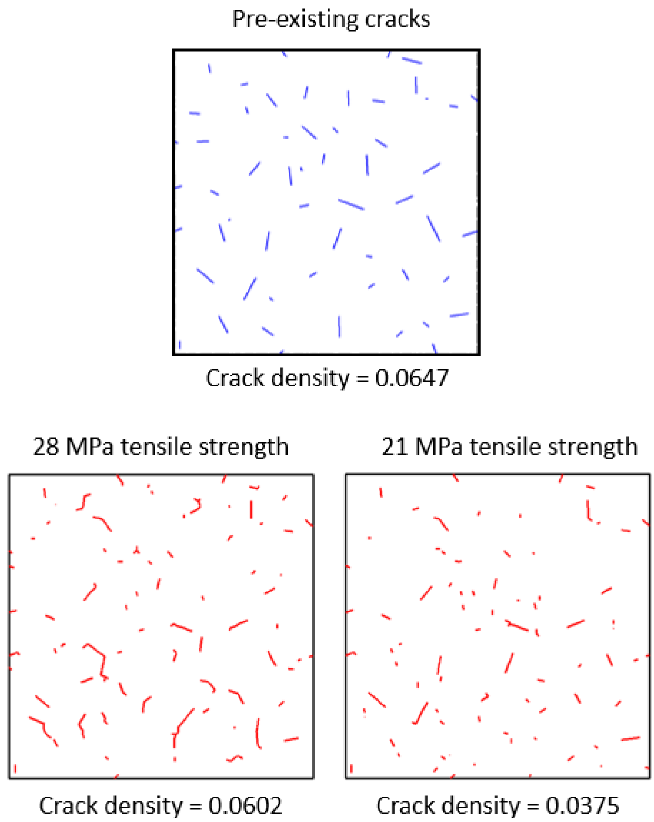

Figure 3-11 Propagation of existing sample damage due to the redistributions of residual stress caused by in situ stress unloading with varied interface tensile strengths

The next, and likely the most important step, in examining the effects of residual stress redistributions on the formation and propagation of microcracks investigates results with varied residual stress magnitudes. These models differ from the previous ones in that the magnitude of the displacement boundaries used for the creation of the residual stress fields were altered, while all other steps remained the same. The displacement boundaries were altered to produce the "low" and "high" residual stress magnitudes used in Chapter 3.3.2. The residual stress fields were simulated by applying bi-directional isotropic displacement boundaries with magnitudes of 1.875 mm for the "low" residual stress magnitude, and 3.0 mm for the "high" residual stress magnitudes. Figure 3-12 and Figure 3-13 illustrate the results for crack formation and propagation respectively due to residual stress redistributions with lower and higher initial residual stress magnitudes.

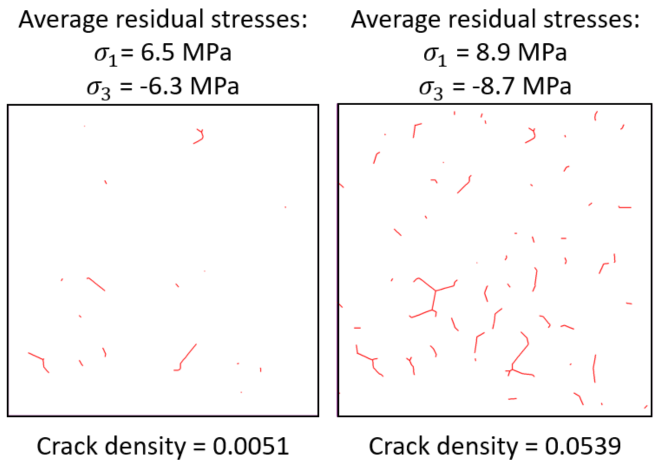

Figure 3-12 Formation of new microcracks due to redistribution of residual stress caused by unloading with varied residual stress magnitudes

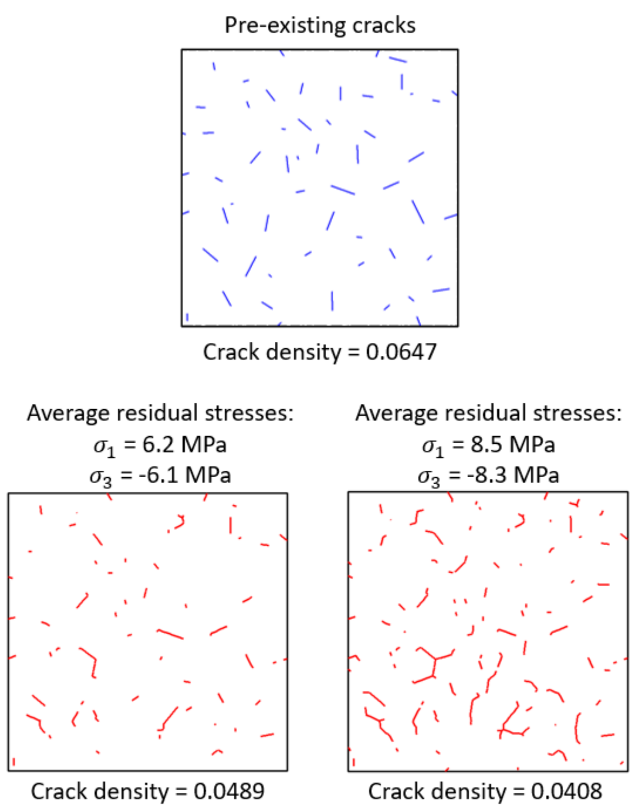

Figure 3-13 Propagation of existing sample damage due to redistributions of residual stress caused by unloading with varied residual stress magnitudes

Figures 3-10 through 3-13 showed that the redistribution of residual stresses can contribute to microcrack formation and propagation. Another form of crack propagation that residual stresses may have implications for is the propagation of a crack under direct tensile loading. With a residual stress field, compressive and tensile magnitudes must be distributed throughout the specimen. When a crack tip propagates and intersects a grain or grain boundary influenced by residual stress, the propagation of the crack could be influenced by the local residual stress state. Figure 3-14 illustrates how encountering a compressive residual stress may stall or resist the growth of a microcrack; as well as how encountering a tensile residual stress may promote the growth of a microcrack.

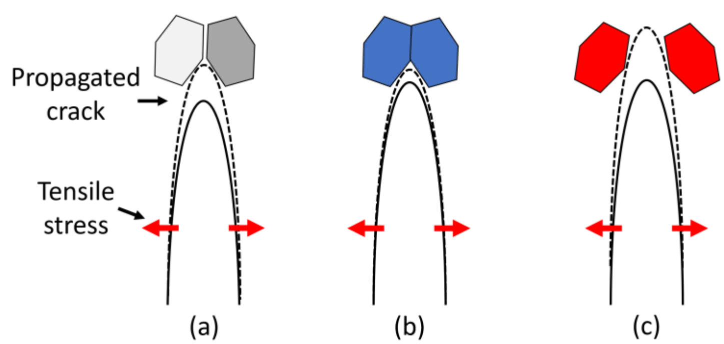

Figure 3-14 Effects of residual stress on the propagation of a microcrack. Dashed lines represent the extent of crack propagation. a) Extent of microcrack propagation without residual stress. b) Lower extent of microcrack propagation when encountering compressive residual stress due to an increased resistance to tensile microcracking. c) Higher extent of microcrack propagation when encountering tensile residual stress due to a lowered resistance to tensile microcracking

To determine if the concepts presented in Figure 3-14 are accurate, numerical simulations were utilized. Two scenarios were considered for modelling: (1) the propagation of a slot cut in a specimen containing residual stress, and (2) the propagation of a slot cut in a specimen without residual stress. Both modelling scenarios followed the same methodology and only differed in their residual stress magnitudes (i.e., present, or not). The modelling procedure was built on the crack formation model discussed previously. In stages 1 – 4, the specimen underwent the residual stress-building process and was unloaded to free boundary conditions resulting in a state of equilibrium for the residual stresses. After reaching the equilibrium state in stage 5, a slot was created at the bottom of the geometry to hypothetically simulate an open microcrack. In stage 6, a tensile load of 1 MPa was implemented by applying stress boundaries with equal magnitudes in opposite directions along the edges of the slot cut. The tensile load was then incremented by 1 MPa/stage until a maximum tensile load of 40 MPa was reached. It should be noted that the specimen without residual stresses could be loaded further, but the modelling scenario with residual stresses encountered model instability after 40 MPa of loading, and therefore this was used as the maximum induced stress for the comparison of models.

In the scenario where residual stress was not present, the first sign of damage at the tip of the slot cut occurred when the tensile load reached 17 MPa. In contrast, in the scenario that contained residual stress, the first sign of damage occurred when the tensile load reached 23 MPa. The 6 MPa tensile strength increase is likely associated with compressive residual stresses ahead of the cut that aided in resisting the propagation of the cut. Although the damage in the specimen with residual stress was stalled compared to that without residual stress, failure progressed more rapidly when residual stresses were present. Without residual stress, damage progressed gradually with the increase in applied tensile magnitude. When residual stresses were present, the damage did not follow a linear path. The initial damage remained fairly similar until a tensile load of 34 MPa; at which point, the damage instantly progressed to the damage state associated with 40 MPa of tensile loading. In comparing the damage states of the two models, when residual stresses were present, the damage progressed quicker and farther into the specimen than in a scenario where residual stresses were not present. If residual stresses were omitted, under 40 MPa of tensile loading, the level of damage within the specimen was about ⅓ the damage when residual stresses were present. It is likely that due to the increase in tensile magnitude required to overcome the initially increased tensile strength, the damage was stalled and progressed more rapidly as the tensile magnitudes were elevated. It is also likely that due to the tensile residual stresses distributed throughout the specimen, local weak zones existed ahead of the slot cut, and when in conjunction with the increased magnitude of tensile stress, the damage progressed at a quicker rate. Due to the increased levels of damage under a lower magnitude of tensile stress in comparison, the modelling results suggest that the presence of a residual stress field may increase the inherent brittleness of a specimen. Figure 3-15 summarizes the discussed modelling results and illustrates the different levels of damage associated with each reported stage.

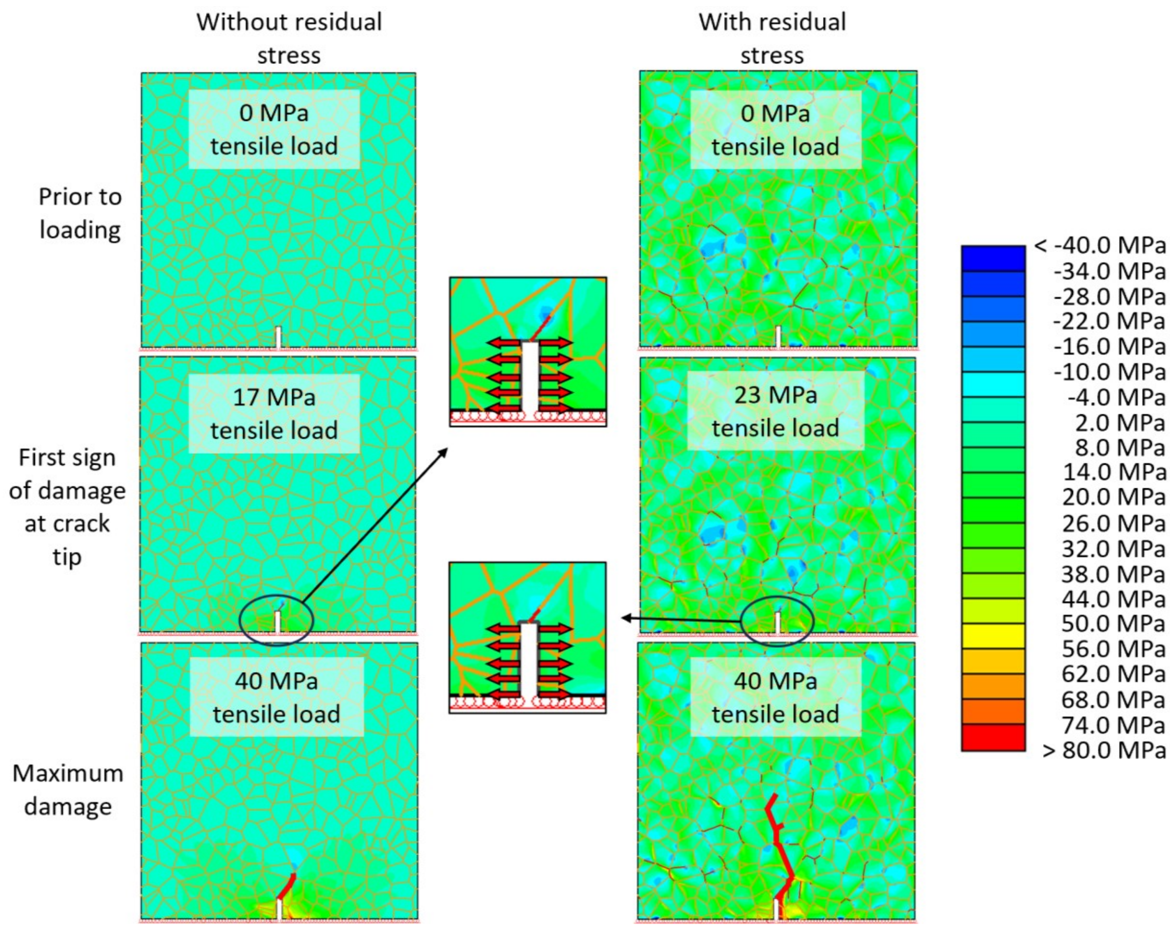

Figure 3-15 Modelled effects of residual stress on the propagation of a slot cut under direct tensile loading

3.3.4 Residual Stress Around Openings

Residual stresses have been shown to mobilize at different scales when an excavation or cut was introduced (Nichols 1975; Read 1990) and mobilized residual stress will have a resulting displacement or strain. This section presents results for models investigating the potential impacts that residual stresses may have surrounding hypothetical excavations in rock. To perform the analysis, additional staging to the initial residual stress-building model was required. Once residual stresses were initialized and the in situ load was removed, a stage was added to the model and a small-scale circular excavation (a hypothetical representation of a small scale borehole) with a 20 cm radius was placed within the center. After the excavation was introduced, changes in stress and strain on the excavation boundary and at depths into the rock were measured under both free boundary conditions, i.e., no in situ stress, and with an isotropic in situ stress boundary condition. Figure 3-16 illustrates the model setup, as well as the direction and depth of the model queries (radial lines).

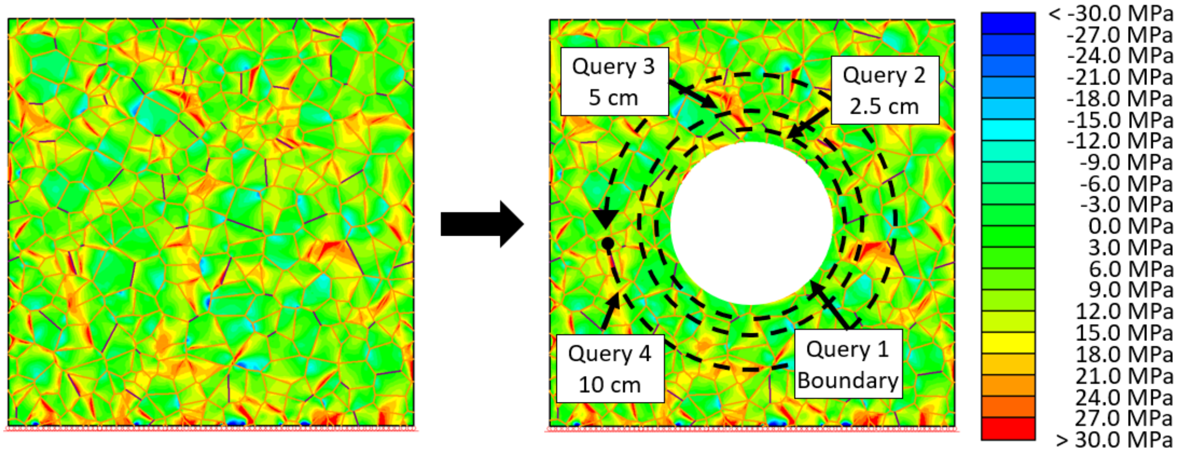

Figure 3-16 Addition of a 20 cm circular hole within a sample containing residual stress and query locations. The circle and arrow on query 4 indicate the starting query point (circle), and the direction of the query line (arrow)

As a result of placing an excavation within the sample free from in situ stress boundary conditions, residual stresses were mobilized throughout the entirety of the model. The changes in stress at all four query locations described in Figure 3-16 were plotted. Figure 3-17 illustrates the changes in stress due to the excavation by plotting the stresses prior to excavation, and the stresses post-excavation, and taking the difference between them. The magnitudes of released residual stresses, or the change in the stress at a location, varied by position. Near the excavation boundary, the change in stress magnitude is near a maximum stress of 40 MPa, while at a further location of 10 cm from the excavation the changes in stresses are all less than 10 MPa.

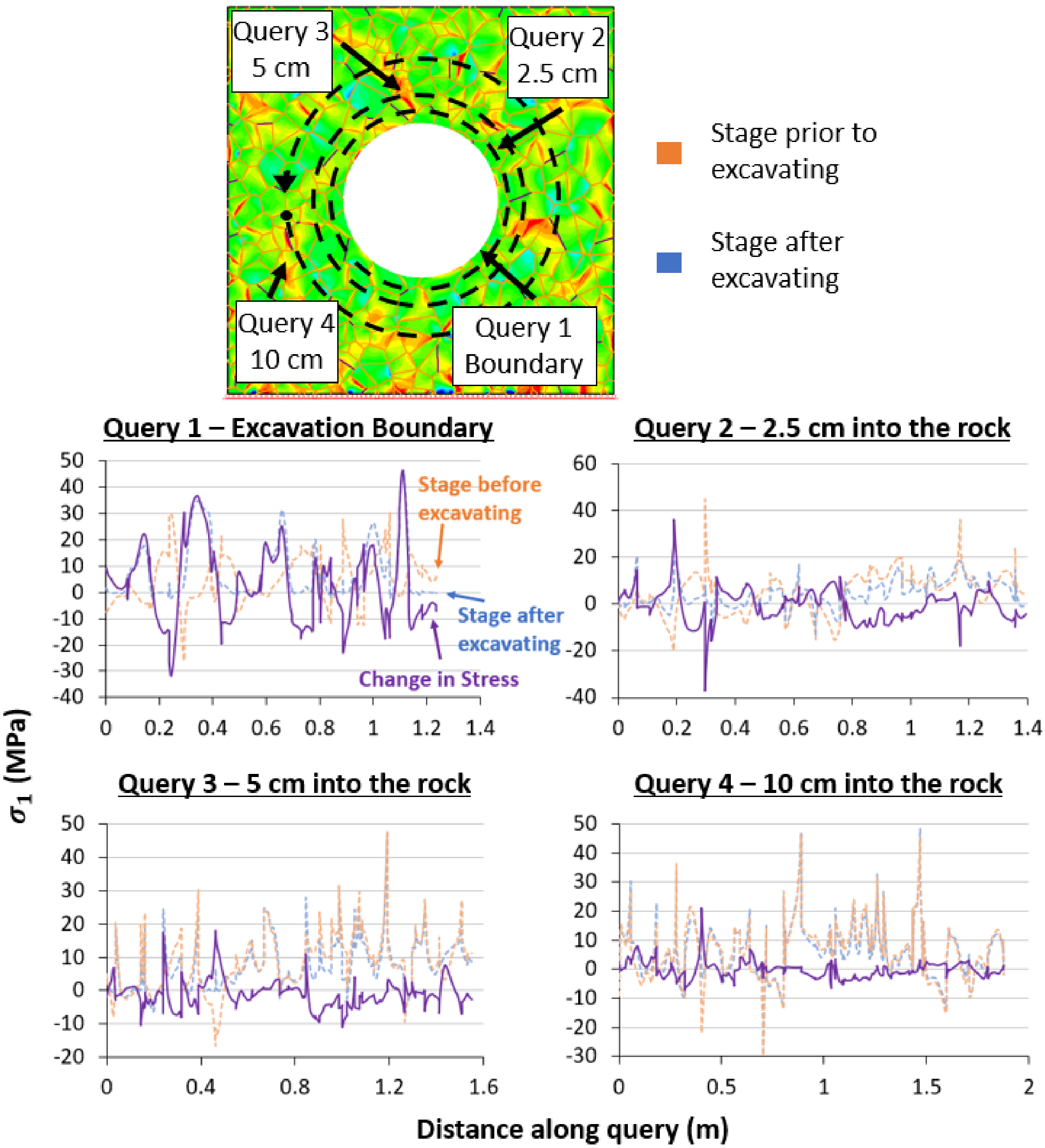

Figure 3-17 Residual stress redistribution plots at four locations due to the addition of a 20 cm radius circular excavation in a sample containing residual stress

The ϵ_X and ϵ_Y strains in the stages prior to, and post-excavation were extracted from the model and the resulting change in strain was calculated using a Mohr's circle of strain conversion. The resulting plots illustrate the strains that would be measured if a strain gauge or other measuring device was present during the excavation process. Typical magnitudes of the released strains were up to 50 με within both the major and minor plots. Figure 3-18 provides a visual representation of the calculated change in strains under free boundary conditions by post-processing the RS2 data using Mathematica software and overlaying the associated damage within the sample illustrated through the red lines.

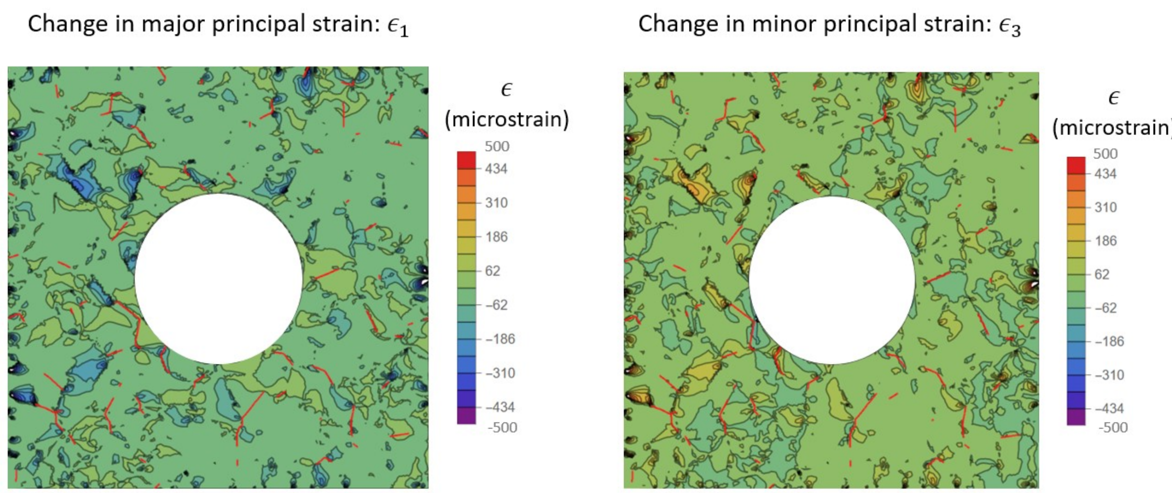

Figure 3-18 Measured strains as a result of a 20 cm radius circular hole placed in a sample containing residual stress field

Residual stresses under free boundary conditions redistribute and result in measurable stresses and strains. The effects of residual stress redistributions in samples under in situ stresses were investigated to determine any differences in the measured displacements that can arise when residual stresses are superimposed with field stresses. The models considering in situ stresses were constructed in the same manner as the free boundary models with a slight adjustment in the final two stages. In the free boundary models, the in situ stress used to build residual stresses was completely removed. In the in situ stress models, the displacement boundary at the stage for removing all external loading was replaced with a bi-directional isotropic stress boundary with a magnitude of 40 MPa. The stress boundary was applied in this stage, and it was not removed. Hence in the final stage when the excavation was introduced, both residual stresses and field stresses were superimposed within the model.

This process was repeated for three separate scenarios. The first scenario used the typical geometry and properties used herein. The other two scenarios only considered one material to represent all of the mineral grains, with either weighted average elastic properties (weighed by their mineralogy %), or elastic properties measured off of the stress-strain curves produced in Chapter 3.3.2. In all three scenarios, models that contained residual stresses had been shown to significantly alter the anticipated magnitude of displacements around the excavation. Figures 3-19a and 3-20a, 3-19b and 3-20b, and 3-19c and 3-20c illustrate the results for each scenario respectively, showing the anticipated displacements around the excavation with the superimposed stress state (i.e., residual stress and in situ stresses), and a state purely representative of in situ stresses (i.e., no residual stresses are present). Figure 3-19 and Figure 3-20 plot the same changes in displacement but with different visual representations.

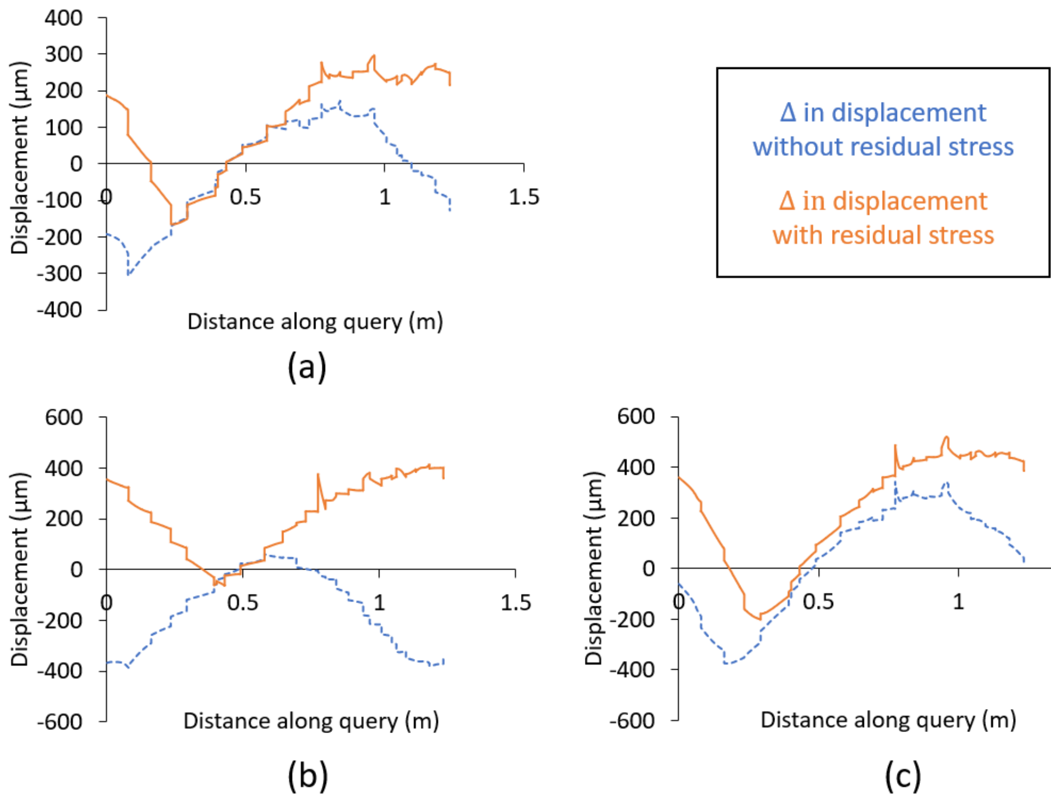

Figure 3-19 Change in displacement plots around a 20 cm radius excavation on the excavation boundary under in situ stresses. a) Three mineral grains with typical mineral properties. b) One mineral grain with weighted average elastic properties from the main three minerals. c) One mineral grain with Young's modulus measured from compression testing

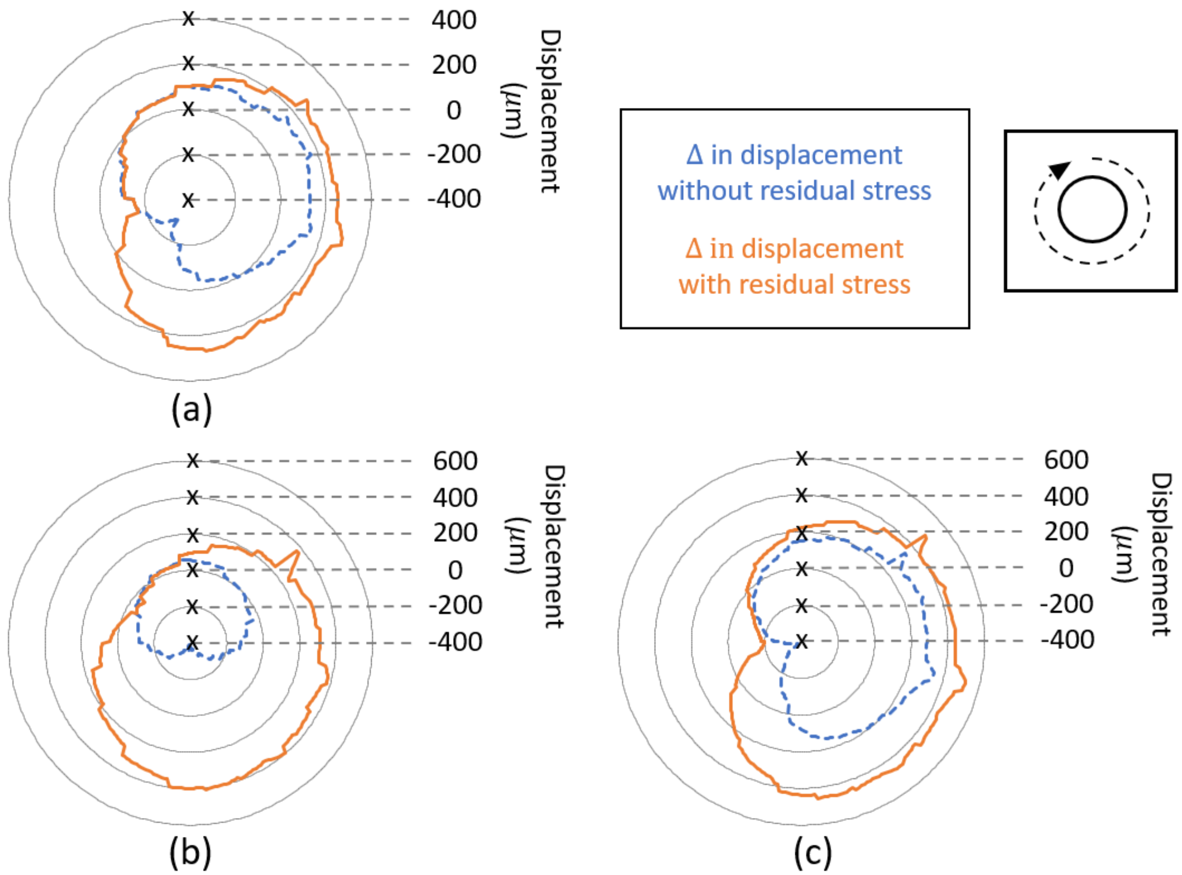

Figure 3-20 Change in displacement plots around a 20 cm radius excavation on the excavation boundary under in situ stresses. a) Three mineral grains with typical mineral properties. b) One mineral grain with weighted average elastic properties from the main three minerals. c) One mineral grain with Young's modulus measured from compression testing

3.4 Discussion

Through the context of observations reported in the literature and the use of micromechanical numerical models, potential implications for residual stresses in rock mechanics were explored. Modelling residual stress as a mechanism for crack closure successfully reproduced crack closure strains without explicitly simulating an initial state of open microfractures, which is the standard practice in today's models attempting to capture such strains. In a study to characterize the crack closure effect of rocks, Peng et al. (2015) implemented the effective medium theory in their work to induce crack closure strains. This theory requires an understanding of the microstructure and divides the measured strains into two components, the matrix strains (representing the rock grains in the matrix) and the microcrack strains. The strains are superimposed, and at a pre-defined level of stress, the crack closure strain reaches a maximum, thus representing a state of closed microcracks. Simulating crack closure strains in this method requires a detailed understanding of the existing magnitude of open microcracks within the sample, and additional testing is required to provide thresholds to limit the strains. In contrast, using residual stresses as a means to simulate crack closure requires only an understanding of the average local residual stress state which can then be implemented through methods discussed in Chapter 3.3.1. To the extent of the author's knowledge, this is the only method that exists for simulating the crack closure effect seen in stress-strain curves without explicitly simulating the pre-existing state of damage within the specimen.

Other attempts at quantifying crack closure strains have been investigated through drilling-induced damage that occurs during sample recovery. Bahrani et al. (2015) discussed the effects of stress path during drilling in situ and its effects on sample damage and microcrack presence. The drilling stress path was determined through 3D finite element modelling, and a simplified version was adapted. A 2D finite element method and a 3D distinct element method analysis were used to examine if the stress path could result in the formation of sample damage. Exposing a specimen to the stress path resulted in damage within the sample. To try and quantify the level of damage, compression tests were performed to measure crack closure strains. Within their models, little to no crack closure was observed even though the sample had undergone a damaging process that researchers typically associate with crack closure strains. What this paper proposes is that residual stress could be a missing mechanism from these models that produces a state of open microcracks. Within the microstructure, compressive and tensile residual stresses are distributed throughout. If microcracks form near tensile residual stresses, when the crack forms and the stress dissipates, the grain boundaries relax and separate from each other, opening the microcrack. Figure 3-21 illustrates the effects of local residual stress fields, and how a state of tension within a grain could be the missing mechanism for opening microcracks to produce crack closure strains.

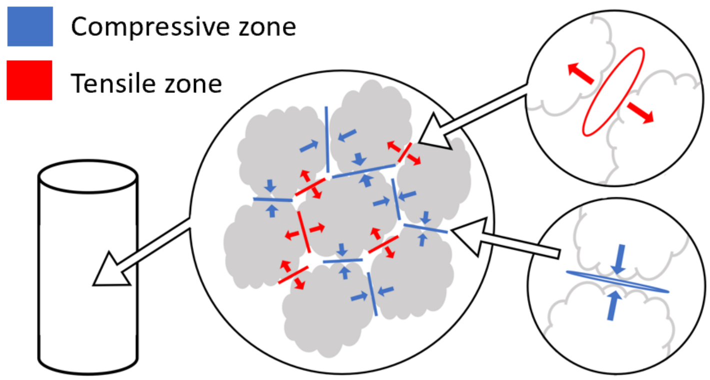

Figure 3-21 Local residual stress field illustrating how tensile stress magnitudes could be responsible for opening existing microcracks after the stress state (in situ and residual) overcomes the local interface strength

A connection between the magnitude of residual stress and crack closure strains was illustrated in Chapter 3.3.2. Similarly, this phenomenon may be exhibited in situ as well. In the residual stress analyses performed at the URL discussed in Chapter 3.2.3, both authors measured low levels of residual stress (about 1 MPa). Due to the low magnitude confirmed by multiple tests, the presence of residual stress at the site was deemed negligible and therefore these stresses were omitted from future studies at the site. Although the residual stress state appeared negligible at the locations of measurement, this may not be the case at greater depths. Martin and Stimpson (1994) investigated sample damage within various levels of the URL. It was noted that at shallow depths, including the 240 level investigated for residual stress, the magnitude of existing damage and crack closure strains were low. With increasing depth, the authors noted that the levels of sample damage increased. Due to the low measured residual stresses at the 240-m level, a large presence of open microcracks likely does not exist, and therefore crack closure strains would be little to none as measured by the authors. Illustrated with micromechanical models, as the magnitude of residual stress increases, so does the magnitude of crack closure strain. It is hypothesized that if residual stress measurements were repeated at the URL but at greater depths (420-m level), larger residual stress magnitudes would be measured to produce the crack closure strains observed in the samples from depth.

As illustrated in Figure 3-7, when higher crack densities exist in a sample containing residual stresses, higher crack closure strains were measured. While these results were not identical to those of Griffiths et al. (2017), a similar trend was observed. While the modelled compression tests captured reduced overall crack closure strains compared to Griffiths' work, the peak stresses were similar and crack closure strains were observed in both cases with larger crack closure strains occurring in specimens with higher damage. In samples containing higher levels of damage, more free surfaces existed to redistribute residual stresses and to free tensile residual stress interfaces. As a result of more cracks, higher crack closure strains were anticipated as more tensile interfaces were freed. This trend was seen in both the modelled result and the work of Griffiths et al. (2017).

While residual stresses have been shown to open pre-existing microcracks, their presence can also form new cracks or propagate existing ones. Removing the boundary conditions on a sample containing residual stress disrupts the state of equilibrium and therefore causes the residual stresses to redistribute. As a result of their redistribution, local residual stress magnitudes may exceed the local strength resulting in the formation of a microcrack. The results from modelling in Chapter 3.3.3 indicated that these stresses could form new microcracks and propagate existing cracks. Residual stresses can also lead to an increase in the brittleness of a sample. If a microcrack forms and wants to propagate, but the crack tip is met with a grain containing compressive residual stresses, then the propagation of the crack is stalled, and energy is stored in the tip. If a redistribution of stress, or the fracturing of neighbouring local grains occurs, a redistribution of stress might overcome the strength of the grain at the crack tip which would then release the stored energy at the tip and propagate the crack even more, effectively increasing the brittleness of the rock at various locations within the microstructure.

As discovered by Nichols (1975), the redistribution of residual stress was higher when measured near the excavated surface and decreased as the distance from such surface increased. A similar trend was observed in the numerical simulations where in Figure 3-17, the change in stress magnitude decreased and approached zero as the distance increased. As this model was measuring the redistribution of stress only 10 cm into the rock, the effects of residual stress on a large scale may not be as important as on a smaller scale say, for in situ stress measurements. It is also likely that the redistribution of residual stress on a larger scale is already accounted for through dilation effects. Nonetheless, at the small scale used in overcoring methods to measure in situ stress, the presence of residual stress should be considered as it can result in significant strains that alter the results of stress measurements. If residual stress is not considered in the estimation of the in situ stresses, large uncertainties are likely to exist which can severely impact the results of engineering design. Neglecting to include a residual stress field (if one is present at the site) in the design of excavations may lead to other issues with unaccounted deformations, especially if strain factors of safety are used on supports such as split-set bolts or for early-age shotcrete strength.

As illustrated in Figure 3-18 the average residual stress redistributions were on the magnitude of 50 $\mu\epsilon$. Comparing these strains to those of Nichols (1975) indicated that the magnitudes of residual stress used were lower than the actual values reported in the literature as their measurements were in the range of 150 – 250 $\mu\epsilon$. Although the methods used for residual stress implementation could not be used to explore increased magnitudes for numerical stability reasons, if a method is used to reach such stress magnitudes, further implications for residual stresses may be derived from micromechanical simulations for rock engineering.

3.5 Conclusion

Residual stresses are well studied and documented in the fields of metallurgy and glass, and engineers in these fields have been able to take advantage of such stresses to obtain desirable material behaviour characteristics. Research into these stresses in rock has confirmed their presence at various geologic scales. Although known to exist, little research has been presented beyond the existence of such stresses to further understand residual stresses and their implications in the field of rock engineering. In this paper, residual stresses were investigated with a grain-based modelling approach to examine the potential implications of their presence providing insight into the mechanism as a possible component of rock behaviour.

Residual stresses were incorporated within continuum-based micromechanical models using RS2 software using a simplified method that produced residual stress magnitudes similar to those reported in the literature. These stresses were investigated through multiple modelling scenarios examining the impacts they may have on rock behaviour. Compression testing was first performed, and crack closure strains were measured as a result of samples containing residual stress. Varying the magnitude of residual stresses altered the shape of the stress-strain curve, specifically in the crack closure region, where lower magnitudes of residual stress produced low crack closure strains and vice-versa. Due to the presence of residual stress, grain interfaces were largely tensile in a state free of external loads which provided reasoning on how open microcracks could exist within a specimen.

The formation and propagation of microcracks was also related to residual stresses. When removing applied loads on a specimen containing residual stresses (simulating the removal of a specimen from in situ), a redistribution of stresses occurs to maintain a state of equilibrium. During the redistribution, micromechanical models have illustrated the magnitudes associated with such processes can overcome the local strength of grain boundaries and result in further sample damage. It was also presented that the distribution of compressive and tensile stresses within the specimen could influence the continued propagation of a crack.

The results obtained from modelling suggested that as an internal microstress field exists within bodies of rock (residual stresses), associated strains and displacements were to be expected as a result of their presence. Excavations in samples containing residual stress were performed and compared to the results of models without residual stress. When these stresses were present, the stresses and displacements surrounding the excavation were largely different from models without residual stress. The redistribution of stresses and their associated strains were larger on the excavation boundary and persisted into the sample, decreasing with depth. The local redistribution of stresses and strains may not be as influential for large-scale excavations, but for small-scale excavations such as in situ stress measurement, the presence of these stresses becomes significantly more important.

While this paper does not perfectly recreate the processes associated with residual stress formation, it does present a method for inducing residual stress fields, as well as some potential implications. This study included residual stress in rock mechanics models to determine if researchers were correct in omitting these stresses from their analyses. The results presented within this study indicate that excluding residual stresses would produce results that were not indicative of the true state if residual stresses were present within the actual rock. Although the results of this study provided additional information on the topic, further research related to residual stress in the field of rock engineering is required to deepen the collective knowledge on the subject.

CHAPTER 4 - *3DEC* MODELLING EXPLORATION OF RESIDUAL STRESS MECHANISMS

A version of a conference paper submission for ARMA 2024. Status: Accepted

4.1 INTRODUCTION

Residual stresses exist as a natural phenomenon found in situ and as a byproduct of formation for certain man-made materials. The state of residual stress contains both compressive and tensile stress magnitudes which allows for the residual stress field to reach a state of equilibrium independently from external stresses. As a result of this self-equilibrating nature, residual stresses are often overlooked as they exist separately from both in situ stress and excavation-induced stresses. However, if a residual stress field is disturbed (e.g., fracture formation), the stresses will mobilize in an attempt to reach a new state of equilibrium and will accompany a measurable strain. Although these stresses exist separately from other common stresses, it is important to understand their existence as they may have consequential impacts if not properly understood. An example of this in steel is the case of the split I-beam (Nau, 2015) where due to casting, residual stresses were created within the beam. Once fully hardened the beam was cut at an angle on both ends which disturbed the state of equilibrium and caused a redistribution of the residual stresses. As a result of their redistribution, the I-beam fully split through the web which then destroyed the beam.

In the field of rock mechanics, a residual stress state exists in equilibrium with its own forces, as well as the in situ stresses. The common approach when designing rock structures is to analyze the structure's response to mining-induced stresses and in situ stresses. But as previously mentioned, residual stresses also exist and can be mobilized with potential impacts on design. In current practice, residual stresses are omitted from design as most engineers in this field either are unaware of their presence or believe they are negligible in nature. The purpose of this study was to investigate residual stresses in rock mechanics using the 3D discontinuum software, *3DEC*. Through the use of a grain-based model, the presence of damage due to redistributions of residual stresses is investigated. To further quantify the damage, compression tests were performed on a specimen containing only residual stresses to investigate the possibility of crack closure, a commonly observed phenomenon in the early stages of compression tests due to the presence of open microcracks which occur as a result of sample damage.

4.2 Background

Residual stresses exist within microstructures of crystalline materials like glass, metal, and rock. One of the earliest observations of residual stress was displayed in Prince Rupert's drops. These structures provided a clear demonstration of how residual stresses could impact the mechanical behaviour of a material that contained them. Prince Rupert's drops were discovered in the early 1600s (Brodsley et al. 1986) when these structures were delivered to the Royal Society. These drops form when molten glass is dropped into cold water. Due to the large thermal gradient that takes place when molten glass contacts cold water, hardening takes place at different rates throughout the material. Once the glass touches the water, the material on the exterior surface starts to harden while the interior remains in a molten state. As the glass continues to be exposed to the cold water, the molten inner core starts to solidify. The continued solidification causes the material to contract as it transitions from a liquid state (molten) to a solid state, pulling on the already hardened exterior shell thus inducing compressive stresses into it. Once the glass becomes fully hardened, a state of stress exists within the material where the compressive stresses on the exterior surface are balanced by tensile stresses at the core. It is the balance between the compressive and tensile magnitudes that allows this state of stress to exist within the microstructure of a material without the need for any load to be applied to the external boundaries to produce such stresses.

What makes Prince Rupert's drops interesting is when an attempt is made to break these structures, the magnitudes of residual stresses within the sample are illustrated. Due to the compressive residual stresses at the exterior surface, when the material is impacted it has an increased resistance to the formation of microcracks. This increased microcrack resistance effectively strengthens the glass to the point where it can withstand continuous impacts from a hammer. However, due to the balancing nature of residual stresses, the large magnitudes of compressive stresses required to increase the strength must be balanced by tensile stresses with an equal and opposite magnitude. The associated large magnitude of tensile stresses contained within the core is visualized when the sample breaks. Upon breakage, the residual stress field is no longer in a state of equilibrium and the large tensile stresses at the core rapidly dissipate which causes the entire specimen to disintegrate into fine granular-like pieces.

Early studies on residual stresses in glass' and metals shed light on the concepts that were then adapted to the field of rock mechanics. Friedman (1967) was one of the first researchers in this field to investigate residual stresses in bodies of rock. Using sandstone samples retrieved from two separate locations, residual stresses were measured using X-ray Diffraction (XRD) techniques. XRD measures the spacing between the layers of atoms that comprise a crystal structure, known as the d-spacing, which can change with applied load and therefore be used as a source of measurement. Changes in d-spacing can be monitored throughout loading/unloading by the diffraction of x-rays through the atomic structure which are then interpreted to produce a measured value of d-spacing that can be correlated to strain (Fitzpatrick et al. 2005). In Friedman's work, they used acid etching to remove the boundary constraints on grains within the sandstones to release residual stresses. Using XRD methods, the change in d-spacing was measured until no further change in d-spacing was noticed with increased acid etching. As a result of removing the constraints around grains in the sandstone, residual strains were mobilized with magnitudes of up to 240 microstrains ($\mu\epsilon$) being reported.

Another method of measurement that can be used to quantify residual stresses in rock is destructive methods such as overcoring or undercoring. Nichols (1975) used a concentric overcoring technique in conjunction with 34 strain gauges across the "top" and "side 2" to measure the release of residual stresses constrained within a sample of granite under laboratory conditions. Their procedure consisted of first coring the top of the sample with a

5.1 cm core barrel to a depth of just under halfway, and strain readings were then recorded for 48 hours. The process was then repeated, but this time a 10.1 cm core barrel was used and placed concentrically over the initial cut. After another 48 hours of strain readings, this process was again repeated on the top for a final time with a 15.0 cm core barrel. This process in its entirety was repeated on the bottom surface. After these cuts were complete, a cut was then made on side 2 with a 10.1 cm core barrel which marked the end of their coring programme. As a result of all the newly created free surfaces (cuts), residual stresses were mobilized with strain readings of up to 275 $\mu\epsilon$ reported.

Similar to overcoring methods, undercoring methods have also been used to show the existence of residual stresses in bodies of rock. Bock (1979) employed the undercoring technique using a specialized rosette comprised of three strain gauges centred around a pilot hole for the undercoring location. Using this method, they performed 22 undercores across the surface of an 18 cm wide basaltic column. Over the 22 measurements, compressive and tensile stresses were reported with magnitudes of up to 15.2, and 12.6 MPa respectively. Destructive methods, such as the concentric overcoring method, have also been utilized in situ to measure residual stresses at the Underground Research Laboratory (URL) located in Manitoba Canada. Lang (1986) employed the concentric coring method by first overcoring with a 200 mm bit to remove the in situ stresses, and then a 150 mm and 96 mm concentric overcore were drilled to release residual stress from the remaining intact rock. From their measurements, a magnitude of about 1 MPa was reported.

Some implications for residual stress were presented by Zang (1989) where residual stress redistributions were measured and correlated with microcrack investigations and strength anisotropy. A sandstone core was retrieved from just over 5 km depth and was used in their analysis. The retrieved core then had strain gauges installed on the center and external shell, and a secondary overcore was performed. After secondary overcoring, residual stress redistributions were noted with the core indicating anisotropic contraction, or the pure contraction of the core but with magnitudes larger in one direction. These contractions were the largest at an orientation of 45° and were the least at an orientation of 135°. A microscopic investigation on thin samples cut from the secondary overcore indicated that microcracks were present with an average strike of 135°. A possibility for the anisotropic contraction can then be related to the closing of open microcracks as the normal of the microcracks (the orientation of opening) is at 45° and correlates with the largest contraction. Brazilian and point load tests were also performed on thin sections of the secondary overcore. Point load testing indicated a typical failure orientation of 135° which aligned with the direction of least compressive redistributions. As noted with the Prince Rupert's drops, compressive residual stresses can resist the formation of microcracks effectively strengthening the material, and in the case of point loading testing, the least amount of compressive residual redistributions were also at an orientation of 135°. Brazillian testing was performed with two loading directions, one at 45° and another at 135°. When loading against 45°, or the orientation with the most compressive residual redistribution, the tensile strength was reported to be approximately 4 MPa higher than the 135° orientation. The main implications derived from Zang's (1989) study were in the strengthening effect of compressive residual stresses, and the influence of residual stress on the aperture of existing microcracks.

4.3 Numerical Modelling

Residual stress exists at the grain scale of rock, and therefore a grain-based model is required to adequately represent the structure, as well as the grain-to-grain interactions. Using Itasca's *3DEC* software (Itasca, 2023), a 3D Voronoi geometry was created for the investigation of residual stress in rock-like specimens. The geometry was then subjected to various residual stress implementation methods to create a specimen containing residual stress without any externally applied load remaining. The specimens were then investigated for damage, which was quantified through crack measurements, and unconfined compression tests.

4.3.1 Model Formulation and Validation

Voronoi structures have previously been used to simulate brittle failure processes and grain-based structures (Sanipour et al. 2022; Li and Bahrani 2021). For the purposes of this study, a Voronoi network was used to simulate a grain-based structure that was representative of the microstructures found in real rock specimens. It is important to note that the specimen created in this study was not intended to replicate a specific rock structure but to be representative of a typical rock structure with properties that were realistic for high-strength granites. To produce such a specimen, one must first start by producing a grain-based geometry that is true to scale for rock, and then assign micromechanical properties to the grains and grain boundaries.

To produce a grain-based model in *3DEC*, a geometry must first be created and filled with Voronoi blocks. When performing such operations, the grains tended to have vertical or horizontal preferences in their alignment near the external boundaries of the geometry. To prevent this from occurring, the initial geometry was created larger than the intended final specimen to produce a sort of “master block” that could then be cut to the desired size. The initial geometry was generated to be 0.25 m larger than the intended final geometry in all directions. After the removal of the 0.25 m excess, the final dimensions of the specimen were 1 m tall, by 1 m wide, by 0.4 m deep and the preferential alignment of grains was no longer observed throughout the sample. The model was upscaled for the convenience of modelling, which resulted in grain sizes that were representative of realistic smaller-grained structures. The size of the implemented Voronoi blocks was scaled to that of the final specimen dimensions to ensure a sufficient number of grains were placed across each of the specimen lengths and resulted in a microstructure that was realistic for rock. This process resulted in a Voronoi structure that was approximately 16 grains wide, by 16 grains tall, by 7 grains deep. A total of 1696 Voronoi blocks were created within the specimen, and all blocks were zoned with a maximum element size of 0.015 m, or approximately 5 subdivisions per grain.

Griffiths et al. (2017) quantified damage in heat-treated samples of Garibaldi grey granite to examine the effects of microcracking on the ultimate strength. In their study, they investigated the microstructure of specimens thermally treated to a variety of temperatures and provided properties for the microstructure to predict the varied levels of ultimate strength based on the level of damage. Due to the detailed description of the microstructure and some of the associated stiffness properties, the material properties used in this model were loosely based on their description of Garibaldi grey granite. The mineralogy of Garibaldi grey granite was described as 45 % feldspar minerals, 45 % quartz minerals, and 10 % mica minerals. This mineralogy was randomly applied to the *3DEC* model to produce a heterogeneous specimen with contrasting grain stiffnesses. Within the model, the mineralogy was randomized by assigning a uniform random value between 0 and 1 as an "extra" type to each block. The extra allows each nodal point to store additional information, which in this case will be used for the random assignment of mineral type. Blocks with extra values from 0 to 0.45 were assigned feldspar minerals, blocks with extra values from 0.45 to 0.9 were assigned quartz minerals, and blocks with extra values from 0.9 to 1 were assigned mica minerals. The modelled dimensions and associated mineralogy are illustrated in Figure 4-1.

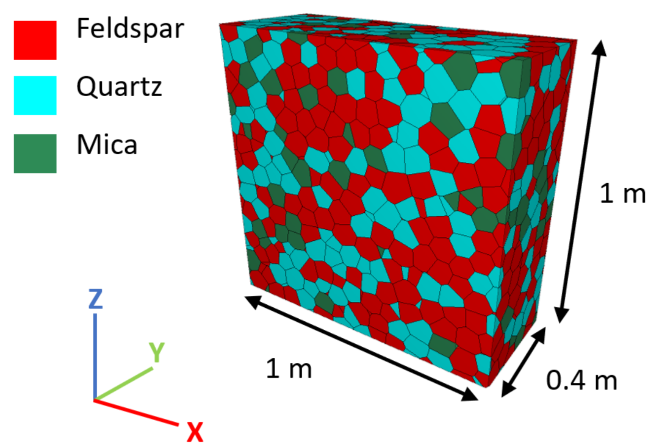

Figure 4-1 Dimensions and mineralogy for the modelled *3DEC* grain-based specimen

The elastic properties for each mineral type were described by Mavko et al. (2020) and were applied to each of the three minerals respectively. To reduce the number of variables that must be calibrated, the grain elements were assigned a purely elastic constitutive model, while the grain boundaries, termed joints in *3DEC* which are discretized into numerous subcontacts, were assigned an elastoplastic behaviour with some simplifications. For the subcontacts, the simplifications are as follows; residual tension and cohesion properties were assigned 0 strength, residual friction was assigned the same value as the initial friction, a normal to-shear modulus ratio of 2 was used, and residual normal and shear moduli were assigned values similar to those of rock joints. Subcontacts were assigned initial values based on legacy micromechanical properties from Khorassani and Corkum (2023), and their strength and stiffness properties were then calibrated iteratively with compression tests until a peak strength and bulk stiffness similar to that reported by Griffiths et al. (2017) were obtained. All elastic grain properties and elastoplastic subcontact properties used within the model are summarized in Table 4-1 and Table 4-2 respectively.

Table 4-1 Elastic properties for mineral types in Garibaldi grey granite

Mineral	E (GPa)	ν	ρ (kg/m^3)
Feldspar	69	0.35	2630
Quartz	96	0.07	2650
Mica	85	0.21	3050

Table 4-2 Elastoplastic properties for modelled subcontacts

Property	Value
K_N	6000 GPa/m
Residual K_N	100 GPa/m
K_S	3000 GPa/m
Residual K_S	50 GPa/m
Tension	26 MPa
Residual tension	0 MPa
Cohesion	95 MPa
Residual cohesion	0 MPa
Friction angle	45 °
Residual friction angle	45 °

To validate if the calibrated properties assigned to the model were representative of high-strength granites, a compression test and direct tension test (pull test) were performed on the specimen. Load was applied to both the top and bottom in either compression or tension depending on the test through applied velocities. The resulting stresses were then monitored at both the top and bottom surfaces of the specimen, as well as throughout the central zones of the specimen to verify if the loading rate was slow enough for the stresses to transfer evenly throughout to prevent a dynamic loading effect. If the stresses reported at the middle lagged behind the stresses reported at the top and bottom, the applied velocity used for loading was reduced until both measurements reported similar values. The results from both compression and tension tests were indicative of high-strength rock materials and can be seen in Figure 4-2.

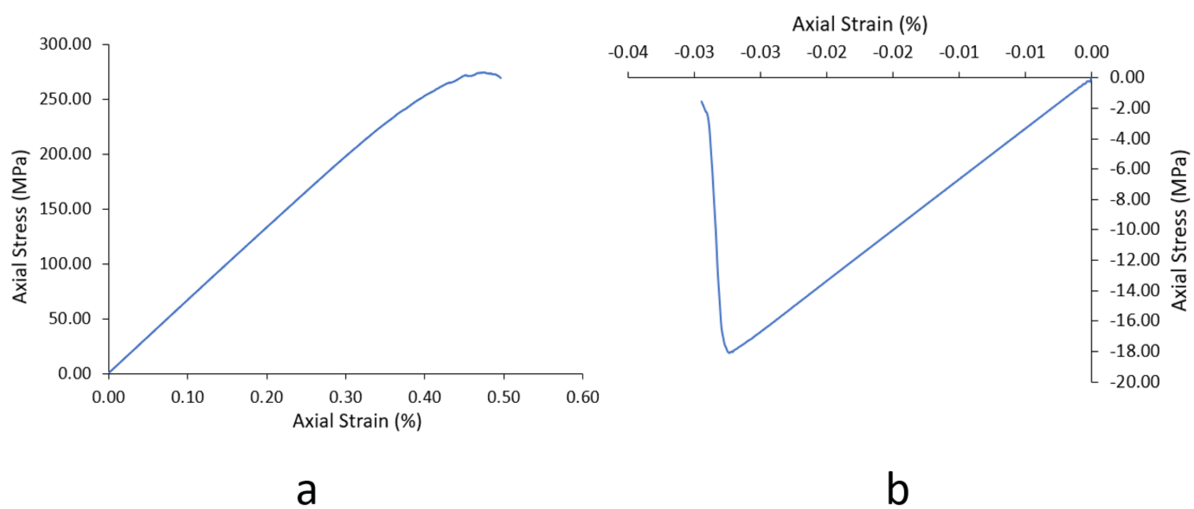

Figure 4-2 a) Stress-strain curve for compression test model validation. b) Stress-strain curve for direct tension test model validation

4.3.2 Modelling Methodologies

A total of three methods were used to simulate a residual stress field within the modelled specimen. The first of which is termed "sliding interface" and is a method to imitate the sliding and gliding processes that occur between the grain boundaries throughout the geological history of a rock material. This method is adapted from an initial study using discrete element grain-based modelling to explore residual stress (Khorassani and Corkum 2023). To initialize residual stress using this method, the material properties of the subcontacts were manipulated. At the start of the residual stress initiation process, subcontact properties were overridden to be purely frictional, i.e. no tensile or cohesive strength exists. The specimen then underwent a triaxial loading scheme with a stress ratio of $\sigma_z = 2\sigma_y = 3\sigma_x$. The maximum magnitudes of applied stress were altered between model iterations to increase the magnitudes of residual stresses that were created to be similar to the levels reported in the literature. Once the maximum magnitude of induced stress was reached, the subcontact state was reset to an elastic state to omit any flags within the model that represented a damaged state. The subcontact properties were then re-assigned their values from Table 4-2, and the model was then unloaded. When the strength was reassigned, the material was unable to relax to the full extent prior to loading, and thus a residual stress field was created as a result.

The second method employed to initialize residual stress is termed "solidification", and it follows a similar pattern to that of the sliding interface method. This method simulates residual stresses that are derived from the solidification or cooling of a magmatic material that is exposed to in situ stresses. To create residual stress using this method, the Young's moduli of the blocks were manipulated. At the initial stage of residual stress building, the Young's moduli for each of the mineral types were reduced to 1% of their value listed in Table 4-1. The model then underwent the same triaxial loading scheme until a maximum stress was reached. Once this stress threshold was hit, the Young's moduli were then reassigned to their full values, and the sample was unloaded. Similar to the previous method, residual stress was stored as a result of the hardening of the material as this prevented the complete relaxation of the specimen.

The final method utilized to initialize residual stress is termed the "combination" method and is a combination of the sliding interface and the solidification methods. Both elastic block properties and subcontact strength properties were manipulated in the same manner as previously described, and the applied load was cycled to the maximum desired stress. The specimen then underwent unloading and as a result of property manipulation a residual stress field was created. It is important to note that in all residual stress initialization methods, the maximum magnitudes of applied stresses could be fairly large (>180 MPa) as these were the required magnitudes to produce the residual stress field with magnitudes nearing 12 to 15 MPa as measured by Bock (1979). The maximum stress values utilized may also be representative of the stresses encountered at great depths where rock formation occurs. As a result of geologic processes, the material could then be uplifted to the stress states that are more commonly found in rock engineering design with residual stresses derived from its geologic history. Figure 4-3 is a visual example of the property manipulation processes that are being utilized for the formation of residual stress.

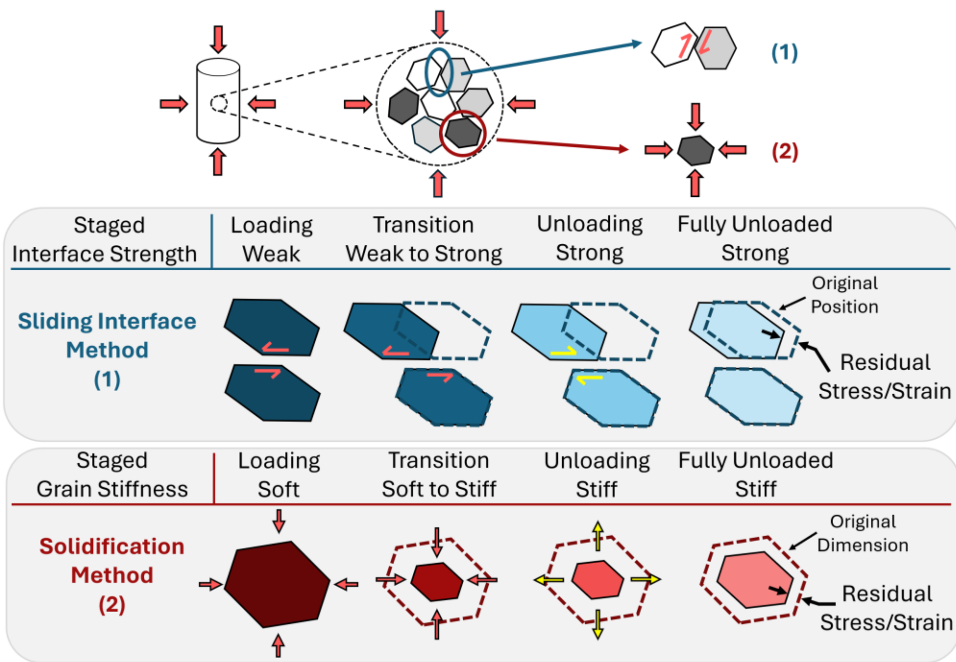

Figure 4-3 Visualization of residual stress initialization methods

To ensure the models were unloaded in a stable manner to prevent damage from occurring due to rapid unloading, a multistage process was employed to gradually release the applied stresses. Once the desired maximum induced stress threshold was reached, the velocity boundary used to induce stress was removed and replaced with a force boundary condition of equal magnitude. The model was then cycled for 1000 time steps to allow for the stresses to partially equilibrate to the new level. The magnitude of the force boundary was then gradually reduced over numerous stages, allowing for progressive unloading at each stage through cycling for partial stress relaxation. At the final unloading stage, the force boundary was completely removed, and the model was cycled until the induced stresses were completely dissipated and the residual stress field reached a state of equilibrium.

4.3.3 Residual Stress Modelling Results

The three methods described in Chapter 4.3.2 were utilized to initialize a residual stress field within the sample that had magnitudes similar to those reported in the literature (Nichols 1975; Bock 1979). The target stress threshold for all models was in the 12 to 15 MPa range with these stresses being reached in both tension and compression. Due to the heterogeneity of the model (contrasting stiffness and irregular grain shape), the target stress threshold could not be reached within all zones but rather the maximum compressive and tensile zones within the model should be indicative of the desired residual stress range. The average residual stress states are illustrated in Table 4-3, and Figure 4-4 illustrates a residual stress field created through the combination method and is indicative of the typically created residual stress field for this study.

Table 4-3 Average residual stresses for each residual stress implementation method

Residual stress implementation method	Average tensile residual stress (MPa)	Average compressive residual stress (MPa)
Sliding interface	3.96	3.94
Solidification	7.13	7.09
Combination	6.06	6.59

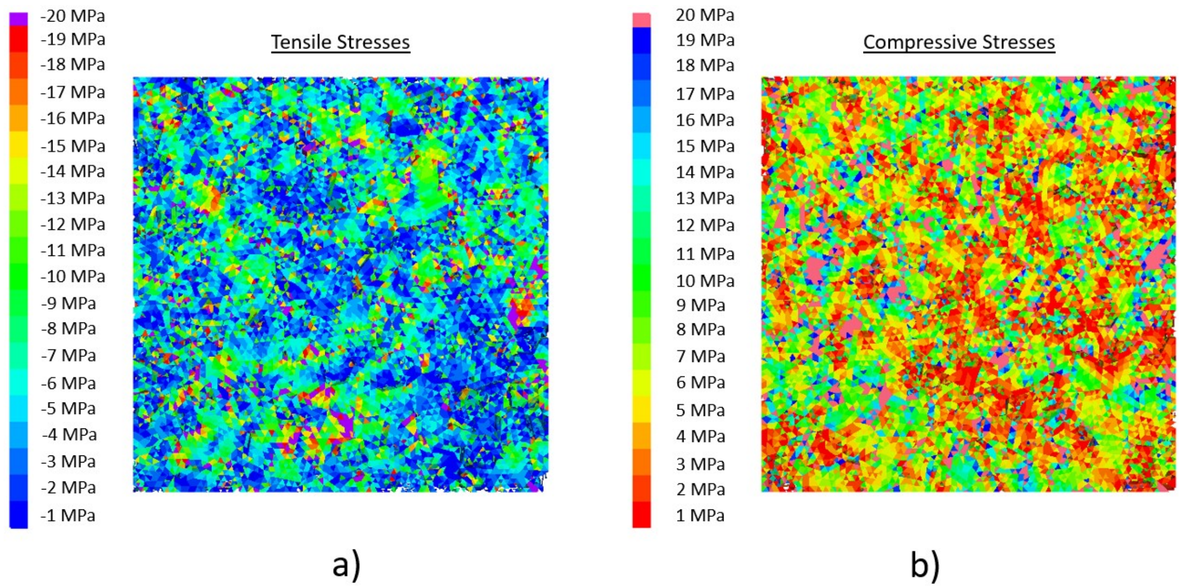

Figure 4-4 Example residual stress field from the combination method. A representation of the typically expected magnitudes of residual stress for modelling use in this project. a) Tensile magnitudes from zones. b) Compressive magnitudes from zones. (Note that the *3DEC* stress convention has been adapted to positive in compression)

As a result of unloading, the newly created residual stress field was constantly changing with the variations in induced stress. Once the specimen was fully unloaded and the residual stress field re-equilibrated, the presence of damage (interface failure) was investigated. As the specimen was exposed to a load/unload scheme, a baseline model was created with no residual stress and was exposed to the same loading scheme to understand the level of damage associated with the loading/unloading processes with and without the presence of residual stresses. Damage was investigated in samples with residual stresses derived from the three methods outlined in Chapter 4.3.2 and was compared to that of the specimen without residual stress. Damage was monitored through the use of a *FISH* function (Itasca's internal programming language) that measures the number of broken subcontacts within the model after unloading occurs and the residual stress field had reached a state of equilibrium. Table 4-4 summarizes the levels of damage associated with unloading each of the residual stress implementation methods.

Table 4-4 Summary of damage due to unloading with and without the presence of residual stress

Formation method	Damage
No residual stress (baseline)	0.31%
Sliding interface	1.79%
Solidification	21.78%
Combination	24.67%

It is a common phenomenon in rock compression tests for a region termed the ‘crack closure region’ to exist in the early stages of loading. Crack closure is only measured when a state of ‘open’ microcracks exists within the specimen. It is hypothesized here that residual stresses may be a factor that could result in a state of open microcracks due to the distribution of tensile residual stresses that can cause a crack to open. To determine if a correlation between the opening of cracks and residual stress exists, unconfined compression tests were performed on the unloaded samples once the residual stress field reached a state of equilibrium. This process was undertaken to determine if crack closure could be measured as a result of the damage produced from unloading with residual stresses present to propagate or open the microcracks. It should be noted that the compression tests were not intended to reach the peak strength of the specimen, but rather only to showcase the early regions of the stress-strain curve to illustrate the crack closure region more effectively. Figure 4-5 illustrates the results of the compression tests on three specimens with different methods of residual stress installation. The test performed on the sliding interface sample illustrated no crack closure and the stress-strain relationship follows a linear elastic path. The specimen with solidification residual stresses illustrated a small region of crack closure that was followed by a region of linear elasticity. Finally, the specimen with combination residual stresses clearly illustrated a region of crack closure that was followed by a linear elastic region after the microcracks had been closed due to the applied stress.

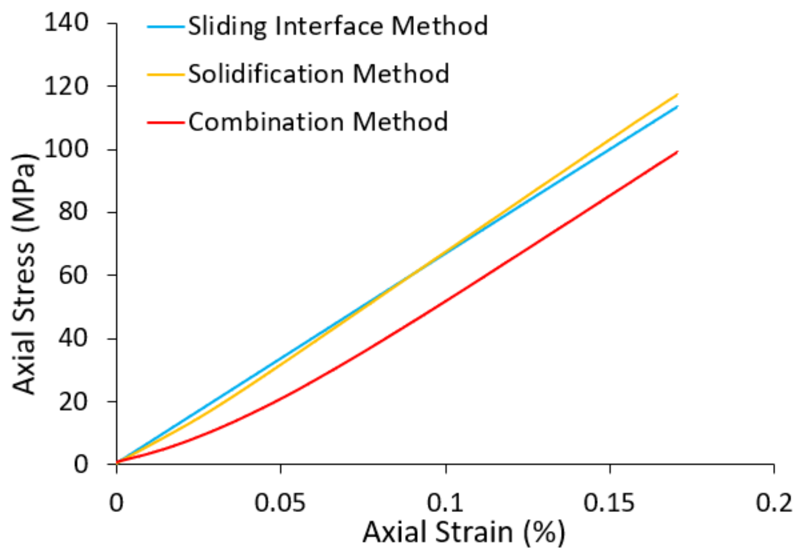

Figure 4-5 Quantification of damage through crack closure strains in compression tests

4.4 Discussion and Conclusions

It was shown that residual stresses from all three installation methods could produce levels of damage that were greater than the damage produced by the loading scheme alone. When these samples were exposed to unconfined compression tests, only the combination method clearly illustrated the crack closure behaviour. Although the solidification method had some non-linearity, the magnitude of crack closure was quite low. The level of damage produced from the sliding interface method was significantly lower than the other methods, and therefore the likelihood of crack closure strains to be present was quite small. A possible explanation for the low level of damage is that when residual stresses were formed from this method alone, the magnitudes of residual stresses were lower in comparison which may not have had the required magnitude to overcome the material strength during their redistribution. It is also likely that any damage formed during the redistribution could not be opened or propagated due to the lower magnitudes of tensile residual stresses that formed as a result of this method.

It had been shown that residual stresses existed within bodies of rock with magnitudes of up to 15 MPa. These stresses are in a state of equilibrium balanced by the tensile and compressive magnitudes that exist within the stress field. Some implications such as strength anisotropy and the influence of microcrack aperture were illustrated by Zang (1989). As little advancement has been introduced on the topic of residual stress in rock mechanics, this study examined the potential impacts of residual stress on a high-strength rock specimen. It was shown that damage could occur as a result of the redistribution of residual stresses due to unloading, and in some cases, the damage could result in crack closure strains that were observable in compression tests.

CHAPTER 5 - CONCLUSION

This chapter marks the conclusion of this thesis and presents findings and observations related to residual stress in rock. Observations found in the literature that may be explained using residual stresses are presented in a discussion section. The main conclusions derived within this thesis are presented, as are recommendations for future work on the topic to continue the development and understanding of residual stress concepts in rock.

5.1 Discussion

The development of microcracks, and therefore sample damage, can be related to residual stress redistributions. In a rock subjected to a stress path (unloading from in situ, drilling, etc.), microstresses acting within the microstructure will redistribute as the applied stress changes. When these induced stress field redistributions are overlain with residual stress redistributions, which take place simultaneously, the magnitudes of stress acting within the microstructure are then influenced by residual stresses. Tensile stresses generated due to heterogeneities (grain shape, size, stiffness, etc.) or changes in applied load magnitudes during stress redistribution, are the main concern for damage formation as the tensile strength of rock is typically much lower than its compressive strength. When tensile residual stresses are superimposed with applied tensile stresses throughout the stress path, the likelihood for damage formation increases. Therefore, when a rock contains residual stress, during the redistribution of stress, the possibility for damage formation is influenced by residual stress magnitudes as the tensile stresses increase the possibility for damage formation. Conversely, compressive residual stresses may resist the formation of local damage as these magnitudes decrease the tensile stresses generated during stress redistributions.

The propagation of an existing crack is also influenced by residual stress. Due to the random distribution of compressive and tensile residual stresses within the microstructure, a propagating crack that encounters residual stress will be influenced by their magnitude as illustrated in Figure 3-15. The propagation of a crack is related to the magnitude of tensile stresses acting on it. When the crack tip encounters compressive residual stresses, the propagation is then stalled as the tensile stresses must now overcome a greater material strength due to the resistance provided by the compressive residual stresses. When a crack then overcomes this increased strength, the magnitude of the tensile load is then elevated which can allow for greater crack propagation to occur. If the crack encounters a local tensile residual stress, the local tensile strength is essentially decreased which then allows the crack to propagate much easier through this zone. As compressive residual stresses can resist or stall tensile damage, and tensile residual stresses promote the growth of damage, it is likely that residual stresses contribute to the brittleness of a rock. As illustrated with Prince Rupert's drops, when damage formation occurs (glass breaking), the large magnitude of tensile stresses rapidly dissipates, and compared to regular annealed glass, the glass breaks into much finer shards. The residual stresses acting in these glass structures can then be related to its brittleness, and therefore in rock, it is also likely that they contribute to its brittleness. This is an important consideration for scenarios such as fracture toughness measurements in rock, as the presence of residual stress have a direct correlation to brittleness and therefore the resistance to fracturing.

Residual stress magnitudes were shown to have a connection to crack closure strains and sample damage. With low magnitudes, low crack closure strains and minor sample damage were observed. With high magnitudes, large crack closure strains and moderate to high sample damage were observed. This connection may be noticed in situ as well. At the URL, on the 240 m level, residual stresses were reported to be fairly low (around 1 MPa). This level also exhibits little sample damage, and when cores from this level undergo UCS testing, they exhibit little to no crack closure strains (Martin and Stimpson 1994). It was observed that at greater depths (420 m level) significant sample damage occurs and crack closure strains were visible (Eberhardt et al. 1998). The numerical models in this thesis illustrated that with larger magnitudes of residual stress, larger sample damage and crack closure strains are observed. It is therefore hypothesized that if residual stress measurements were to be undertaken at the 420 m level of the URL, then larger residual stresses may be reported compared to the measurements on the 240 m level.

A connection between sample damage occurring from in situ drilling stresses, and crack closure magnitudes was examined by Bahrani et al. (2015). In their study, they determined the stress path during drilling with 3D modelling and then applied a simplified version of this stress path in 2D models. When exposing specimens to the simplified stress path, the presence of damage was observed. In an attempt to correlate the damage from drilling to crack closure strains, UCS tests were undertaken on the samples after damage formation. It was noted that little to no crack closure strains occurred in the models even though damage was created. It is typically assumed in rock engineering that the damage process alone results in crack closure strains. This thesis proposes that residual stress is a missing mechanism in producing crack closure. Although damage forms from drilling, there exists no internal stress to influence the aperture of the newly formed microcracks and thus there exists no force to open them. If residual stresses were present in their model, the damage produced during drilling would likely result in crack closure due to the internal forces required to open the microcracks.

By implementing residual stress into numerical models, crack closure strains can be obtained without explicitly simulating open microcracks as is today's standard practice. Peng et al. (2015) implemented the effective medium theory in their analysis to produce crack closure strains. To implement this theory, the microstructure must be well defined, and two magnitudes of strain exist. The first is the matrix strains which consist of strains produced in the grains of a material and are related to the Young's modulus of the material. The second is the microcrack strains which essentially represent the crack aperture. These strains are then superimposed during loading to produce the strain history. At a pre-defined stress threshold, the microcrack strains reach their maximum and are no longer present and the system strain is then represented by the matrix strains only. Potyondy and Fu (2024) use a different method than that of Peng et al. (2015) to obtain crack closure strains in numerical models where a predefined crack closure stress is used as a model input to limit the non-linear section of the stress-strain curve. Including residual stress in rock simulation to achieve crack closure strain requires no predefinition of any micro-parameters such as crack length or aperture, nor does it require a stress threshold that defines the non-linear section of a stress-strain curve. Instead of using the current methods, using residual stress, a phenomenon known to occur in rock, to implement crack closure strains requires only the knowledge of the residual stress state prior to testing.

When excavating in rock containing residual stress, these stresses can mobilize and result in increased stresses acting on the boundaries of the excavation and can result in increased strains. When designing rock supports for underground and surficial excavations, the mobilization of residual stress can then act on the support components and impact their effectiveness. If supports are applied soon after excavation, and the complete redistribution of residual stress does not occur, then these stresses will mobilize and result in an additional stress component that then acts on them. The mobilization of residual stress due to excavating can also impact in situ stress measurement. When performing overcoring measurements, a strain cell is typically placed within a small excavation and then overcored to remove in situ stresses, and the relaxation of the rock is then measured and related to the in situ stresses. If residual stresses are present, the strains acting on the excavation-stress cell boundary can be influenced by their redistribution. If overcoring occurs before the complete relaxation of the residual stresses surrounding the strain cell location, then these stresses will continue to mobilize and will therefore influence the measurements. As illustrated by Nichols (1975), as the distance from the measurement point to the area of coring increases, measured residual strains become lower. This suggests that if the measurement point is located close to the overcore, then the cut will introduce residual stress redistributions that will influence the measurement. But, if the overcore takes place far enough from the strain measurement then its influence may be able to be mitigated and its influence on the results negligible.

5.2 Conclusions

Residual stresses exist in rock and have been measured in situ and in the laboratory. The standard procedure in rock mechanics and rock engineering is to omit residual stress from consideration. This thesis analyzed the outcomes of numerical models that contained residual stress to determine if their omission could result in discrepancies compared to simulations without residual stress. Using both 2D continuum (*RS2*) and 3D discontinuum (*3DEC*) software, residual stress was successfully implemented into the modelled geometries. In *RS2* models, the maximum magnitude of residual stress that could be obtained with the residual stress implementation used for storing strains in crack elements was about 7.7 MPa in both compression and tension. Using the Young's modulus manipulation method, residual stress magnitudes of about 8.8 MPa in compression and tension could be obtained. No further increase in residual stresses could be achieved with the current model configurations. In the *3DEC* models, residual stresses were created with the sliding interface method, solidification method, and combination method. The maximum compressive and tensile magnitudes investigated for each method were approximately 3.95 MPa, 7.11 MPa, and 6.33 MPa respectively. Within the *3DEC* models, the magnitudes of residual stress could be increased, but no further attempts at increasing the magnitudes were performed in this study.

Numerical specimens had residual stresses initialized, and compression tests were performed to investigate a relationship between residual stress and crack closure strains. It was noted that with increasing magnitudes of residual stress, increased crack closure strains were observed in specimens with equal levels of pre-existing damage. In specimens with equal residual stress magnitudes, but varied levels of damage (low and high), larger crack closure strains were observed in the higher damaged specimen which is likely due to the increased ability to dissipate residual stress and therefore open microcracks. In both continuum and discontinuum models, crack closure strains were observed. Although in the discontinuum models obvious crack closure strains were only noticed using the combination method, by increasing the magnitudes to achieve values closer to those reported in the literature, crack closure strains may be observed with the sliding interface and solidification methods as well.

The effects of a residual stress field on the formation and propagation of microcracks was investigated in continuum and discontinuum models, and the propagation of a singular microcrack under tensile loading was examined using continuum models only. By creating residual stress fields under applied loads, unloading the specimen results in the formation and propagation of damage within the microstructure due to the mobilization of residual stresses. Damage from residual stress redistribution was illustrated using all residual stress formation methods in both continuum and discontinuum models. In samples undergoing the same loading and unloading processes without residual stress, no damage was observed. This indicates that the presence of residual stress is a factor in damage formation during unloading. With continuum models, a slot cut was created in a rock block with and without residual stresses and was then subjected to applied tensile loading to simulate the propagation of a microcrack. The results illustrate that residual stresses can influence the propagation of the slot cut due to their random distribution of stress magnitudes. The presence of compressive residual stresses ahead of the cut resulted in the stalling of damage, and the tensile strength of the material was effectively increased compared to a simulation without residual stress. After the damage was initialized, it then propagated further into the specimen containing residual stress due to the distribution of tensile residual stress causing local weak zones ahead of the crack. Residual stresses were shown to be a factor in the formation of new damage and to influence the propagation of damage which indicates that they should be considered when examining rock fracture mechanics.

Residual stresses surrounding an excavation were shown to mobilize and result in measurable strains. As the distance from the excavation surface into the rock increases, the magnitude of mobilized residual stresses decreases. This observation was also noticed in the laboratory by Nichols (1975). Stress redistributions in specimens with and without residual stress were measured while in situ stresses were acting on the external boundaries, and when residual stresses were present, the results were significantly different. In in situ stress measurement, if residual stresses are omitted then this would act as a large source of uncertainty due to its effects on the excavation boundary where strains are measured in situ. After the addition of an excavation in the model, the magnitude of the released strain was measured, and lower strains compared to the literature measurements were observed. This indicates that larger magnitudes of residual stress should be implemented to achieve residual stress fields comparable to physical measurements.

Residual stresses are currently thought to have little to no implications in the field of rock mechanics and rock engineering. Results from the models undertaken in this thesis suggest that these stresses may have direct implications in rock. As illustrated in the simulations undertaken here, some implications for these stresses include the formation and propagation of damage, opening of microcracks resulting in crack closure strains in compression tests, the influence of compressive and tensile magnitudes in fracture mechanics, additional stress and strain components on excavation supports, and a source of error for in situ stress measurement. The implications presented in this thesis likely only represent some of the implications within this field. With continued investigation of residual stress mechanisms in rock, more implications for these stresses are likely to be discovered.

5.3 Recommendations for Future Study

Due to the limited study of residual stress in rock mechanics and rock engineering, many areas could benefit from its continued study. The model results presented in this thesis indicate that there may be a connection between residual stress and crack closure. A study that relates residual stresses and crack closure strains measured in a laboratory could be used with the numerical modelling procedures presented here to further explore this relationship. By using concentric coring with strain gauges to release residual stresses, this process can be modelled and used as a source of calibration for the magnitude of residual stresses contained within it by iteratively increasing the magnitudes until similar strains are reported. Once similar magnitudes are implemented, the numerical simulations could be used as a means to predict the crack closure that might be measured within the physical specimen recovered from the rock block. By comparing the magnitudes of crack closure strains with similar residual stress magnitudes, the possibility for a connection between these two phenomena may be further explored.

Numerous researchers have performed laboratory investigations of residual stress in rock, and many different investigations such as XRD, coring, p-wave velocity analysis, SEM investigations, and fracture tests have performed. Researchers have yet to include all of these methods in one investigation, nor have any included compression tests along side of these results. To develop a large dataset that may be used to relate residual stresses to other laboratory measurements, it is suggested that all the methods used in individual studies should be repeated in a singular study as well as including other tests, such as UCS, that have not been previously investigated with the main research question surrounding residual stress. A rock block may be overcored and subjected to XRD to measure residual strains, and using the secondary overcoring process illustrated by Zang and Berckhemer (1989), p-wave velocities before and after residual stress redistributions may be measured along with fracture tests and an SEM investigation on thin sections of the secondary overcore recovered after preparing a UCS test specimen from the same core. By performing numerous laboratory investigations on rock specimens with known magnitudes of residual stress, new implications may be revealed and related to observations that may not currently be well known or accurately predictable with the tools and understanding currently available.

While coring and diffraction techniques are typically used to quantify residual stress in rock, other methods may be explored to assess their effectiveness. While not able to directly quantify residual stress, acoustic emission (AE) sensors may be an effective means to monitor residual stress redistributions. During redistribution, movement may occur in the microstructure and result in frequencies that can be picked up by AE sensors. If paired with p-wave velocity measurements after coring, using AE as a means to monitor the redistributions may result in additional data that can be used to investigate residual stress. Another uncommon method that may be further explored to investigate residual stress is with the use of microscopic measurements. If a microscope has sufficient accuracy (± 10 to 20 $\mu\epsilon$), then measurements (height and width) of the grains contained on the edges of a rock core may be undertaken to measure residual stress. By performing measurements on an intact core and then disaggregating it using thermal loading similar to Rosengren and Jaeger (1968), after the grains have been freed from their neighbouring constraints, residual stresses may be released and could be quantified by comparing measurements before and after disaggregation to determine the residual strain released from within the grain.

Using numerical methods, the exploration of residual stress could be furthered from what was presented in this thesis. By simulating numerous rock types (a sandstone, metamorphic and igneous rock) with more variations in the simulated residual stress magnitudes (5 to 20 MPa), the illustrated connection between the magnitude of residual stress and crack closure strain may be further explored. It was also presented that a connection between residual stress and sample damage occurred. With further investigation into other damaging processes, such as drilling with in situ stresses, core discing, and tunnel EDZs, the relationship between sample damage and residual stress redistributions may be further explored. The magnitudes of residual stress implemented in this study were generally lower than values reported in the literature as illustrated by Figure 3-18, where the redistributions of residual stress were about 25% of the values presented by Nichols (1975), and if the magnitudes are increased, then further implications may be observed or explored. Residual stresses in rock mechanics and rock engineering are still poorly understood, and more research is required to further the understanding of its formation mechanisms and implications in rock engineering and rock mechanics.

BIBLIOGRAPHY

Aben H, Anton J, Ois M, Viswanathan K, Chandrasekar S, Chaudhri MM (2016) On the extraordinary strength of Prince Rupert's drops. Applied Physics Letters 190.

Aptukov VN, Volegov SV (2020) Modeling Concentration of Residual Stresses and Damages in Salt Rock Cores. Journal of Mining Science 56(3): 331-338.

Aronen A, Karvinen R (2018) Effect of glass temperature before cooling and cooling rate on residual stresses in tempering. Glass Structural Engineering 3: 3-15.

Bahrani N, Valley B, Kaiser PK (2015) Numerical simulation of drilling-induced core damage and its influence on mechanical properties of rocks under unconfined condition. International Journal of Rock Mechanics and Mining Sciences 80:40-50.

Barla G, Barla M (2000) Continuum and Discontinuum Modelling in Tunnel Engineering. The Mining-Geological-Petroleum Engineering Bulletin 12: 45-57.

Bock H (1979) Experimental determination of the residual stress field in a basaltic column. 4th ISRM Congress. ISRM-4CONGRESS-1979-006.

Brodsley L, Frank C, Steeds JW (1986) Prince Rupert's drops. Notes and Records of the Royal Society. 41(1):1-26.

Chen K, Kunz M, Tamura N, Wenk HR (2011a) Deformation twinning and residual stress in calcite studied with synchrotron polychromatic X-ray microdiffraction. Physics and Chemistry of Minerals 38: 491-500.

Chen K, Kunz M, Tamura N, Wenk HR (2011b) Evidence for high stress in quartz from the impact site of Vredefort, South Africa. European Journal of Mineralogy 23(2): 169-178.

Chen K, Kunz M, Tamura N, Wenk HR (2015) Residual stress preserved in quartz from the San Andreas Fault Observatory at Depth. Geology 43(3): 219-222.

Chen K, Kunz M, Li Y, Zepeda-Alarcon E, Sintubin M, Wenk HR (2016) Compressional residual stress in Bastogne boudins revealed by synchrotron X-ray microdiffraction. Geophysical Research Letters 43: 6178-6185.

Corkum AG, Damjanac B, Lam T (2018) Variation of the horizontal in situ stress with depth for long-term performance evaluation of the Deep Geologic Repository project access shaft. International Journal of Rock Mechanics and Mining Sciences 107: 75-85.

Corkum AG (2020) A Model for Pore Pressure Response of a Claystone due to Liberated Residual Stress Dilation. Rock Mechanics and Rock Engineering 53: 587-600.

Damjanac B (2008) Phase 1 Long-Term Cavern Stability. OPG's Deep Geologic Repository for Low & Intermediate Level Waste: Supporting Technical Report. OPG 00216-REP-01300-00005-R00.

Durrance EM (1969) Release of Strain Energy as a Mechanism for the Mechanical Weathering of Granular Rock Material. Geological Magazine 106(5): 496-497.

Eberhardt E, Stead D, Stimpson B (1998) Effects of sample disturbance on the stress-induced microfracturing characteristics of brittle rock. Canadian Geotechnical Journal 36: 239-250.

Eijpe MPIM, Powell PC (1997) Residual stress evaluation in composites using a modified layer removal method. Composite Structures 37(3): 335-342.

Ekmekci B, Ekmekci N, Tekkaya AE, Erden A (2004) Residual Stresses Measurement with Layer Removal Method. 1st Cappadocia International Mechanical Engineering Symposium (1).

Engelder T, Sbar ML (1977) The Relationship Between In Situ Strain Relaxation and Outcrop Fractures in the Potsdam Sandstone, Alexandria Bay, New York. Pure and Applied Geophysics 115: 41-55.

Engelder T, Sbar ML, Kranz R (1977) A Mechanism for Strain Relaxation of Barre Granite: Opening of Microfractures. Pure and Applied Geophysics 115: 27-40.

Engelder T, Geiser P (1984) Near-Surface in Situ Stress 4. Residual Stress in the Tully Limestone Appalachian Plateau, New York. Journal of Geophysical Research 89(B11): 9365-9370.

Fan J, Liu W, Jiang D, Chen J, Tiedeu WN, Daemen JJK (2020) Time Interval Effect in Triaxial Discontinuous Cyclic Compression Tests and Simulations for the Residual Stress in Rock Salt. Rock Mechanics and Rock Engineering 53: 4061-4076.

Farahmand K, Diederichs MS (2020) Calibration of coupled hydro-mechanical properties of grain-based model for simulating fracture process and associated pore pressure evolution in excavation damage zone around deep tunnels. Journal of Rock Mechanics and Geotechnical Engineering 13: 60-83.

Fitzpatrick ME, Fry AT, Holdway P, Kandil FA, Shackleton J, Souminen L (2005) Determination of Residual Stresses by X-ray Diffraction – Issue 2. Measurement Good Practice Guide 52.

Friedman M (1967) X-ray analysis of residual elastic strain in quartzose rocks. 10th U.S. Symposium on Rock Mechanics (USRMS) ARMA-68-0573.

Friedman M, Logan JM (1970) Influence of Residual Elastic Strain on the Orientation of Experimental Fractures in Three Quartzose Sandstones. Journal of Geophysical Research 75(2): 387-405.

Friedman M (1972) Residual elastic strain in rocks. Tectonophysics 15:197-330.

Gentry DW (1972) Horizontal residual stresses in the vicinity of a breccia pipe. International Journal of Rock Mechanics and Mining Sciences & Geomechanics Abstracts 10(1): 19-36.

Ghorbani Y, Nwaila GT, Zhang SE, Bourdeau JE, Canovas M, Arzua J, Nikadat N (2023) Moving towards deep underground mineral resources: Drivers, challenges and potential solutions. Resource Policy 80: 103222.

Griffiths L, Heap MJ, Baud P, Schmittbuhl J (2017) Quantification of microcrack characteristics and implications for stiffness and strength of granite. International Journal of Rock Mechanics and Mining Sciences 100: 138-150.

Guo J, Fu H, Pan B, Kang R (2019) Recent progress of residual stress measurement methods: A review. Chinese Journal of Aeronautics 34(2): 54-78.

Gy R (2008) Ion exchange for glass strengthening. Materials Science and Engineering B 149: 159-165.

Harker YD, She CY, Edwards DF (1970) Raman Spectra of α Quartz Under Uniaxial Stress. Journal of Applied Physics 41: 5274-5278.

Holzhausen GR, Johnson AM (1979) The concept of residual stress in rock. Tectonophysics 58: 237-267.

Hosseinzadeh F, Kowal J, Bouchard PJ (2014) Towards good practice guidelines for the contour method of residual stress measurement. The Journal of Engineering 8: 453-468.

Itasca Consulting Group, Inc. (2023) 3DEC — Three-Dimensional Distinct Element Code, Ver. 7.00.155 Minneapolis: Itasca.

Jacobus K, DeVor RE, Kapoor SG (2000) Machining-Induced Residual Stress: Experimentation and Modelling. Journal of Manufacturing Science and Engineering 122(1): 20-31.

Khorassani AG, Corkum AG (2023) Discrete element grain-based model for residual stress mechanisms and resulting microcrack formation in crystalline granite. Internal Dalhousie Engineering report: unpublished.

Lang PA, Thompson PM, NG LKW (1986) The effect of residual stress and drill holes size on the in situ stress determined by overcoring. ISRM International Symposium ISRM-IS-1986-072.

Lee MJ, Hill MR (2007) Intralaboratory Repeatability of Residual Stress Determined by the Slitting Method. Experimental Mechanics 47: 745-752.

Li X, Peng K, Peng J, Hou D (2021) Effect of thermal damage on mechanical behaviour of a fine-grained sandstone. Arabian Journal of Geosciences 14: 1212.

Li Y, Bahrani N (2021) A continuum grain-based model for intact and granulated Wombeyan marble. Computers and Geotechnics 129.

Mainprice D, Nicolas A (1989) Development of shape and lattice preferred orientations: applications to the seismic anisotropy of the lower crust. Journal of Structural Geology 11(1-2): 175-189.

Maleki E, Bagherifard S, Unal O, Bandini M, Farrahi GH, Guagliano M (2021) Introducing gradient serve shot peening as a novel mechanical surface treatment. Scientific Reports 11: 22035.

Martin CD, Stimpson B (1994) The effect of sample disturbance on laboratory properties of Lac du Bonnet granite. Canadian Geotechnical Journal 31:692-702.

Mavko G, Mukerji T, Dvorkin J (2020) The rock physics handbook. Cambridge University Press.

Molli G, Heilbronner R (1999) Microstructures associated with static and dynamic recrystallization of Carrara marble (Alpi Apuane, NW Tuscany, Italy). Geologie en Mjnbouw 78: 119-126.

Montross CS, Wei T, Ye L, Clark G, Mai YW (2002). Laser shock processing and its effects on microstructure and properties of metal alloys: a review. International Journal of Fatigue 24: 1021-1036.

Nau A (2015) A Contribution to Enlarge the Application Limits of Residual Stress Analyses by the Hole-Drilling and the Ring-Core Method. Kassel University Press.

Nelson DV (2010) Residual Stress Determination by Hole Drilling Combined with Optical Methods. Experimental Mechanics 50: 145-158.

Nichols TC (1975) Deformations associated with relaxation of residual stresses in a sample of Barre granite from Vermont. Geological Survey Professional Paper 875.

Passchier CW, Trouw RAJ (2005) Microtectonics 2nd edition. Springer.

Peng J, Rong G, Tang Z, Sha S (2019) Microscopic characterization of microcrack development in marble after cyclic treatment with high temperature. Bulletin of Engineering Geology and the Environment 78: 5965-5976.

Potyondy DO, Cundall PA (2004) A bonded-particle model for rock. International Journal of Rock Mechanics and Mining Sciences 41: 1329-1364.

Potyondy DO, Fu W (2024) A 3D Subspring Network Breakable Voronoi Model for Rock: Laboratory-Scale Behaviour. ARMA 24-0493.

Price NJ (1969) Laws of Rock Behaviour in the Earth's Crust. 11th US Symposium on Rock Mechanics ARMA-69-0003.

Read RS (1990) Residual strain, scale effects, and time-dependent behaviour at the 240-m level of the underground research laboratory. Atomic Energy of Canada Limited.

Rocscience (2023) Joints Overview. RS2 User Guide.

Rong G, Peng J, Yao M, Jiang Q, Wong LNY (2018) Effects of specimen size and thermal-damage on physical and mechanical behaviour of a grained-grained marble. Engineering Geology 232: 46-55.

Rosengren KJ, Jaeger JC (1968) The Mechanical Properties of an Interlocked Low-Porosity Aggregate. Géotechinque 18: 317-326.

Rossini NS, Dassisti M, Benyounis KY, Olabi AG (2011) Methods of measuring residual stresses in components. Materials and Design 35: 572-588.

Russell JE, Hoskins ER (1972) Residual Stresses in Rock. 14th US Symposium on Rock Mechanics ARMA-72-0001.

Sanipour S, Bahrani N, Corkum A (2022) Simulation of Brittle Failure Around Canada's Mine-By Experiment Tunnel Using 2D Continuum-Based Voronoi Tessellated Models. Rock Mechanics and Rock Engineering 55: 6387-6408.

Savage WZ (1978) The development of residual stress in cooling rock bodies. Geophysical Research Letters 5(8).

Schajer GS (2010) Relaxation Methods for Measuring Residual Stresses: Techniques and Opportunities. Experimental Mechanics 50: 1117-1127.

Sekine K, Hayashi K (2009) Residual stress measurements on a quartz vein: A constraint on paleostress magnitude. Journal of Geophysical Research 114.

Sharma A, Hesterberg D (2020) Synchrotron radiation-based spatial methods in environmental biogeochemistry. Multidimensional Analytical Techniques in Environmental Research: 231-265.

Tan TK, Wang WF (1980) Locked in Stresses, Creep and Dilatancy of Rocks, and Constitutive Equations. Rock Mechanics 13: 5-22.

Tebedge N, Alpsten G, Tall L (1973) Residual-stress measurement by the sectioning method. Experimental Mechanics 13: 88-96.

Terakado N, Sasaki R, Takahashi Y, Fujiwara T, Orihara S, Orihara Y (2020) A novel method for stress evaluation in chemically strengthened glass based on micro-Raman spectroscopy. Communications Physics 3(37).

Tullis TE (1977) Reflections on Measurement of Residual Stress in Rock. Pure and Applied Geophysics 115: 57-68.

Ulutan D, Ozel T (2011) Machining induced surface integrity in titanium and nickel alloys: A review. International Journal of Machine Tools & Manufacture 51:250-280.

Varnes DJ (1969) Model For Simulation of Residual Stress in Rock. 11th US Symposium on Rock Mechanics ARMA-69-0415.

Varnes DJ, Lee FT (1972) Hypothesis of Mobilization of Residual Stress in Rock. Geologic Society of America Bulletin 83(9): 2863-2866.

Voight B (1966) Residual stresses in rocks. 1st ISRM Congress ISRM-1CONGRESS-1966-140.

Voigtlander A, Leith K, Walter JM, Krautblatter M (2020) Constraining Internal States in Progressive Rock Failure of Carrara Marble by Measuring Residual Strains With Neutron Diffraction. Journal of Geophysical Research: Solid Earth (125).

Wang T, Ye W, Tong Y, Jiang N, Liu L (2023) Residual stress measurement and analysis of siliceous slate-containing quartz veins. International Journal of Minerals, Metallurgy and Materials 30(12): 2310-2320.

Wenk HR, Chandler BC, Chen K, Li Y, Tamura N, Yu R (2020) Residual lattice strain in quartzites as a potential palaeo-piezometer. Geophysical Journal International 222(2): 1363-1378.

White JM (1984) Residual strain measurements in selected materials from the Black Hills, South Dakota. Rocky Mountain Geology 23(1): 37-43.

Withers PJ, Webster PJ (2001) Neutron and Sychrotron X-ray Strain Scanning. Strain 37(1).

Wolfram (2023) Mathematica. Version 13.2.1.0.

Zang A, Berckhemer H (1989) Residual stress features in drill cores. Geophysical Journal International 99: 621-626.

Zang A, Lienert M, Zinke J, Berckhemer H (1996) Residual strain, wave speed and crack analysis of crystalline cores from the KTB-VB well. Tectonophysics 263: 219-234.